

AFOSR-TR- 80-0065

Q

Acc4563

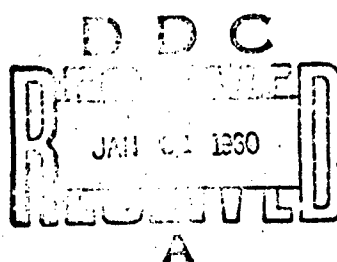
777-1111

AD A 080135

20000727286

Reproduced From
Best Available Copy

DDC FILE COPY



80 1 30 068

Approved for public release;
distribution unlimited.

TIME-TEMPERATURE STUDIES OF HIGH TEMPERATURE
DETERIORATION PHENOMENA IN LUBRICANT SYSTEMS:
SYNTHETIC ESTER LUBRICANTS

By

L. R. Mahoney, S. Korcek, P. A. Willermet,
E. J. Hamilton, Jr., R. K. Jensen, M. Zinbo,
S. K. Kandah, J. M. Norbeck, and L. A. Scheich

Engineering and Research Staff

Research

Ford Motor Company

Dearborn, Michigan 48121

AIR FORCE OFFICE OF SCIENTIFIC RESEARCH (AFSC)
NOTICE OF TRANSMITTAL TO DDC

This technical report has been reviewed and is
approved for public release IAW AFN 100-12 (7b).
Distribution is unlimited.

A. D. BLOSE
Technical Information Officer

Unclassified

SECURITY CLASSIFICATION OF THIS PAGE (When Data Entered)

19 REPORT DOCUMENTATION PAGE

READ INSTRUCTIONS
BEFORE COMPLETING FORM

1. REPORT NUMBER

18. GOVT ACCESSION NO.

3. RECIPIENT'S CATALOG NUMBER

19 AFOSR/TR-80-0065

4. TITLE (and Subtitle)

5. Time-Temperature Studies of High Temperature
Deterioration Phenomena in Lubricant Systems:
Synthetic Ester Lubricants

9. TYPE OF REPORT / PERIOD COVERED

Final rep't.
1 Apr 1976 - Sep 1979

6. PERFORMING ORG. REPORT NUMBER

7. AUTHOR(S)

8. CONTRACT OR GRANT NUMBER

10. L. R. Mahoney, S. Korcek, P. A. Willmett, E. J.

Hamilton, Jr., R. K. Jensen

K. J. M. Verbeek and D. W. Schatz

11. PERFORMING ORGANIZATION NAME AND ADDRESS

Ford Motor Company

Dearborn, Michigan 48121

15. F44620-76-C-0097

16. PROGRAM ELEMENT, PROJECT, TASK AREA & WORK UNIT NUMBERS

17. 2303 1600 17/A2

12. CONTROLLING OFFICE NAME AND ADDRESS

Air Force Office of Scientific Research, NC
Bolling Air Force Base, DC 20332

18. REPORT DATE

19. 1979

20. NUMBER OF PAGES

143

14. MONITORING AGENCY NAME & ADDRESS (if different from Controlling Office)

15. SECURITY CLASS. (of this report)

Unclassified

15a. DECLASSIFICATION/DOWNGRADING SCHEDULE

16. DISTRIBUTION STATEMENT (of this Report)

Approved for public release: Distribution unlimited

17. DISTRIBUTION STATEMENT (of the abstract entered in Block 20, if different from Report)

18. SUPPLEMENTARY NOTES

19. KEY WORDS (Continue on reverse side if necessary and identify by block number)

Synthetic Ester Lubricants, Pentaerythrityl tetraheptanoate, Chemical Kinetics, Deterioration, Stirred Flow Reactor, Wear, Antioxidants.

alpha, gamma and alpha, delta

401 367 9M

20. ABSTRACT (Continue on reverse side if necessary and identify by block number)

A kinetic and mechanistic study of the autoxidation of liquid pentaerythrityl tetraheptanoate, PETH, in a stirred flow reactor at 180 to 220°C was completed. The results are consistent with the occurrence of a chain reaction scheme similar to that proposed for n-hexadecane autoxidation. This scheme includes the formation of monohydroperoxides by the intermolecular abstraction reaction (1), formation of α , γ and α , β -dihydroperoxides and hydroperoxyketones by intramolecular peroxy radical abstraction reactions (2) and (3), bimolecular termination reaction of peroxy radicals, reaction (4), and rapid conversion of α , γ -hydroperoxyketones to cleavage acids and

Unclassified

Unclassified

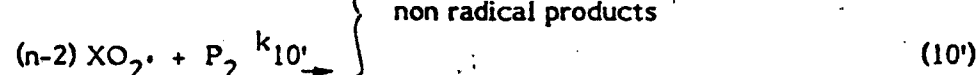
SECURITY CLASSIFICATION OF THIS PAGE (When Data Entered)

methylketones, reaction (7).

Comparisons of various rate parameters for the n-hexadecane and PETH systems reveal that the values of k_7 and $(k_3/\text{H-atom})/(2k_6)$ are within experimental uncertainties identical for the two systems at 180°C.

Laboratory studies showed that small degrees of autoxidation produce large increases in metal wear when PETH functions as a boundary lubricant. The results indicate that monoesters of dicarboxylic acids produced in reaction (7) are the products which in conjunction with hydroperoxides result in the increased wear.

We find that upon the introduction of an antioxidant, AH, the radical termination reactions (6) are replaced by the termination reaction sequences,



where P_1 and P_2 are antioxidant active intermediate products of the reactions of the initial antioxidant radical A^\bullet and n is the total number of XO_2^\bullet radicals consumed by the reactions of a molecule of AH and its reactive products.

The results for the 4,4'-dioctyldiphenylamine inhibited autoxidation of PETH at 180 to 220°C are consistent with the occurrence of reaction sequence (8) through (10) where $k_{-8}(\text{XOOH}) \gg k_9(\text{XO}_2^\bullet)$ and n is very large, ca. 19. This large value of n requires that reactions (9) and (10) be cyclic processes involving the consumption and then the regeneration of species such as nitroxy radicals and hydroxylamine products of A^\bullet .

The results for the 4,4'-methylenebis(2,6-di-tert-butylphenol) inhibited autoxidation of PETH at 180 to 220°C are consistent with the occurrence of reaction scheme (8) - (10) where $k_9(\text{XO}_2^\bullet)$ and $k_9'(\text{A}^\bullet) \gg k_{-8}(\text{XOOH})$ and n is equal to ca. 4.0. The product of reaction (9') has been shown to be the quinone methide, QM. From the consumption of AH and the growth and the decay of QM a general rate equation for the disappearance of AH has been derived.

Based upon the results of these inhibited autoxidation studies a method for establishing the relationships between structure and thermoxidative stability of synthetic ester lubricants has been developed. Kinetic equations have been derived for the autoxidation of ester systems inhibited by antioxidants for which $k_9(\text{XO}_2^\bullet) \gg k_8(\text{XOOH})$ and numerical procedures have been developed for the solutions of these equations. The solutions yield values of the ratios of the inhibition periods for ester systems as a function of the values of $k_8/(k_3/\text{H-atom})$, n and the relative contribution of intramolecular and intermolecular abstraction reactions in the inhibited ester autoxidations. Utilizing values of $k_4/k_3(\text{RH})$ and $k_4^*/k_3(\text{RH})$ observed in the autoxidation of PETH, values of n equal to 2.0, and $k_8/(k_3/\text{H-atom})$ equal to 2.5×10^3 , the ratios of the inhibition periods calculated by the procedure are found to be in excellent agreement with the experimental ratios for the n-C₅ through n-C₈ pentaerythrityl alkanoates containing 1 weight per cent N-phenyl- α -naphthylamine at 232°C.

Unclassified

TIME-TEMPERATURE STUDIES OF HIGH TEMPERATURE
DETERIORATION PHENOMENA IN LUBRICANT SYSTEMS:
SYNTHETIC ESTER LUBRICANTS

By

L. R. Mahoney, S. Korcek, P. A. Willermet,
E. J. Hamilton, Jr., R. K. Jensen, M. Zinbo,
S. K. Kandah, J. M. Norbeck, and L. A. Scheich

Engineering and Research Staff
Research
Ford Motor Company
Dearborn, Michigan 48121

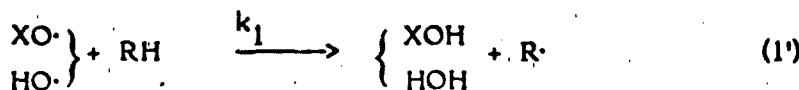
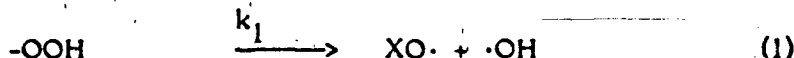
Accession For

MSIS	Code	DL 3 673
Library	Section	Chemical
Jan 1972	Year	
By		
A		

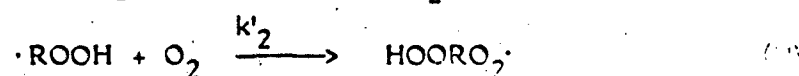
ABSTRACT

A kinetic and mechanistic study of the autoxidation of liquid pentaerythrityl tetraheptanoate, PETH, in a stirred flow reactor at 180 to 220°C was completed. The results are consistent with the occurrence of a chain reaction scheme similar to that proposed for n-hexadecane autoxidation:

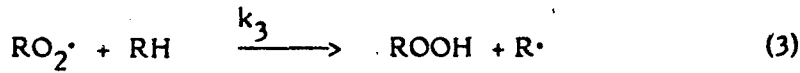
Initiation



Oxidation



Intermolecular Propagation



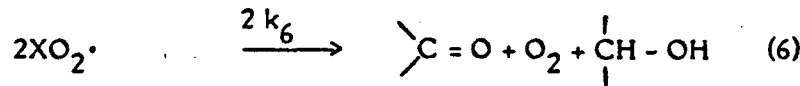
α , γ and α , δ Intramolecular Propagation



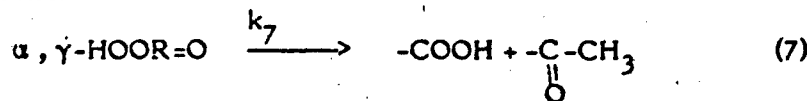
Hydroxy Radical Formation



Termination



Acid Formation

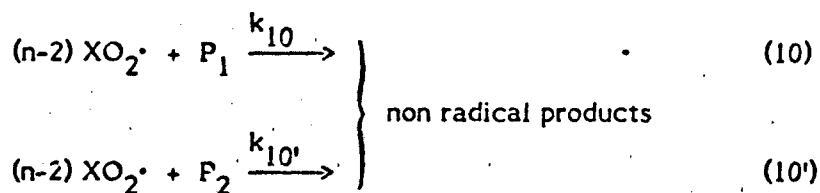
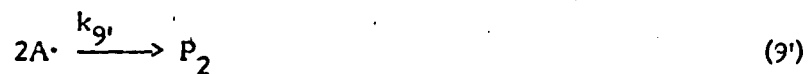
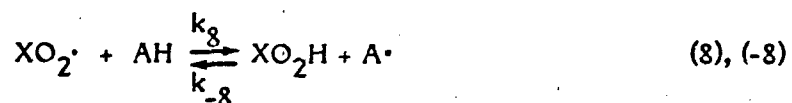


where RH represents PETH, XO_2^\cdot equals to $(\text{RO}_2^\cdot + \text{HOORO}_2^\cdot)$ and XO^\cdot to $(\text{RO}^\cdot + \text{HOOR}^\cdot + \text{O} = \text{RO}^\cdot)$.

Comparisons of various rate parameters for the n-hexadecane and PETH systems reveal that the values of k_7 and $(k_3/\text{H-atom})/(2k_6)^{1/2}$ are within experimental uncertainties identical for the two systems at 180°C.

Laboratory studies showed that small degrees of autoxidation produce large increases in metal wear when PETH functions as a boundary lubricant. The results indicate that monoesters of dicarboxylic acids produced in reaction (7) are the products which in conjunction with hydroperoxides result in the increased wear.

We find that upon the introduction of an antioxidant, AH, the radical termination reactions (6) are replaced by the termination reaction sequences,



where P_1 and P_2 are antioxidant active intermediate products of the reactions of the initial antioxidant radical $A \cdot$ and n is the total number of $XO_2 \cdot$ radicals consumed by the reactions of a molecule of AH and its reactive products.

The results for the 4,4'-dioctyldiphenylamine inhibited autoxidation of PETH at 180 to 220°C are consistent with the occurrence of reaction sequence

(8) through (10) where $k_{-8}(XOOH) \gg k_9(XO_2^{\cdot})$ and n is very large, ca. 19. This large value of n requires that reactions (9) and (10) be cyclic processes involving the consumption and then the regeneration of species such as nitroxy radicals and hydroxylamine products of A^{\cdot} .

The results for the 4,4'-methylenebis(2,6-di-*tert*-butylphenol) inhibited autoxidation of PETH at 180 to 220°C are consistent with the occurrence of reaction scheme (8) - (10) where $k_9(XO_2^{\cdot})$ and $k_{-9}(A^{\cdot}) \gg k_{-8}(XOOH)$ and n is equal to ca. 4.0. The product of reaction (9') has been shown to be the quinone methide, QM. From the consumption of AH and the growth and the decay of QM a general rate equation for the disappearance of AH has been derived.

Based upon the results of these inhibited autoxidation studies a method for establishing the relationships between structure and thermoxidative stability of synthetic ester lubricants has been developed. Kinetic equations have been derived for the autoxidation of ester systems inhibited by antioxidants for which $k_9(XO_2^{\cdot}) \gg k_{-8}(XOOH)$ and numerical procedures have been developed for the solutions of these equations. The solutions yield values of the ratios of the inhibition periods for ester systems as a function of the values of $k_8/(k_3/\text{H-atom})$, n and the relative contribution of intramolecular and intermolecular abstraction reactions in the inhibited ester autoxidations. Utilizing values of $k_4/k_3(\text{RH})$ and $k_4^*/k_3(\text{RH})$ observed in the autoxidation of PETH, values of n equal to 2.0, and $k_8/(k_3/\text{H-atom})$ equal to 2.5×10^3 , the ratios of the inhibition periods calculated by the procedure are found to be in excellent agreement with the experimental ratios for the $n\text{-C}_5$ through $n\text{-C}_8$ pentaerythrityl alkanoates containing 1 weight per cent N-phenyl- α -naphthylamine at 232°C.

TABLE OF CONTENTS

	<u>Page</u>
ABSTRACT	
I. INTRODUCTION	1
II. KINETICS AND MECHANISM OF 4,4'-DIOCTYLDIPHENYLAMINE INHIBITED AUTOXIDATION AT 160 TO 220°C, By R. K. Jensen, S. Korcek, L. R. Mahoney, L. A. Scheich, and M. Zinbo	2
LOW CONCENTRATIONS OF AMINE	2
HIGH CONCENTRATIONS OF AMINE	13
VALUES OF n AND REACTIONS OF AMINO RADICAL PRODUCTS	17
DEPENDENCE OF INHIBITION PERIODS ON $(AH)_o$	20
EXPERIMENTAL	23
REFERENCES	24
III. MECHANISM OF 4,4'-METHYLENEBIS(2,6-DI-TERT-BUTYLPHENOL) INHIBITED AUTOXIDATIONS AT 180 TO 220°C, By R. K. Jensen, S. Korcek, L. R. Mahoney, and M. Zinbo	25
INHIBITION PERIOD STUDIES	25
REACTANT AND PRODUCT ANALYSES	28
PRELIMINARY KINETIC AND MECHANISTIC ANALYSES	34
MAXIMUM INHIBITION PERIODS	41
EXPERIMENTAL	43
REFERENCES	45
IV. EFFECTS OF STRUCTURE ON THE THERMOXIDATIVE STABILITY OF SYNTHETIC ESTER LUBRICANTS: THEORY AND PREDICTIVE METHOD DEVELOPMENT, By L. R. Mahoney, S. Korcek, and J. M. Norbeck	46
BACKGROUND	46
DERIVATION OF KINETIC EQUATIONS	48
n-C ₅ --n-C ₈ ESTERS OF PENTAERYTHRITOL	53
FUTURE WORK	53
REFERENCES	58
APPENDIX 1: DERIVATION OF KINETIC EXPRESSIONS	59
APPENDIX 2: NUMERICAL EVALUATION OF THE RATIO OF INTEGRALS IN EQ. VIII	64
ACKNOWLEDGMENTS	67

TABLE OF CONTENTS (CONT.)

ATTACHMENT I:

KINETICS AND MECHANISM OF THE AUTOXIDATION OF PENTAERYTRITYL TETRAHEPTANOATE AT 180 TO 220°C, by E. J. Hamilton, Jr. S. Korcek, L. R. Mahoney, and M. Zinbo, Int. J. Chem. Kinet., in press

ATTACHMENT II:

LUBRICANT DEGRADATION AND WEAR. IV. THE EFFECT OF OXIDATION ON THE WEAR BEHAVIOR OF PENTAERYTRITYL TETRAHEPTANOATE, by P. A. Willermet, L. R. Mahoney, and S. K. Kandah, to be presented at the 1980 ASME/ASLE Lubrication Conference, San Francisco, California, August 18 - 21, 1980.

I INTRODUCTION

This is the final report on the work carried out during the period April 1, 1976 to September 30, 1979 under the Air Force Office of Scientific Research - Ford Contract, F44620-76-C-0097, entitled "Time - Temperature Studies of High Temperature Deterioration Phenomena in Lubricant Systems: Synthetic Ester Lubricants."

Preprints of technical papers describing the results of autoxidation and of wear studies on pentaerythrityl tetraheptanoate, PETH, are Attachments I and II of the report. The first paper entitled "Kinetics and Mechanism of the Autoxidation of Pentaerythrityl Tetraheptanoate at 180 to 220°C" by E. J. Hamilton, Jr., S. Korcek, L. R. Mahoney, and M. Zinbo has been accepted for publication in the International Journal of Chemical Kinetics. The second paper entitled "Lubricant Degradation and Wear. IV. The Effect of Oxidation on the Wear Behavior of Pentaerythrityl Tetraheptanoate" by P. A. Willermet, L. R. Mahoney, and S. Kandah will be presented at the 1980 ASME/ASLE Lubrication Conference in San Francisco, California.

The work on the kinetics and mechanism of inhibited autoxidation of synthetic ester lubricants is described in sections II - IV. It is anticipated that following the completion of a limited number of additional experiments each of these sections will be prepared and submitted for publication in technical journals. The respective authors of these papers are indicated at the beginning of each section.

II KINETICS AND MECHANISM OF 4,4'-DIOCTYLDIPHENYLAMINE INHIBITED AUTOXIDATION AT 160 TO 220°C

(R. K. Jensen, S. Korcek, L. R. Mahoney, L. A. Scheich, and M. Zinbo)

In the present section we report the results of our work on the inhibition of the autoxidation of PETH and of n-hexadecane by 4,4'-dioctyldiphenylamine. To determine the complex rate expressions describing the kinetics in these systems studies were carried out at very low (less than 5×10^{-5} M) and at very high (up to 5×10^{-3} M) concentrations of the antioxidant. The stirred flow reactor system was utilized for the low concentration experiments while the high concentration experiments were carried out in a batch reactor.

A reaction mechanism is proposed which accounts for the results at both low and high concentrations of the amine. Although various novel features of the proposed reaction mechanism receive support from theoretical considerations and from the results of recent work from other laboratories the detailed elucidation of the mechanism requires additional work.

LOW CONCENTRATIONS OF AMINE - Table I summarizes the results of amine, hydroperoxide, and acid analyses of samples from stirred flow reactor experiments in PETH at 180°C and in n-hexadecane at 160 and 180°C.

TABLE 1
AUTOXIDATION OF PETH AND N-HEXADECANE
INHIBITED BY 4,4'-DIOCTYLDIPHENYLAMINE
(Stirred Flow Reactor Experiments)

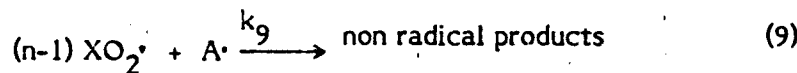
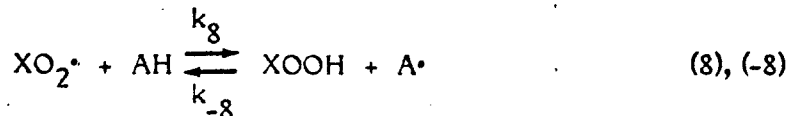
Temp (°C)	τ (s)	Run Number	(AH) ₀	(AH) _τ	(-OOH) ^a	(-COOH)
				$10^4(X)$, M ^c		
n-hexadecane						
160	824	212	0.37(2) ⁸	0.29(1) ⁴	53.0	8.2
	991	213	0.37(2) ⁸	0.24(2) ⁴	107	19.1
	1096	214	0.37(2) ⁸	0.23(2) ⁵	146	28.2
	858	208	0.65(2) ¹⁰	0.56(1) ⁴	38.3	6.7
	906	209	0.65(2) ¹⁰	0.54(1) ³	44.2	8.2
	950	210	0.65(2) ¹⁰	0.51(1) ⁴	70.3	12.2
	1061	211	0.65(2) ¹⁰	0.46(1) ⁴	108	18.9
180	138	204	0.70(0) ²	0.63	22.3	2.4
	154	203	0.70(0) ²	0.55(1) ²	38.9	5.7
	177	202	0.70(0) ²	0.45(2) ²	71.1	11.2
	223	201	2.24(3) ²	1.90 ^b	21.9	3.8
	232	200	2.24(3) ²	1.85 ^b	41.9	7.7
	253	199	2.24(3) ²	1.60(5) ²	60.4	15.0
	277	198	2.24(3) ²	1.56(4) ²	154	41.1
	303	197	2.24(3) ²	1.18(1) ²	202	60.0
	306	196	3.94(7) ²	3.46	30.9	
	320	194	3.94(7) ²	3.40 ^b		
	371	195	3.94(7) ²	2.09(6) ²	219	90.0
	343	193	4.35(3) ²	3.00	107	
	363	192	4.35(3) ²	2.61(6) ²	195	56.6
	382	191	4.35(3) ²	2.19	342	129
PETH						
180	340	71	0.82(4) ³	0.56(3) ²	34.5	11.8
	380	70	0.82(4) ³	0.63	31.5	10.8
	402	72	0.82(4) ³	0.42	78.9	32.0
	832	75	2.49(5) ⁵	1.88(1) ²	54.0	20.9
	1006	76	4.07(3) ⁷	3.31(3) ³	44.5	18.0(8) ²

^a The value of (-OOH) in PETH includes hydrogen peroxide but in n-hexadecane it has been subtracted out. The correction amounts to about 5%.

^b Values from GLC on reduced samples.

^c The uncertainties of measured values are indicated in parenthesis. The values listed are averages obtained by independent analyses; their number is given by a number superscript. For example, 0.37(2)⁸ denotes that eight measured values lay in the range 0.37 ± 0.02 .

The results are consistent with the reaction sequence (1) - (7) proposed earlier for the chain autoxidation of PETH⁽¹⁾ and n-hexadecane⁽²⁾ (cf. Figure 2 in Section IV) and the additional termination reactions of the amine, AH,



In contrast to conventional inhibited autoxidation reaction mechanisms the transfer reactions of amine hydrogen to peroxy radicals, reaction (8), are reversible. As a consequence of this reversibility the rates of product formation are suppressed since the total concentration of chain carrying radicals decreases via reaction (9). However, the distribution of various products is not altered by the presence of the amine.¹ This unique behavior for the amine inhibited systems is clearly demonstrated by the results in Figure 1. In the figure it is shown that the ratios of yields of various products of n-hexadecane to monohydroperoxide products are not altered in the presence of low concentrations of added amine.

¹ If reaction (8) was not reversible the distribution of products would be strongly dependent on amine concentration: at higher amine concentration the ratio of difunctional to monofunctional products would be very low compared to the uninhibited autoxidation.

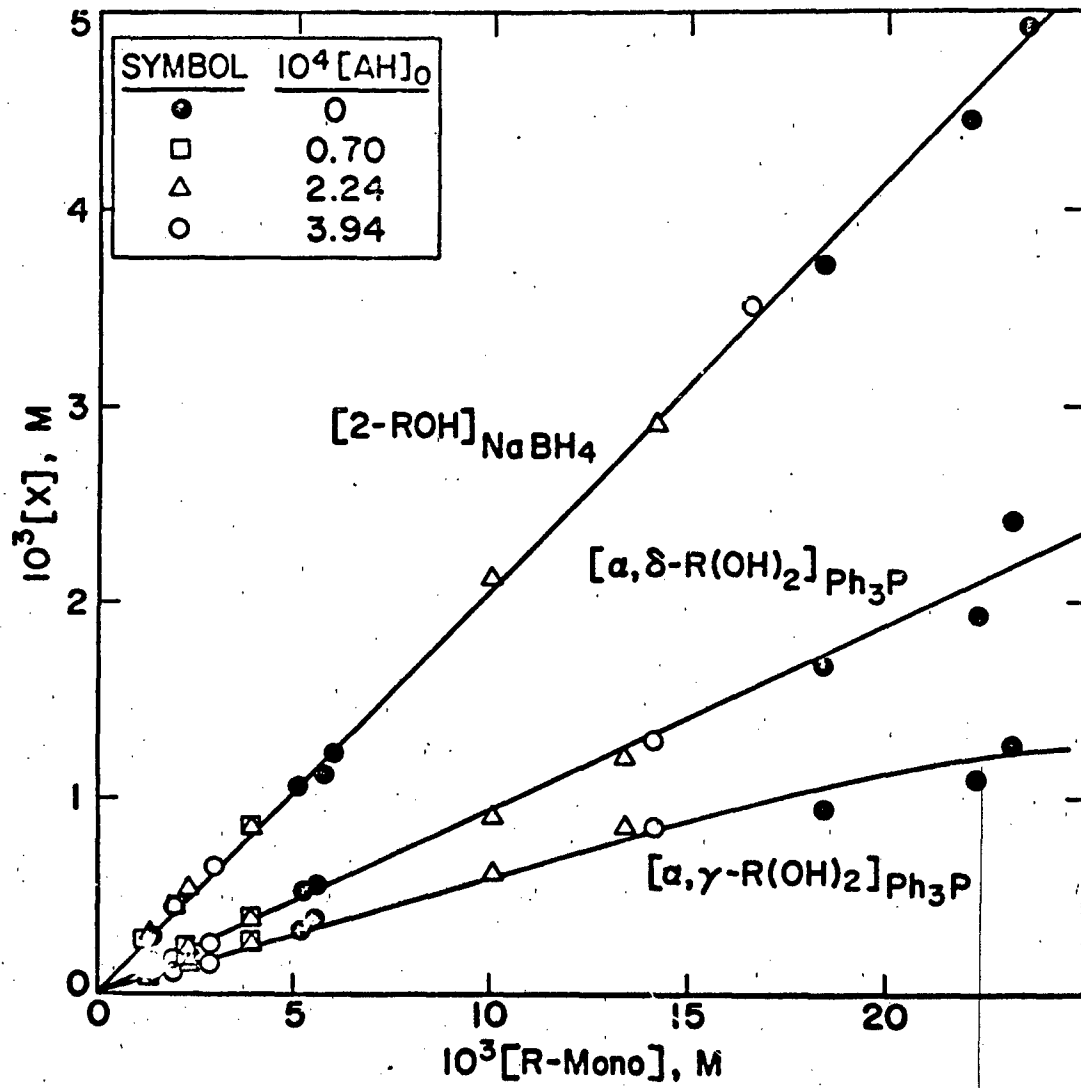


Figure 1 The yields of 2-hexadecanol and α, γ - and α, δ -hexadecanediols vs. the corresponding yields of monofunctional products in the NaBH_4 - and Ph_3P -reduced samples from the inhibited and noninhibited autoxidation of n-hexadecane at 180°C .

Values of $\frac{n k_9 K_8}{2 k_6}$ and n may be obtained from the following kinetic analyses. Utilizing the usual steady state approximations for concentrations of radicals,

$$2 k_1 (-\text{OOH}) = 2 k_6 (\text{XO}_2^{\cdot})^2 + n k_9 (\text{A}^{\cdot}) (\text{XO}_2^{\cdot}) \quad (\text{I})$$

where

$$(\text{XO}_2^{\cdot}) = (\text{RO}_2^{\cdot}) + (\text{HOORO}_2^{\cdot}) + (\text{O} = \text{RO}_2^{\cdot}).$$

When $k_8 (-\text{OOH}) \gg k_9 (\text{XO}_2^{\cdot})$,

$$(\text{A}^{\cdot}) = \frac{k_8 (\text{AH}) (\text{XO}_2^{\cdot})}{(-\text{OOH})} \quad (\text{II})$$

where

$$(-\text{OOH}) = (\text{ROOH}) + 2 (\text{R}(\text{OOH})_2) + (\text{O} = \text{ROOH})$$

Combining (I) and (II) yields,

$$(\text{XO}_2^{\cdot}) = \left[\frac{k_1 (-\text{OOH})}{k_6} \right]^{\frac{1}{2}} \frac{1}{\left[1 + \frac{n k_9 K_8}{2 k_6} \frac{(\text{AH})}{(-\text{OOH})} \right]^{\frac{1}{2}}} \quad (\text{III})$$

In earlier work⁽¹⁾ it was shown that reaction scheme (1) - (7) yields equation (IV) for the sum of the instantaneous rates of formation of hydroperoxides and acids,

$$\begin{aligned}
 \frac{d(-\text{OOH})}{dt} + \frac{d(-\text{COOH})}{dt} &= k_3(\text{RH}) \left[\frac{\frac{k_{4-\alpha, \gamma}}{k_3(\text{RH})} \left[2 + \frac{k_{4-\alpha, \gamma}^*}{k_3(\text{RH})} \right] + \frac{k_{4-\alpha, \delta}}{k_3(\text{RH})} \left[2 + \frac{k_{4-\alpha, \delta}^*}{k_3(\text{RH})} \right]}{1 + \frac{k_{4-\alpha, \gamma}^*}{k_3(\text{RH})} + \frac{k_{4-\alpha, \delta}^*}{k_3(\text{RH})}} \right. \\
 &\quad \left. - \frac{\frac{k_{4-\alpha, \gamma}}{k_3(\text{RH})} + \frac{k_{4-\alpha, \delta}}{k_3(\text{RH})}}{1 + \frac{k_{4-\alpha, \gamma}^*}{k_3(\text{RH})} + \frac{k_{4-\alpha, \delta}^*}{k_3(\text{RH})}} \right] (\text{XO}_2^*) \\
 &= \left[\frac{k_6}{k_1} \right]^{\frac{1}{2}} \eta (\text{XO}_2^*) \quad (\text{IV})
 \end{aligned}$$

Combining (III) and (IV) and squaring yields

$$\left[\frac{d(-\text{OOH})}{dt} + \frac{d(-\text{COOH})}{dt} \right]^2 = \frac{\eta^2 (-\text{OOH})}{1 + \frac{n k_9 K_8}{2 k_6} \frac{(\text{AH})}{(-\text{OOH})}} \quad (\text{V})$$

In Figures 2 and 3 are plots of $(-\text{OOH}) / ((d(-\text{OOH})/dt) + (d(-\text{COOH})/dt))^2$ versus $(\text{AH}) / (-\text{OOH})$ for the PETH system at 180°C and the n-hexadecane system at 160 and 180°C . The plot is linear for PETH but shows significant curvature for n-hexadecane. From the slope of the straight line for PETH a value of $n k_9 K_8 / 2 k_6$ equal to 840 is obtained. The strong curvature in the n-hexadecane plots suggests that either reactions (1) - (8) are not applicable to the system or that additional reactions of amino radicals occur in the system and lead to a systematic lowering of n with increasing concentration of amine, vide infra.

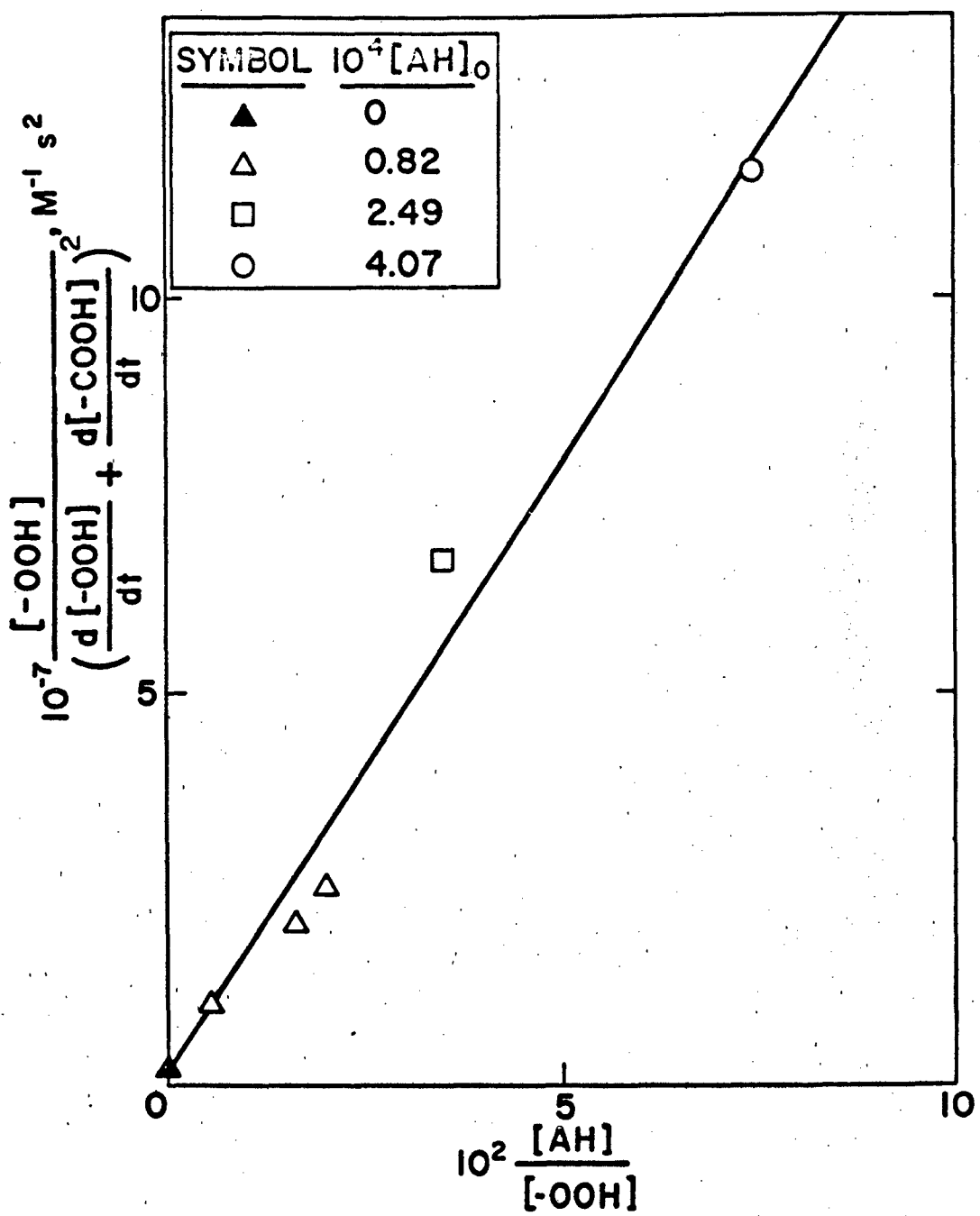


Figure 2 Plot of $(-OOH)/\left((d(-OOH)/dt) + (d(-COOH)/dt) \right)^2$ vs. $(AH)/(-OOH)$ for the inhibited autoxidation of PETH at $180^\circ C$.

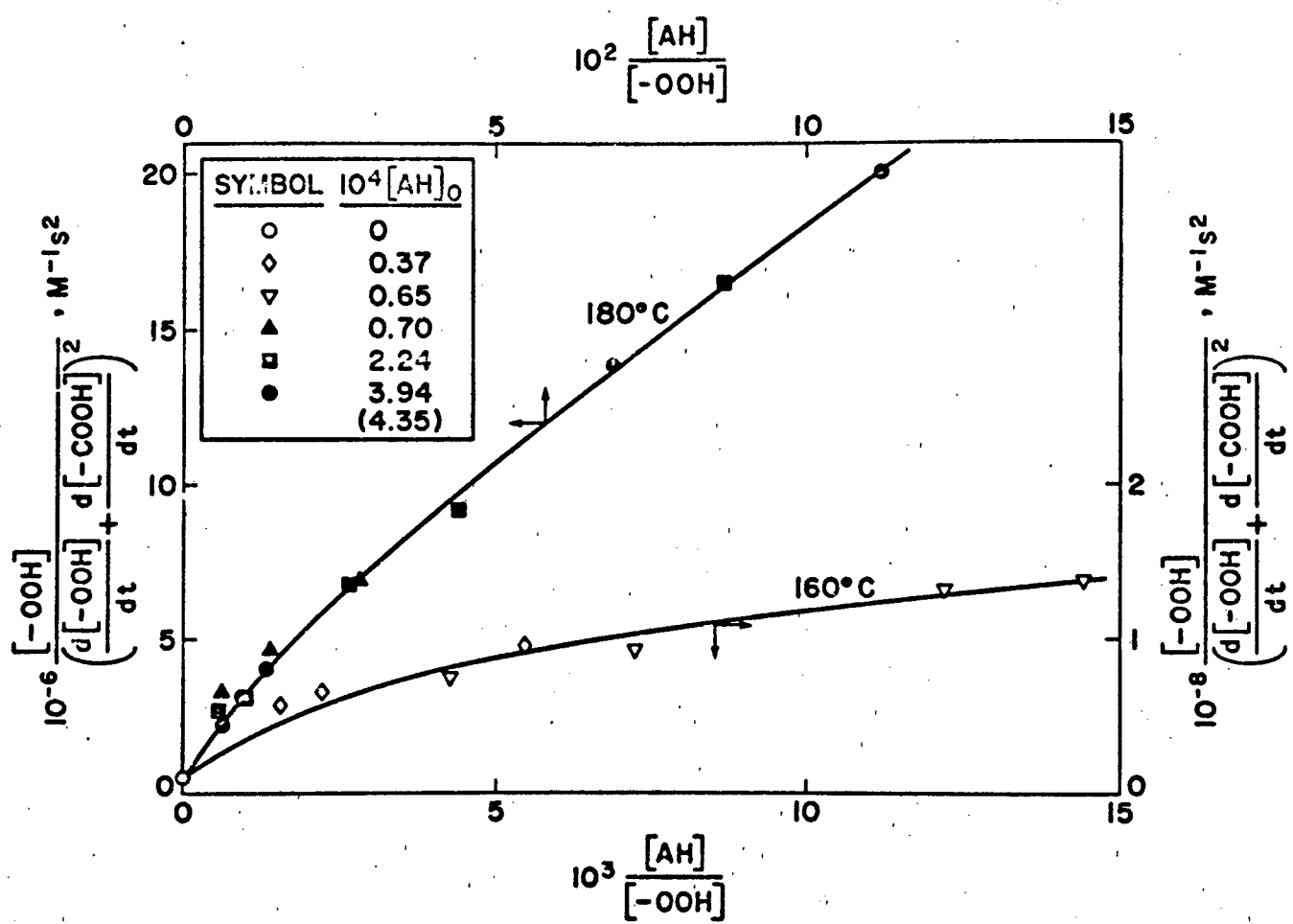


Figure 3 Plots of $(-OOH)/((d(-OOH)/dt) + (d(-OOH)/dt))^2$ vs. $(AH)/(-OOH)$ for the inhibited autoxidation of n-hexadecane at 160 and $180^\circ C$.

Values of n are estimated from the instantaneous rates of consumption of amine which are given by the following equation:

$$-\frac{d(AH)}{dt} = k_9 (XO_2^{\cdot}) (A^{\cdot}) \quad (VI)$$

Combining eq. (II), (III), and (VI) yields

$$-\frac{d(AH)}{dt} = \frac{k_1 k_9 K_8}{k_6} \left[\frac{(AH)}{1 + \frac{n k_9 K_8}{2 k_6} \frac{(AH)}{(-OOH)}} \right] \quad (VII)$$

and after rearrangement

$$\frac{1}{-d \ln(AH)/dt} = \frac{k_6}{k_1 k_9 K_8} + \frac{n}{2 k_1} \frac{(AH)}{(-OOH)} \quad (VIII)$$

In Figures 4 and 5 are plots of $1/(-d \ln(AH)/dt)$ versus $(AH)/(-OOH)$. As in the case of eq. (V), the PETH system obeys eq. (VIII) while the n-hexadecane system shows strong curvature in the plots. The slope for the PETH system is equal to 6×10^4 s. Utilizing this value and a value of k_1 for PETH equal to $1.6 \times 10^{-4} \text{ s}^{-1}$ ⁽¹⁾ yields a value of n equal to 19. From initial slopes in n-hexadecane values of n are equal to 13 (55) at 180 (160)⁰C. These large values of n do not appear to be artifacts generated by neglecting additional reactions of amino radicals^{(3), 2} such as

² Reaction (10) would lead to regeneration of amine and thus would result in the observation of abnormally large n values.

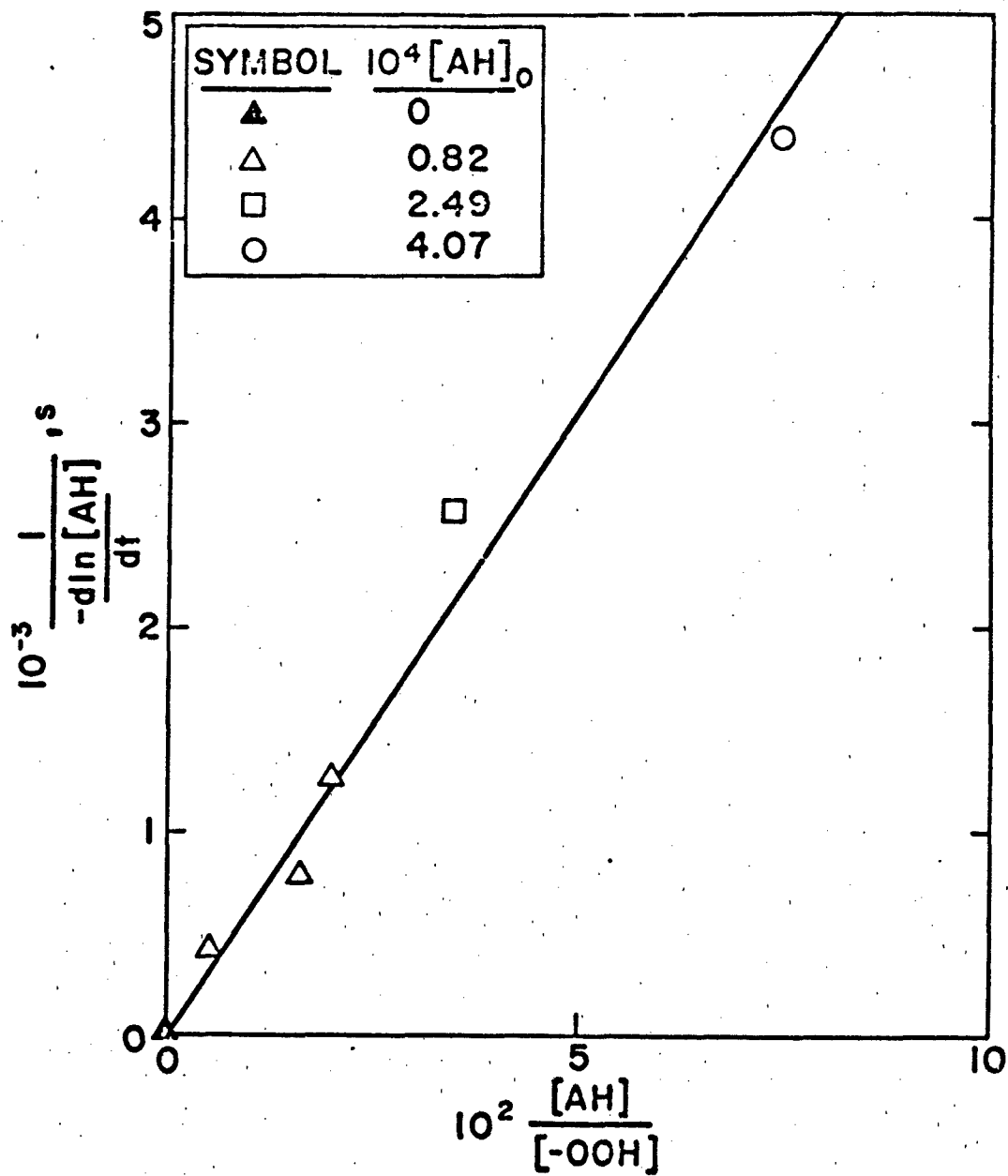


Figure 4 Plot of $1/(-d \ln (AH)/dt)$ vs. $(AH)/(-OOH)$ for the inhibited autoxidation of PETH at 182°C .

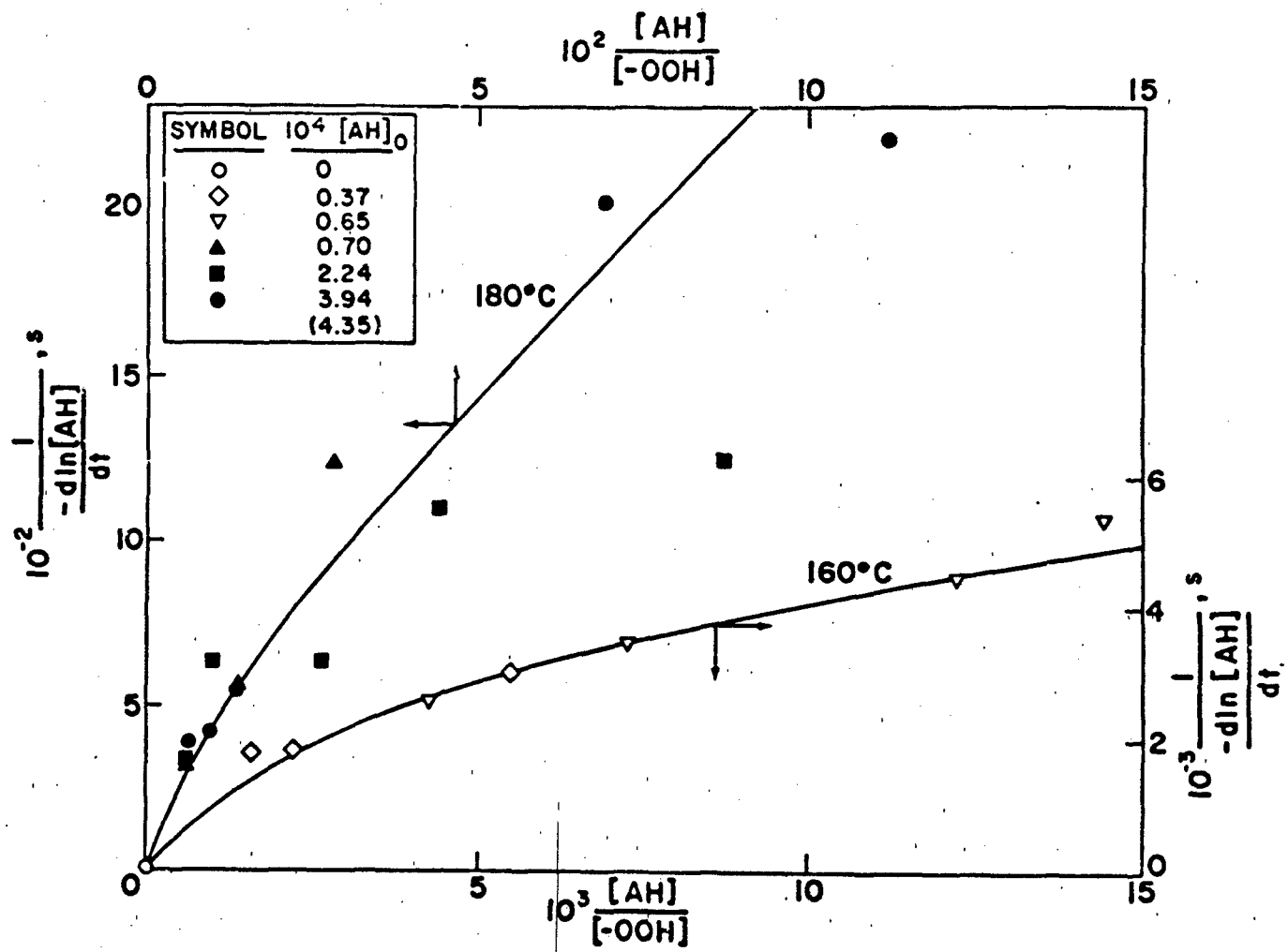


Figure 5 Plots of $1/(-d \ln (AH)/dt)$ vs. $(AH)/(-OOH)$ for the inhibited autoxidation of n-hexadecane at 160 and 180 °C.



since the high concentration experiments described below yield similarly high values of n .

HIGH CONCENTRATIONS OF AMINE - Results from batch reactor studies of hydroperoxide formation and amine consumption at high concentrations of amine in the PETH autoxidation at 180 to 220°C are shown in Figures 6 to 8.

At high concentrations of amine and extended reaction times the contribution of unstable α, γ -hydroperoxyketone products to hydroperoxide titer is negligible and $(nk_9K_8/2k_6)((AH)/(-OOH)) \gg 1$. The rate of formation of hydroperoxide groups is then given by the equation

$$\frac{d(-OOH)}{dt} = \frac{(n-\omega)(-OOH)^{\frac{1}{2}}}{\left[\frac{n k_9 K_8}{2 k_6} \frac{(AH)}{(-OOH)} \right]^{\frac{1}{2}}} + a \left[\frac{-d(AH)}{dt} \right] - k_1 (-OOH) \quad (IX)$$

where n and ω are composite rate parameters for the PETH system reported earlier⁽¹⁾ and a is equal to the number of hydroperoxide groups formed by the reactions of a molecule of amine and its reaction products. Since

$$2k_1(-OOH)_t = -\frac{n d(AH)}{dt} \quad (X)$$

$$\frac{d(-OOH)}{dt} = \left[a - \frac{n}{2} \right] \left[-\frac{d(AH)}{dt} \right] + \frac{n}{2k_1} \frac{(n-\omega)}{\left[\frac{n k_9 K_8}{2 k_6} \right]^{\frac{1}{2}}} \frac{1}{(AH)^{\frac{1}{2}}} \left[-\frac{d(AH)}{dt} \right] \quad (XI)$$

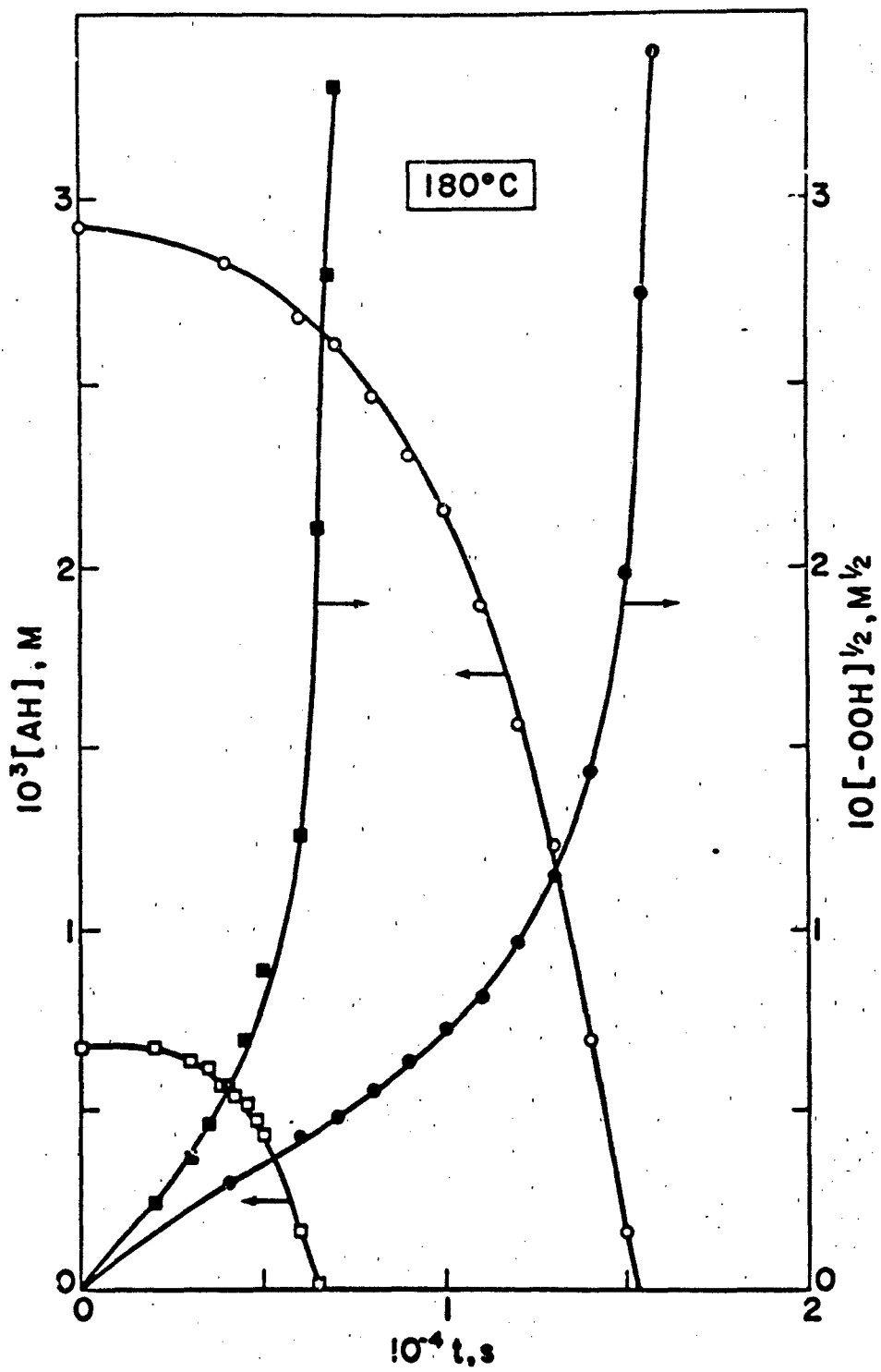


Figure 6 Hydroperoxide formation and amine consumption in the inhibited autoxidation of PETH at 180°C.

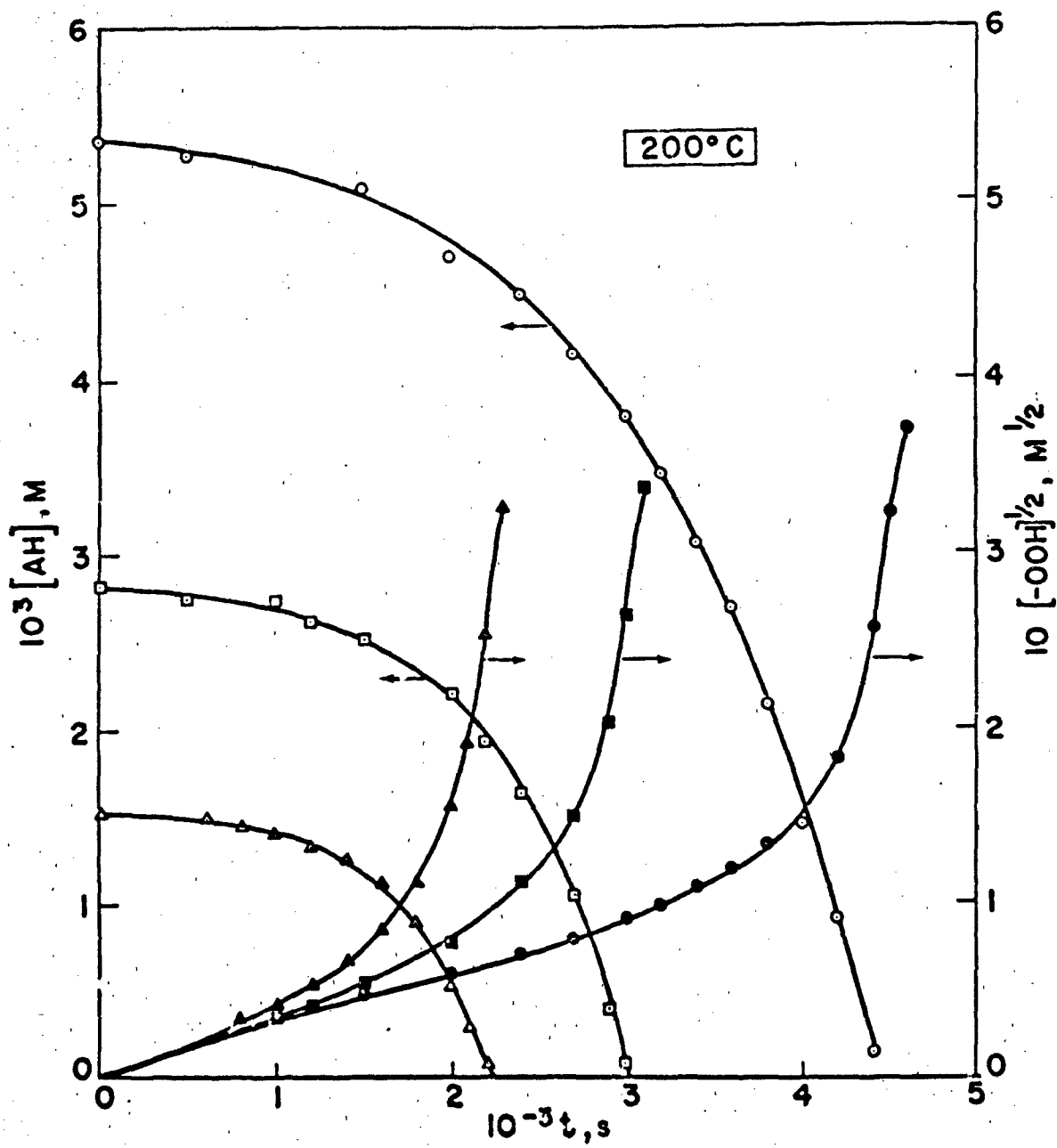


Figure 7 Hydroperoxide formation and amine consumption in the inhibited autoxidation of PETH at 200°C.

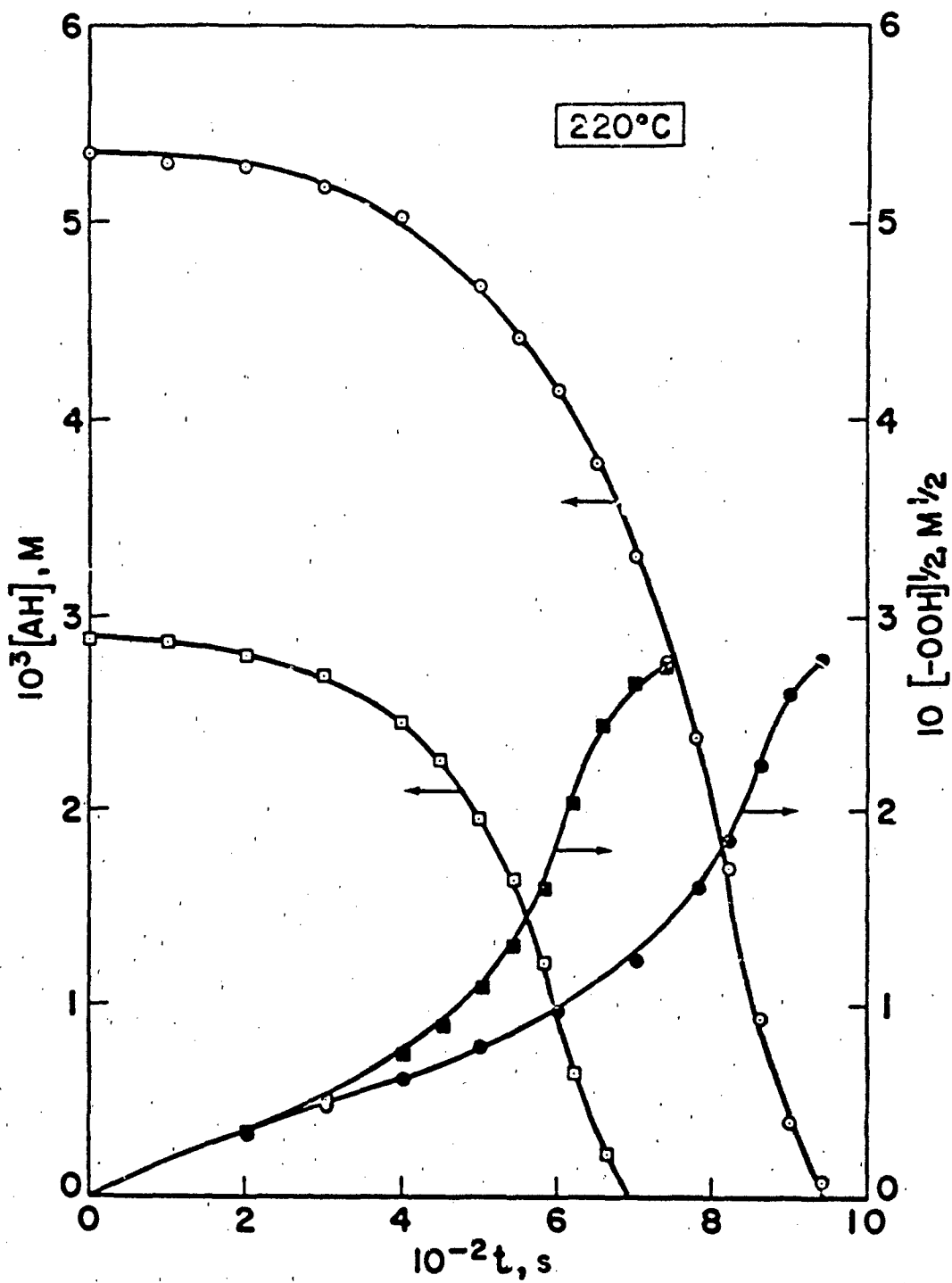


Figure 8 Hydroperoxide formation and amine consumption in the inhibited autoxidation of PETH at 220°C.

Integration and rearrangement of (XI) leads to

$$\begin{aligned}\frac{(-\text{OOH})_t}{(\text{AH})_0 - (\text{AH})_t} &= \left[a - \frac{n}{2} \right] + \frac{n}{2k_1} \frac{\frac{(n - \omega)}{n k_9 K_8} \frac{(\text{AH})_0^{1/2} - (\text{AH})_t^{1/2}}{2k_6}}{(\text{AH})_0 - (\text{AH})_t} \\ &= m + p \frac{(\text{AH})_0^{1/2} - (\text{AH})_t^{1/2}}{(\text{AH})_0 - (\text{AH})_t} \quad (\text{XII})\end{aligned}$$

A master plot of eq. (XII) for all of the PETH data at high concentrations of amine is given in Figure 9. The dashed line in the figure is calculated from eq. (XII) using the 180°C low concentration amine experimental values.

From the reasonably good agreement we conclude that within the experimental uncertainties the rate equation derived from reactions (1) - (9) accurately describes our results over a hundred fold range in amine concentration. Most importantly the values of n appear to be very large, greatly exceeding the normally small integral values shown by conventional antioxidant systems.

In the following section we examine in some detail the source of these large values of n.

VALUES OF n AND REACTIONS OF AMINO RADICAL PRODUCTS - The very large values of n derived from the kinetic analyses of the low amine

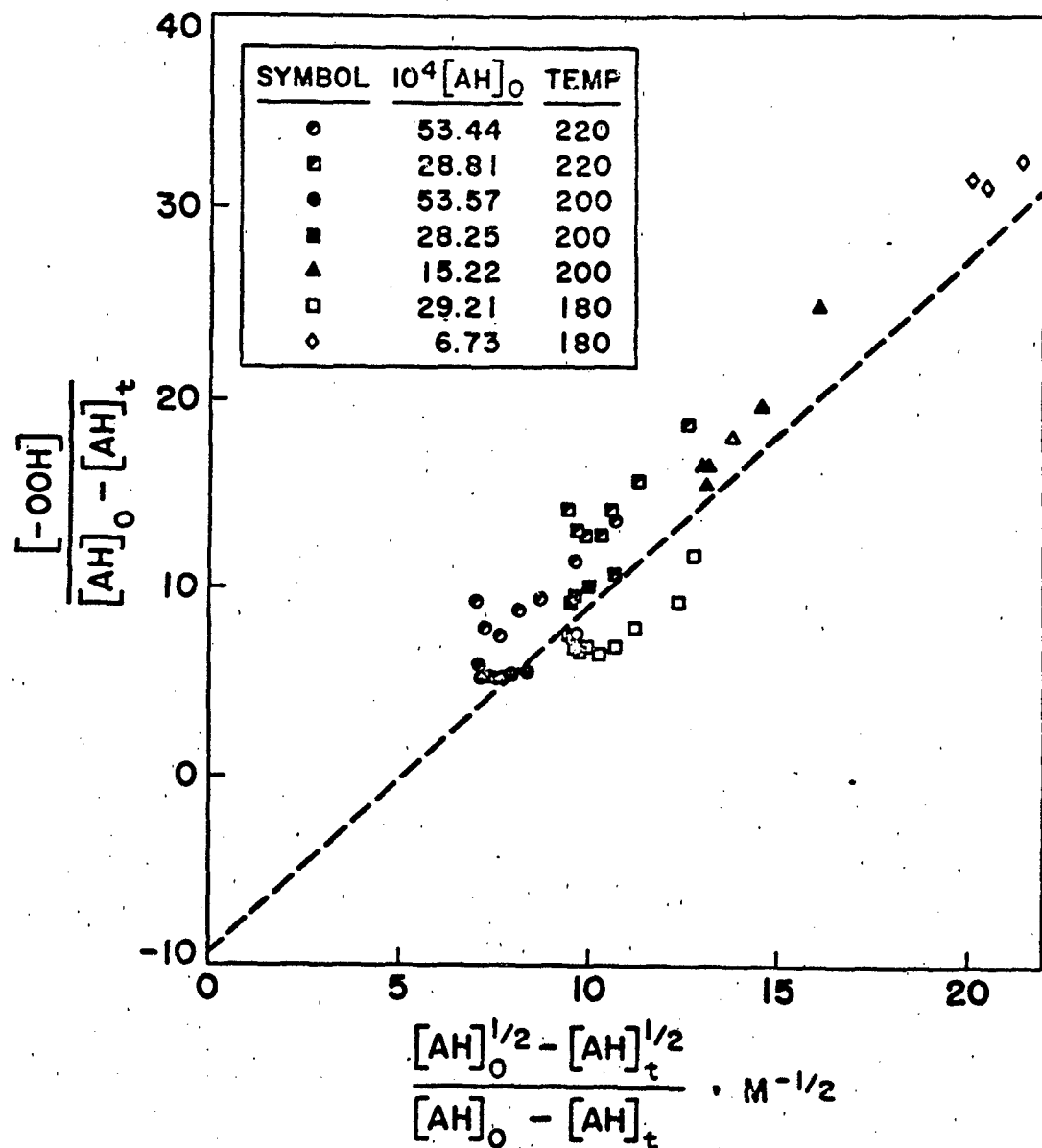
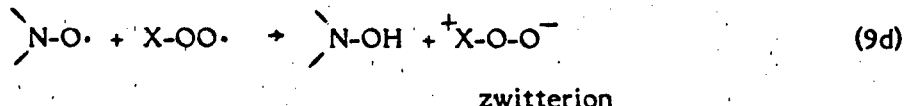
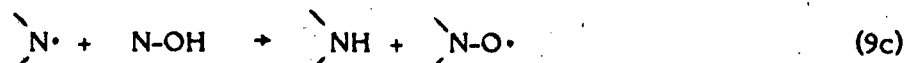
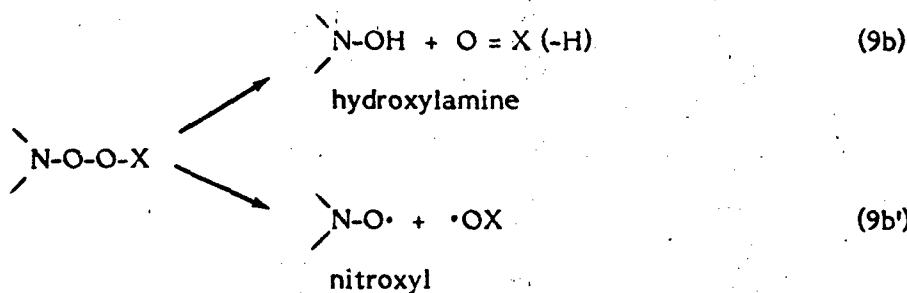
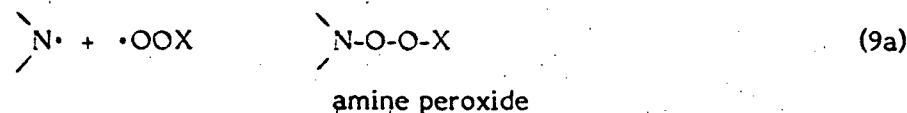


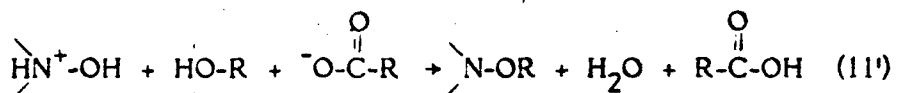
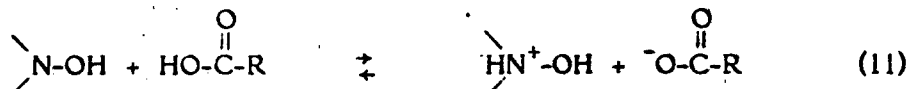
Figure 9 A plot of eq. (XII) for the inhibited autoxidation of PETH at high concentrations of the amine at 180, 200, and 220°C.

concentration results and confirmed by the amine consumption and hydroperoxide formation data in the high concentration experiments suggest the occurrence of a complex series of reactions involving amino radical products. The following is a plausible sequence which accommodates the results:



Recent work by Howard et al.⁽⁴⁾ shows that reactions (9b) and (9b') readily occur at low temperatures with model amine peroxide systems. At elevated temperatures these reactions should be very rapid. Reaction (9c) should be a facile reaction since it involves hydrogen atom transfer between heteroatoms and should be ca. 13 kcal/mole exothermic.⁽⁵⁾ The coupled reactions (9c) and

(9d) represent a cyclic inhibition process. The cycle could be interrupted by molecular reactions of the hydroxylamine intermediate. These reactions include



Reactions (11) and (11') would be very sensitive to the polarity of the autoxidizing media and to the activities of the reactants. The acid-base equilibrium reaction (11) should be much more favorable in n-hexadecane than in PETH and this factor could account for the lower n values observed in the hydrocarbon system at 180°C.

The intermediate nitroxyl radical has been detected in samples from our stirred flow reactor experiments by ESR. Further experiments in which this species is monitored as a function of reaction time could yield more information.

DEPENDENCE OF INHIBITION PERIODS ON $(\text{AH})_0$ - In Table II are summarized the values of the lengths of the inhibition periods, t_{inh} , estimated from the $(-\text{OOH})^{1/2}$ versus time plots, Figures 6 to 8, and the initial amine concentrations in the PETH system at 180 to 220°C and the n-hexadecane system at 180°C. In the final column of the table are given the values of $t_{\text{inh}}/(\text{AH})_0^{1/2}$. The nearly constant values of this ratio contrast with the nearly constant values of

TABLE II
 AUTOXIDATION OF PETH AND N-HEXADECANE
 INHIBITED BY 4,4'-DIOCTYLDIPHENYLAMINE
 (Inhibition Period Experiments)

Temp (C°)	$10^4 (AH)_0$ (M)	$10^{-3} t_{inh}$ (s)	$10^{-4} t_{inh}/(AH)_0^{1/2}$ (M ^{-1/2} s)
n-hexadecane			
180	5.25	1.55	6.7
	7.61	1.96	7.1
PETH			
180	6.73(9) ³	5.90	23
	29.2(3) ²	14.7	27
200	15.2(1) ²	1.96	5.0
	28.2(1) ²	2.73	5.1
	53.6(0) ²	4.22	5.8
220	28.8(1) ²	0.52	1.0
	53.4(2) ²	0.75	1.0

$t_{inh}/(AH)_0$ observed with many other antioxidant systems (cf. the bisphenol results described in the following section of this report). The source of this behavior is likely to be due to reversibility of reaction (8) with this antioxidant.

Combining eq. (X) with eq. (XII) yields

$$-\left[\frac{n}{2k_1}\right] \frac{1}{(AH)_0 - (AH)_t} \frac{d(AH)}{dt} = m + p \left[\frac{(AH)_0^{1/2} - (AH)_t^{1/2}}{(AH)_0 - (AH)_t} \right] \quad (XIII)$$

Rearrangement and integration of eq. (XIII) gives the time interval, $t_2 - t_1$, for the antioxidant concentration to decay from $(AH)_{t_1}$ to $(AH)_{t_2}$,

$$t_2 - t_1 = \frac{n}{2k_1} \int_{(AH)_{t_1}}^{(AH)_{t_2}} \frac{-d(AH)}{m \left[(AH)_0 - (AH)_t \right] + p \left[(AH)_0^{1/2} - (AH)_t^{1/2} \right]} \quad (XIV)$$

Although the length of the inhibition period may not be directly determined from this equation, cf. section IV of this report, the inverse half order term in (AH) will likely lead to observed half order dependence of t_{inh} on $(AH)_0$.

EXPERIMENTAL

MATERIALS - Pentaerythrityl tetraheptanoate, PETH, was purified by methods previously described to yield a PDP material.⁽¹⁾ Hexadecane was purified and deoxygenated as previously described.⁽²⁾

4,4'-Diptyldiphenylamine obtained from R.T. Vanderbilt Co. was recrystallized three times from methanol prior to use.

LIQUID CHROMATOGRAPHIC ANALYSIS - A Waters' HPLC system was used for analysis. The system consists of a Model 600 solvent delivery pump, a model U6K Septumless injector, a model R401 refractive index detector, and a model 440 dual micro UV-VIS detector.

HPLC analysis was accomplished by reverse-phase separation on a μ -Bondapak C₁₈ column obtained from Waters. The column was operated at room temperature in the isocratic mode using CH₃OH/H₂O/CH₃CN (2/5/93) modified with Waters' PIC B-7 reagent as the mobile phase. The 4,4'-diptyldiphenylamine was detected at 280 nm. A Hewlett Packard Model 3380A integrator was used for peak area determination.

ANALYSES OF OXIDATION PRODUCTS - Methods of analyses of individual n-hexadecane oxidation products and hydroperoxide and acid products were previously described.^(1, 2)

REFERENCES

1. E. J. Hamilton, Jr., S. Korcek, L. R. Mahoney, and M. Zinbo, Int. J. Chem. Kinet., in press; Attachment I.
2. R. K. Jensen, S. Korcek, L. R. Mahoney, and M. Zinbo, J. Am. Chem. Soc., 101, in press.
3. L. R. Mahoney, J. Am. Chem. Soc., 89, 1895 (1967).
4. J. A. Howard, National Research Council of Canada, personal communication, 1979.
5. L. R. Mahoney, G. D. Mendenhall, and K. U. Ingold, J. Am. Chem. Soc., 95, 8610 (1973).

III MECHANISM OF 4,4'-METHYLENEBIS (2,6-DI-TERT-BUTYLPHENOL) INHIBITED AUTOXIDATIONS AT 180 to 220°C

(R. K. Jensen, S. Korcek, L. R. Mahoney, and M. Zinbo)

In the following sections are summarized the results obtained from the study of inhibited oxidation of PETH and n-hexadecane in the presence of a phenolic antioxidant 4,4'-methylenebis(2,6-di-tert-butylphenol), BPH, at elevated temperatures. All of these studies were carried out in a batch reactor.¹

INHIBITION PERIOD STUDIES - Figure 1 shows the inhibitory effects of varying amounts of BPH on hydroperoxide formation in the autoxidation of PETH with molecular oxygen at 180°C. Results obtained from a systematic study of the lengths of the inhibition periods, t_{inh} , the time periods for which the chain oxidation is suppressed, in PETH and n-hexadecane as a function of initial antioxidant concentration and temperature are presented in Table I.²

¹ The batch reactor requires the use of only 35 to 40 ml of PETH from which a number of samples may be obtained as a function of time. This compares to the 100 or more ml required for a single stirred flow reactor experiment. The results obtained from these batch reactor experiments have provided, with the minimum consumption of purified PETH, considerable insight into the kinetic behavior of the antioxidant as a function of reaction temperature and concentration.

² Results of the inhibition period studies with pre-oxidized PETH are reported in reference (1), Attachment I of this report.

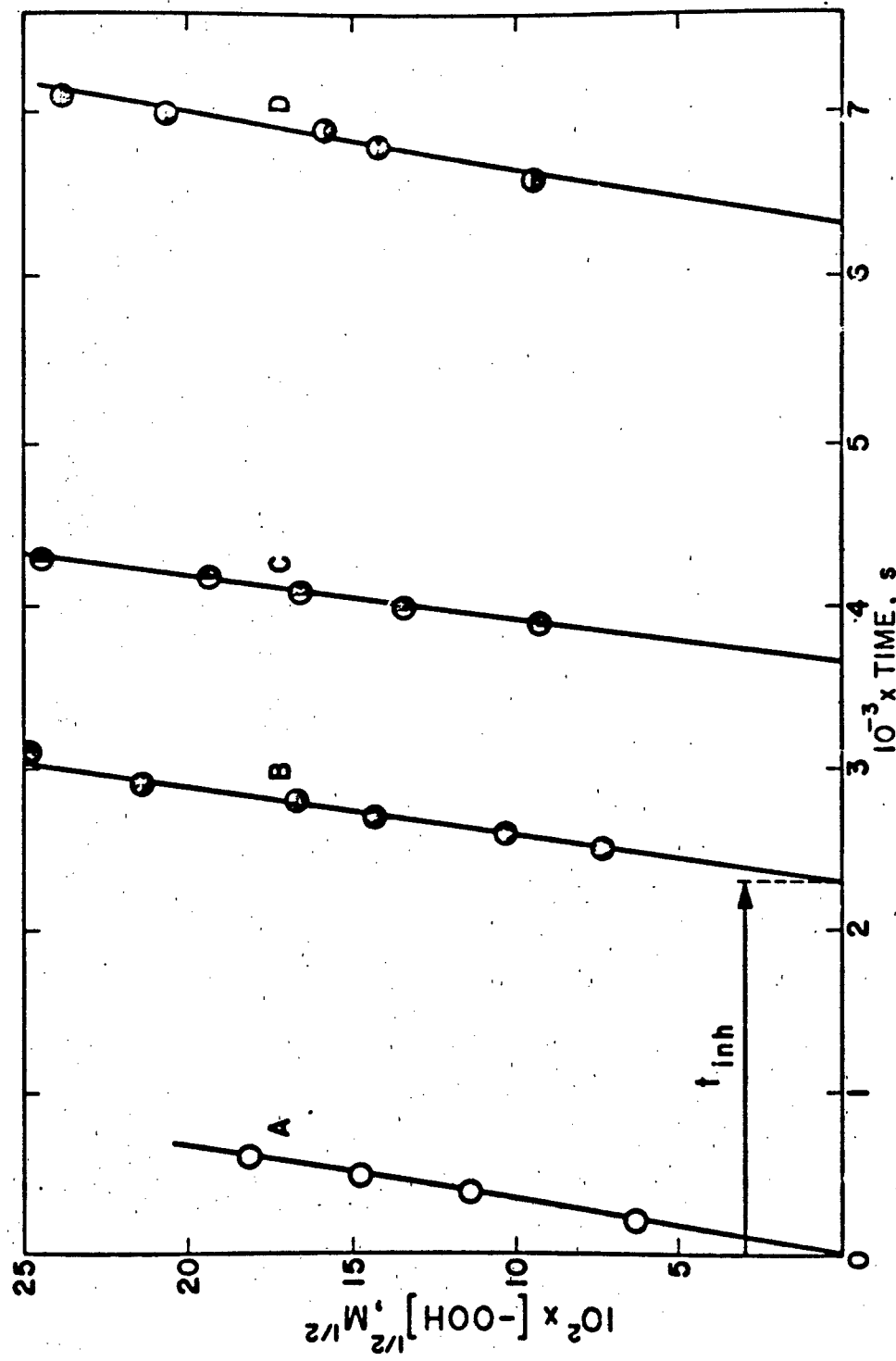


Figure 1 Inhibition period measurements for the BPH inhibited autoxidation of PETH at 180°C.
 Initial BPH concentrations: A - 0, B - 1.09×10^{-4} M, C - 1.86×10^{-4} M, D - 3.45×10^{-4} M.

TABLE I
AUTOXIDATION OF PETH AND N-HEXADECANE
INHIBITED BY BPH
(Inhibition Period Experiments)

Temp (°C)	$10^4 (BPH)_0$ (M)	$10^{-3} t_{inh}$ (s)	$10^{-6} t_{inh}/(BPH)_0^a$ ($M^{-1} s$)
n-hexadecane			
180	2.12	1.91	9.01
	7.96	7.36	9.25
	48.8	22.5	4.61
PETH			
180	1.09	2.23	20.9
	1.86	3.66	19.7
	3.45	6.28	18.2
200	5.3	1.33	2.51
	10.6	2.74	2.58
	15.7	3.48	2.22
220	39.1	1.24	0.32
	50.6	1.28	0.25
	76.2	1.64	0.22

^a From eq. (1) $t_{inh}/(BPH)_0 = n/R_i$

The results are best discussed in terms of the values of $(BPH)_0/t_{inh}$, where $(BPH)_0$ is initial concentration of antioxidant. In the simplest case the values of $(BPH)_0/t_{inh}$ are related to the rates of formation of the free radicals, R_i , in an oxidizing hydrocarbon by the expression, (2)

$$\frac{(BPH)_0}{t_{inh}} = \frac{R_i}{n} \quad (I)$$

where n , the stoichiometric factor, is equal to the total number of free radical species consumed in the complete reaction of one molecule of BPH and its reactive products,



At 60° and 120°C the n values for BPH are equal to 4.0. (3a, b) From the results in Table I we see that the values of R_i/n show small but systematic increase with increasing initial concentration of BPH. The magnitude of this effect was very pronounced at 220°C . This suggests that R_i increases and/or n decreases with increasing $(BPH)_0$.

REACTANT AND PRODUCT ANALYSES - Figure 2 shows the values of the ratios of the integrated signal intensities, $(BPH)_t/(BPH)_0$, determined by HPLC, as a function of time for a series of experiments in which varying concentrations of BPH were added to pure PETH and to n-hexadecane before exposure to oxygen at 180°C . At low initial concentrations of BPH, the decay curves are convex;

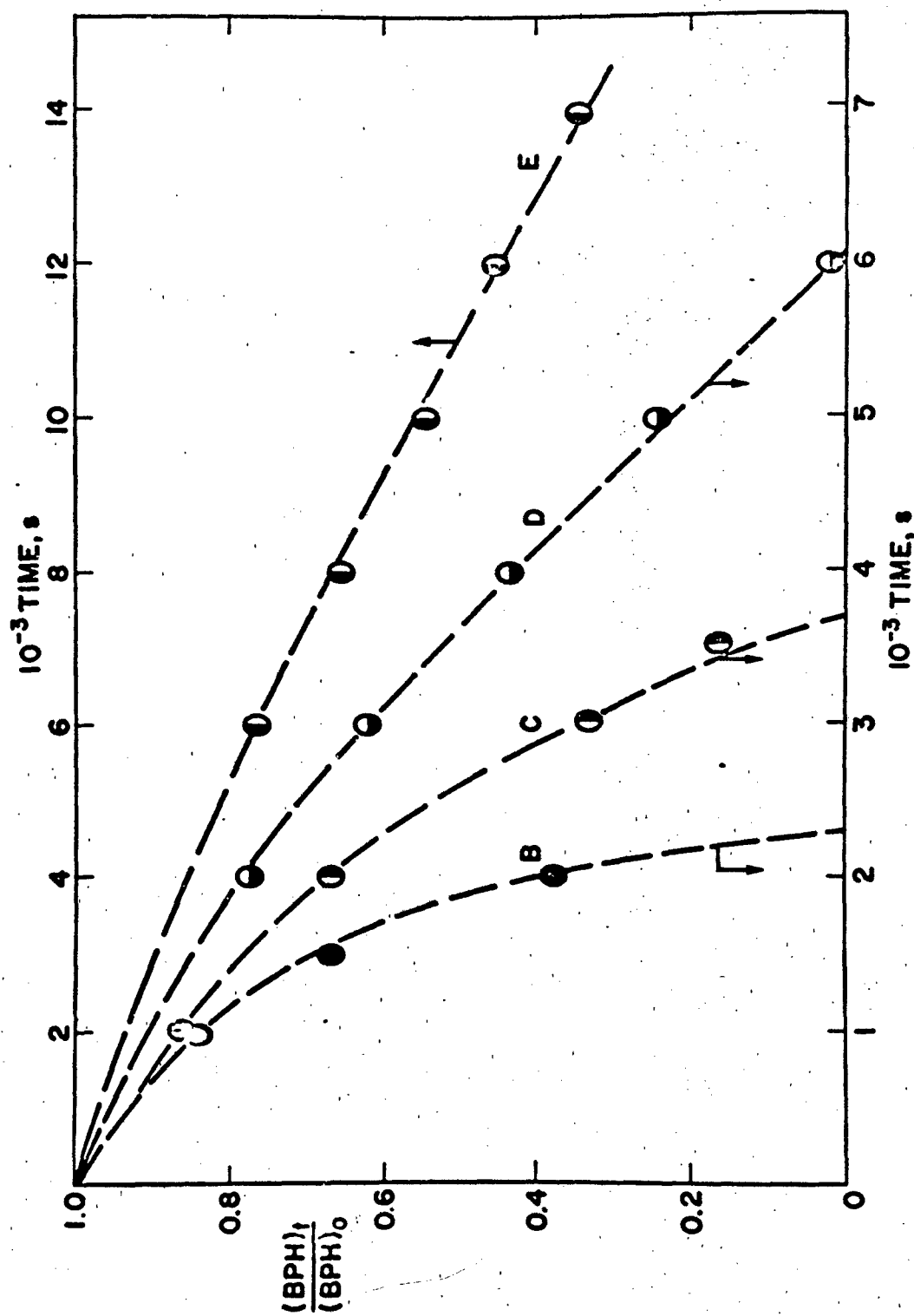


Figure 2 Ratios $(BPH)_t/(BPH)_0$ vs. time for the BPH inhibited autoxidation of PETH and n-hexadecane (curve E) at 180°C . Initial BPH concentrations: B - 1.09×10^{-4} M, C - 1.86×10^{-4} M, D - 3.45×10^{-4} M, E - 48.8×10^{-4} M.

curves B and C. As the initial concentration of BPH is increased, curves D and E, the convexity decreases and the slopes of $(BPH)_t/(BPH)_0$ versus time are approximately constant for each run within the range of the concentrations studied.

Plots of $(BPH)_t/(BPH)_0$ and $(BPH)_t/(BPH)_{18}$ versus time for pure PETH and a PETH system which had been reacted with oxygen to produce 60×10^{-4} M ROOH prior to the addition of PBH are shown in Figure 3. In contrast to the decay curves observed with pure PETRI, curve D, the decay curve for preoxidized PETH, curve F, is concave.

Concurrent with the decay of BPH is the formation of quinone methide, QM. Figure 4 shows plots of $(QM)_t/(BPH)_0$ versus time for the pure PETH (curves C and D), pure n-hexadecane (curve E), and preoxidized PETH (curve F) at 180°C . The nature of these curves is consistent with the view that the QM is an intermediate product of the antioxidant reactions of BPH. Further, the dependence of the maximum yield of QM as a function of the initial concentration of BPH suggests that QM is being consumed by radical species in competition with BPH, vide infra.

Besides BPH and QM peaks there is a number of unidentified peaks in the liquid chromatograms. Some peaks grow and then decay with reaction time, while others first appear toward the end of the inhibition period. In Figure 5 are shown plots of the ratios of integrated signal intensities for QM and two

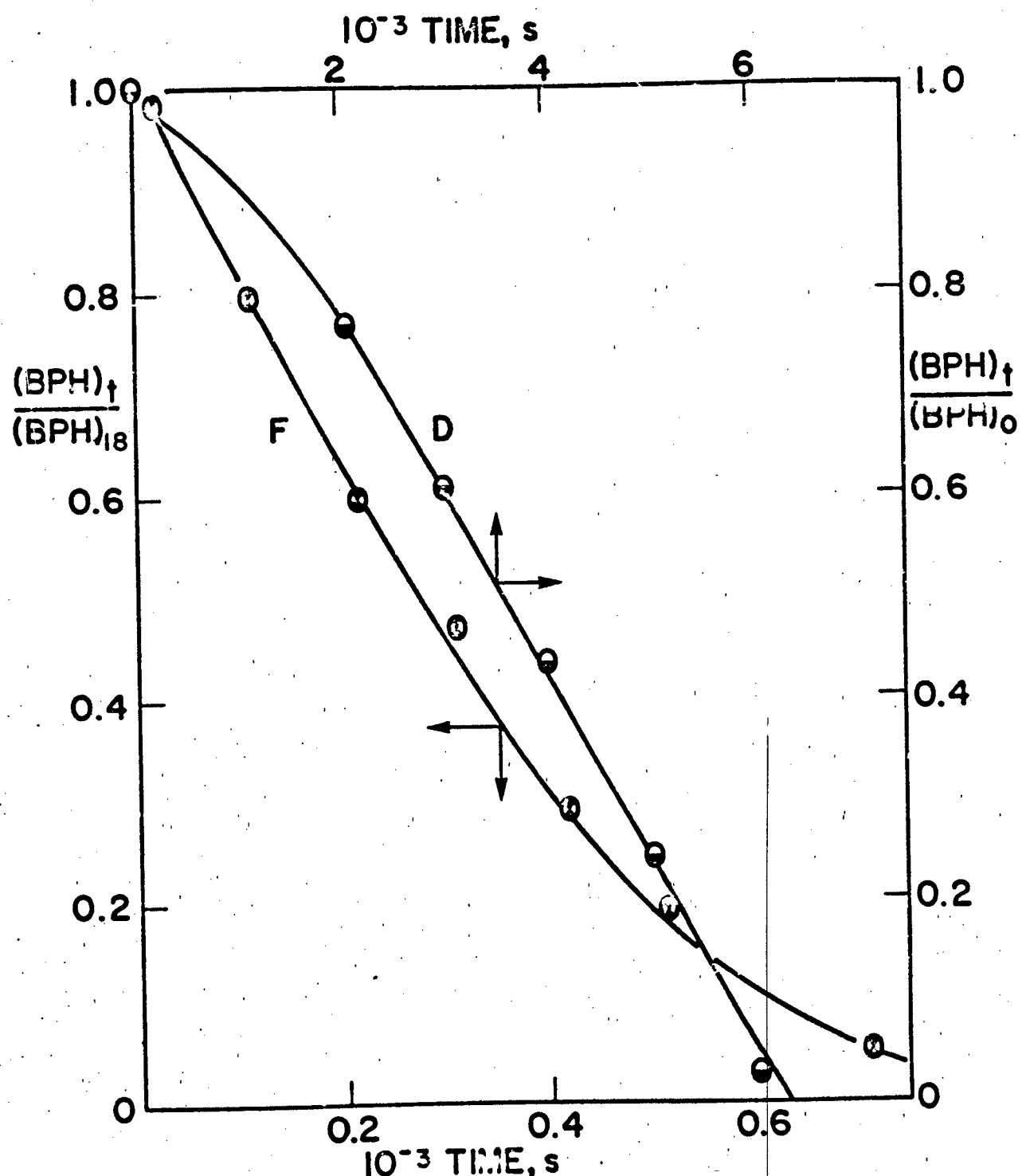


Figure 3 Ratios $(BPH)_t / (BPH)_0$ and $(BPH)_t / (BPH)_{18}$ vs. time for the BPH inhibited autoxidation of pure and preoxidized PETH at $180^\circ C$. Initial hydroperoxide concentrations: D - 0, F - 60×10^{-4} M. Initial BPH concentrations: D - 3.45×10^{-4} M, F - 7.2×10^{-4} M.

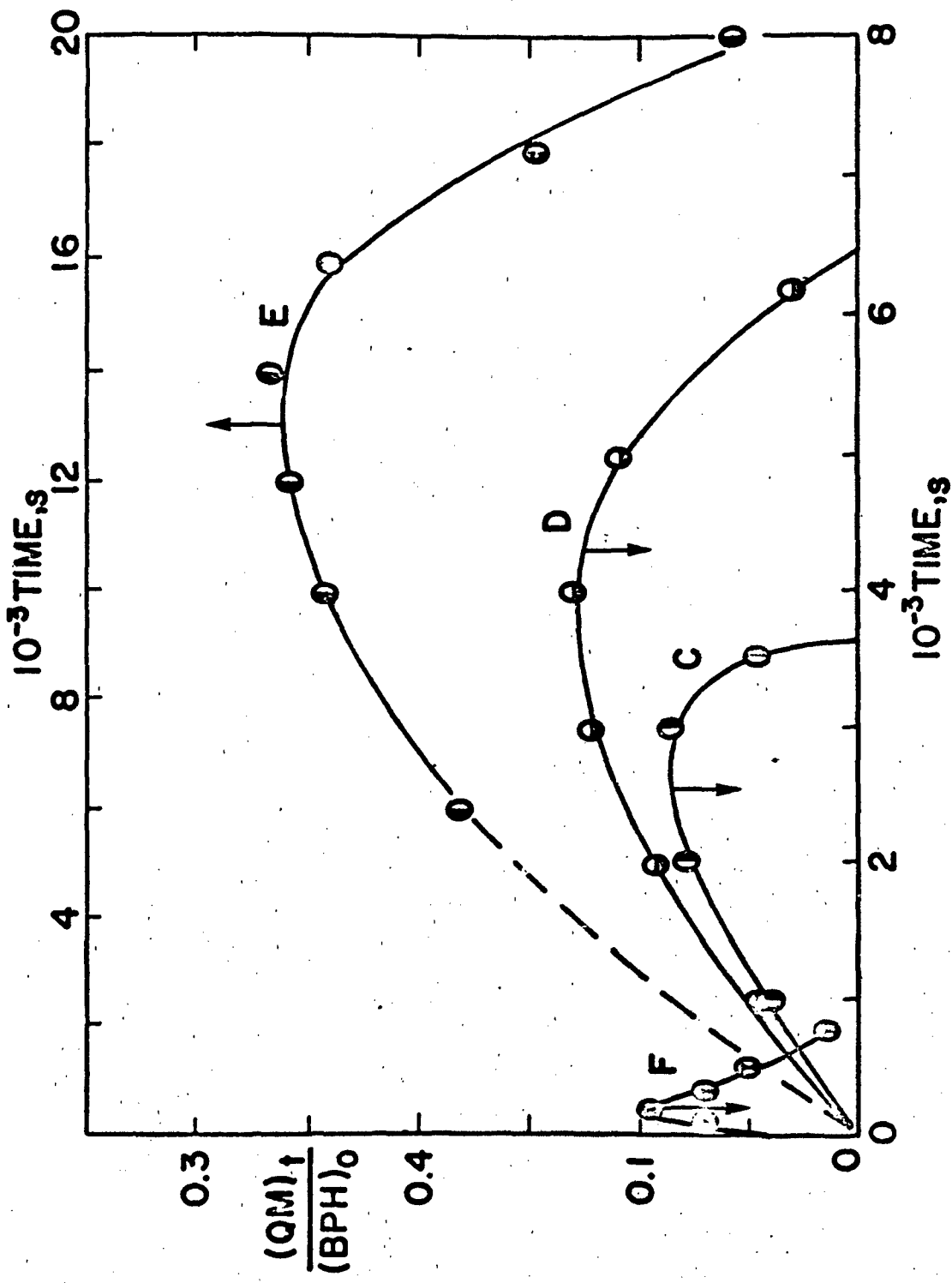


Figure 4 Ratios $(QM)_t/(BPH)_0$ vs. time for the BPH inhibited autoxidation of pure PETH (curves C and D) and n-hexadecane (curve E) and preoxidized PETH (curve F) at 180°C. initial hydroperoxide concentrations: C, D, and E - 0, F - 60×10^{-4} M. Initial BPH concentrations: C - 1.86×10^{-4} M, D - 2.45×10^{-4} M, E - 48.8×10^{-4} M, F - 7.2×10^{-4} M.

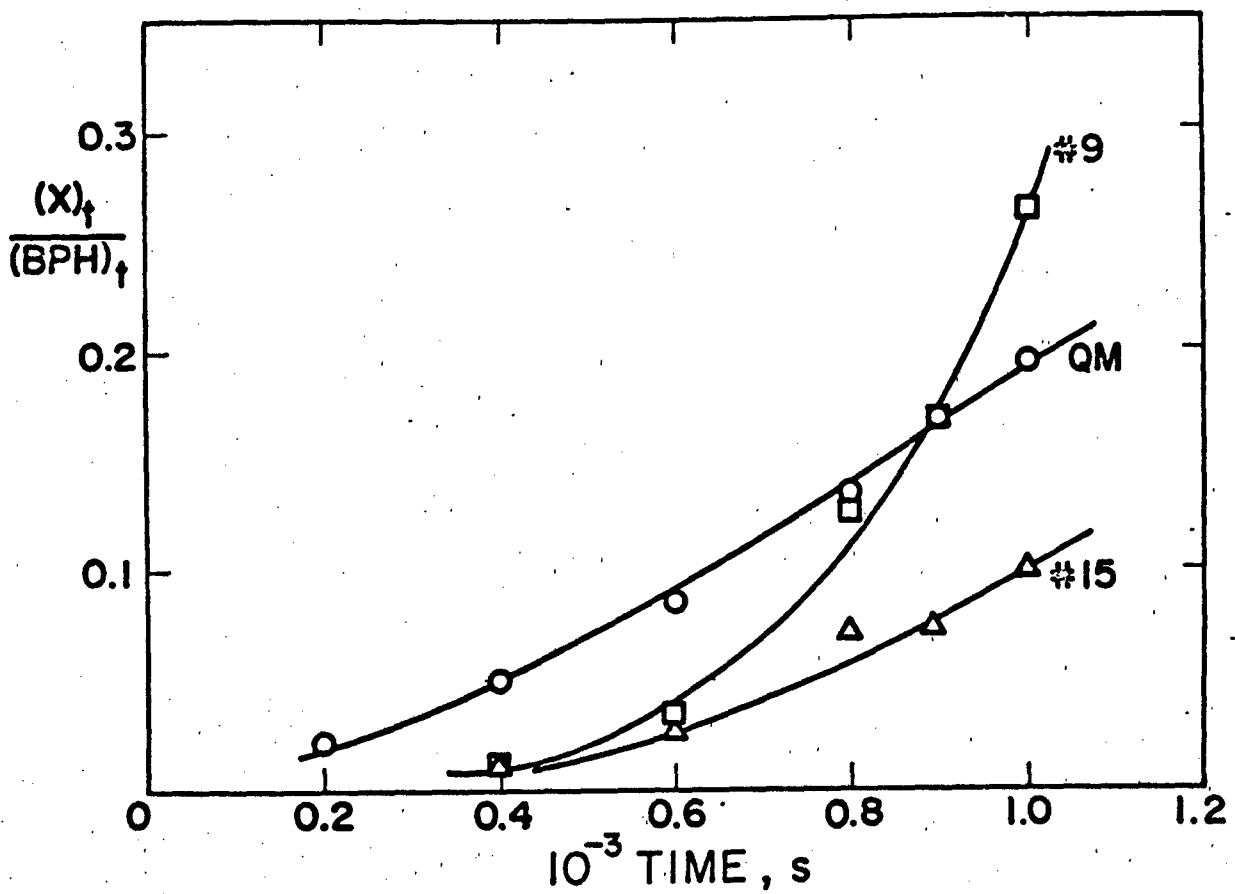
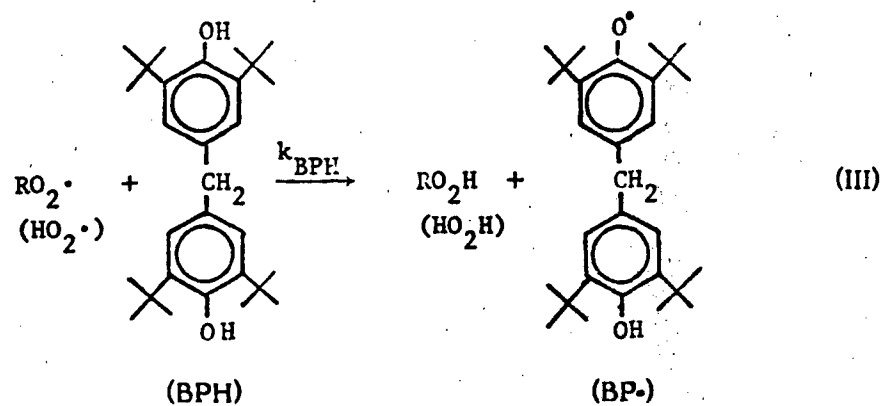


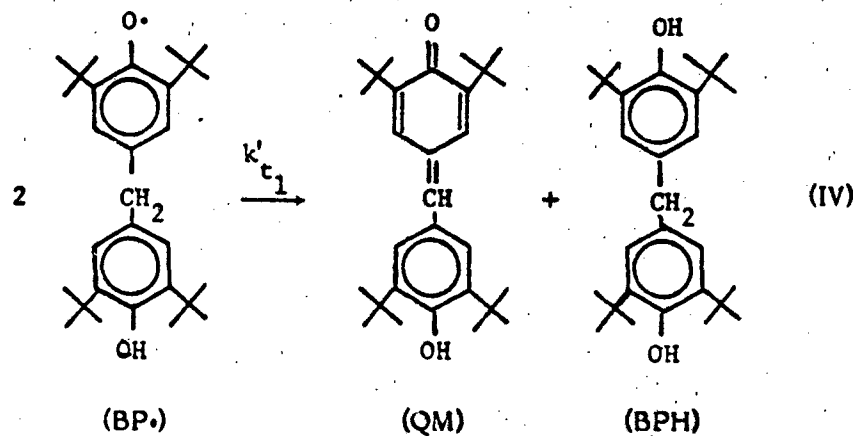
Figure 5 Ratios of concentrations of QM and of two unidentified BPH products, #9 and #15, to concentration of BPH vs. time for the BPH-inhibited autoxidation of PETH at 200°C. Initial concentration of BPH was equal to 5.3×10^{-4} M.

unidentified products to $(BPH)_t$ versus time for a pure PETH system inhibited by BPH at 200°C. In future work we hope to identify these species and develop methods for their quantitative determination.

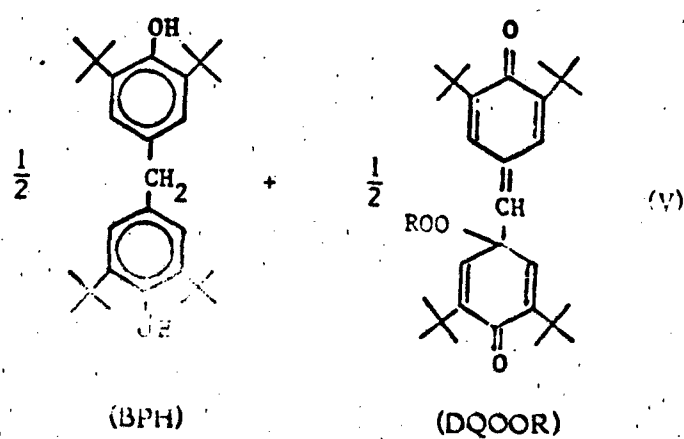
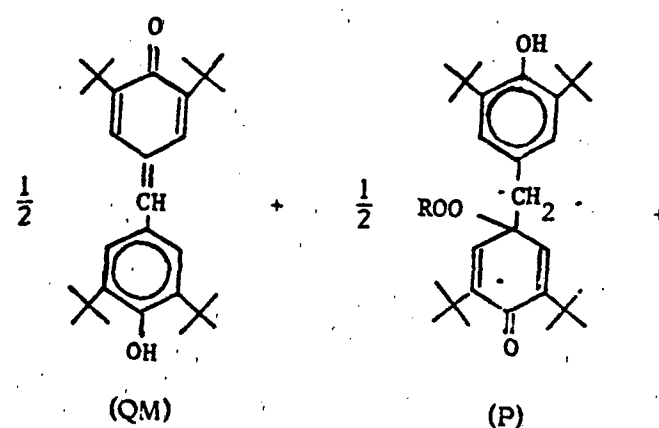
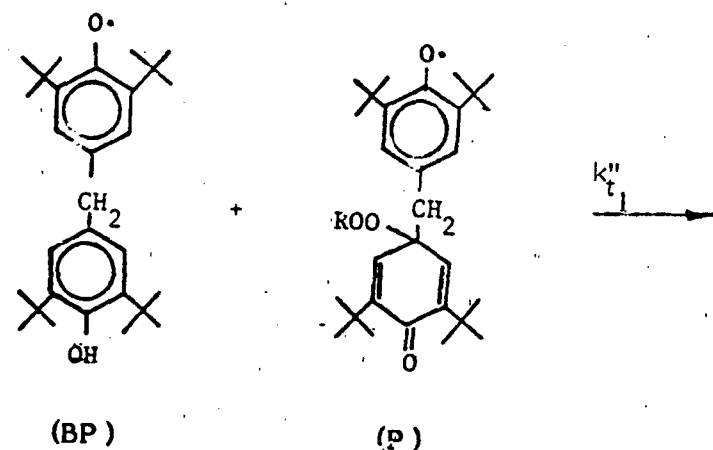
PRELIMINARY KINETIC AND MECHANISTIC ANALYSES - The reactions of peroxy radical species with bisphenol, BPH, are likely to involve facile hydrogen atom transfer reactions to form the corresponding phenoxy radical, BP^\bullet , and hydroperoxide products,⁽²⁾



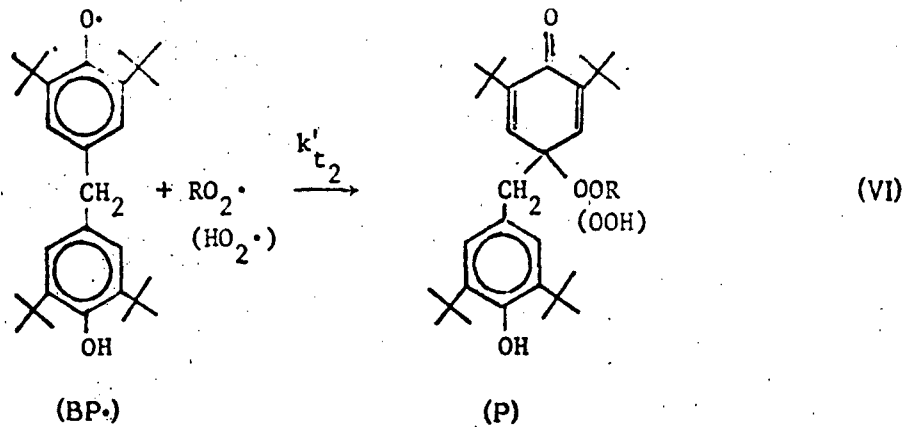
Phenoxy radicals, BP^\bullet , then undergo bimolecular self disproportionation reaction (IV) to form a molecule of quinone methide, QM, and to regenerate a molecule of BPH,⁽⁴⁾



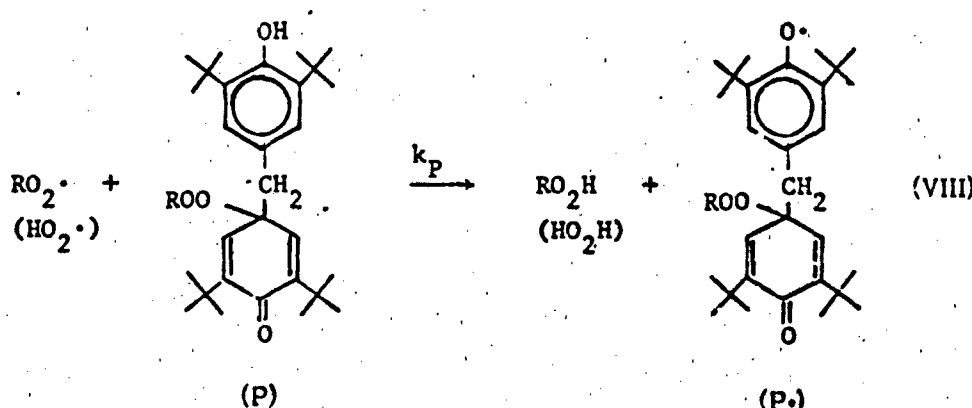
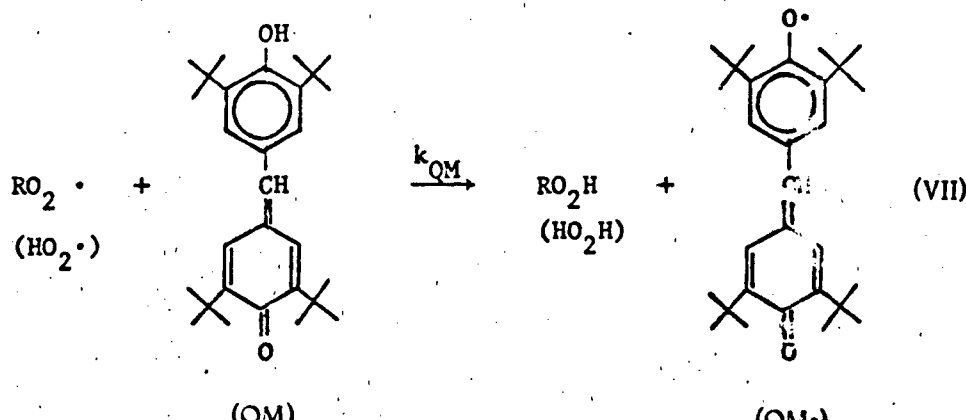
and disproportionation reaction (V) with radical P[•] also leading to a formation of QM and BPH,



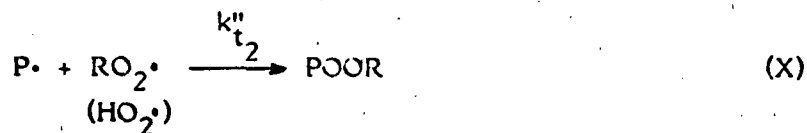
Alternatively, $\text{BP}\cdot$ can react with a peroxy radical to form a second product, P , in reactions such as,



Both QM and P contain reactive phenolic groups and may also function as antioxidants by the transfer reactions,



followed in the case of $P\cdot$ by fast termination reactions (V), (IX), and (X) analogous to those of $BP\cdot$ (V, XV, and VI),



Since radical $QM\cdot$ cannot undergo selfdisproportionation and has weaker bond energy than $BP\cdot$, we assume that $QM\cdot$ reacts only with $RC_2\cdot$



From this reaction sequence the rate of consumption of BPH at any time, t , is given by the expression,

$$-\frac{d(BPH)_t}{dt} = k_{BPH} (RO_2\cdot)_t (BPH)_t \left[1 - \frac{x_t}{2} \right] \quad (XII)$$

where

$$x_t = \frac{2 k'_{t_1} (BP\cdot)_t^2 + k''_{t_1} (BP\cdot)_t (P\cdot)_t}{k_{BPH} (RO_2\cdot)_t (BPH)_t} \quad (XIII)$$

represents the fraction of $BP\cdot$ radicals which is converted to QM and BPH via disproportionation reactions (IV) and (V). Similarly, y_t used below is defined as the fraction of $P\cdot$ radicals which undergoes disproportionation reactions (V) and (IX),

$$y_t = \frac{2 k_{t1}''' (P\cdot)^2 + k_{t1}'' (BP\cdot)(P\cdot)}{k_p (RO_2\cdot)(P)_t} \quad (XIV)$$

Equating the sum of rates of termination reactions with the rate of radical formation at time t , $(R_i)_t$, and making steady state assumptions for all free radicals gives

$$(RO_2\cdot)_t = \frac{(R_i)_t}{(2 - x_t) k_{BPH} (BPH)_t + 2 k_{QV1} (QV1)_t + (2 - y_t) k_p (P)_t} \quad (XV)$$

The rate of radical formation consists of the sum of at least two terms, i.e.,

$$(R_i)_t = w_0 + 2 k_1 (ROOH)_t, \quad (XVI)$$

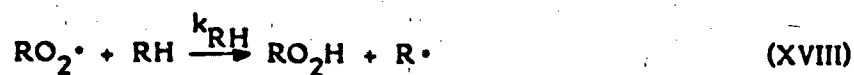
where w_0 is the constant rate of radical formation from the spontaneous reactions of molecular oxygen, k_1 is the composite first order rate constant for homolysis of hydroperoxide, and $(ROOH)_t$ is the hydroperoxide concentration at time t .

Combining eqs. (XII) through (XVI) then yields the general expression for the instantaneous rate of disappearance of BPH at time t ,

$$\frac{-d(BPH)_t}{dt} = \frac{w_0 + 2 k_1 (ROOH)_t}{2 + \frac{4}{(2 - x_t)} \frac{k_{QV1}}{k_{BPH}} \frac{(QV1)_t}{(BPH)_t} + \frac{2(2 - y_t)}{(2 - x_t)} \frac{k_p}{k_{BPH}} \frac{(P)_t}{(BPH)_t}} \quad (XVII)$$

By appropriate choice of values for the rate constants and ratios of rate constants, equation (XVII) could account for the changes in the nature of the decay curves observed for $(BPH)_t/(BPH)_0$ and $(BPH)_t/(BPH)_{18}$ in the absence and presence of preformed hydroperoxide,³ cf. Figures 2 and 3. When $(ROOH)_t \gg w_0/2 k_1$ the numerator does not change significantly while the value of the denominator monotonically increases with reaction time. This leads to the exponential decay of $(BPH)_t/(BPH)_{18}$ observed with preformed hydroperoxides (cf. Figure 3, curve F). When $(ROOH)_t \leq w_0/2 k_1$ the values of the numerator increase with reaction time due to the homolysis of organic hydroperoxides formed via the antioxidant reactions of BPH, QM, and P. This increase can compensate for the increase in the value of the denominator and lead to the observed approximately constant rate of decay of $(BPH)_t/(BPH)_0$ in the pure PETH and pure n-hexadecane systems (cf. curves D and E in Figure 2).

The highly convex decay curves exhibited by BPH when its concentration decays to a low level, see curves B and C in Figure 2, can then be accounted for by the occurrence of an additional mode of organic hydroperoxide formation, namely



³ Values of the ratios $1 \leq (k_{QM}/k_{BPH}) \leq 2$ and k_p/k_{BPH} equal to 0.5 yield calculated rates of BPH consumption in moderately good agreement with experimental values.

The rate of formation of organic hydroperoxides from this process is given by

$$\frac{d(\text{ROOH})}{dt} = k_{\text{RH}} (\text{RO}_2^{\cdot}) (\text{RH}) \quad (\text{XIX})$$

Combining eqs. (XIX) and (XII) and assuming that x_t is very small compared to 1 yields

$$\frac{d(\text{ROOH})}{dt} = \frac{k_{\text{RH}}(\text{RH})}{k_{\text{BPH}}} \left[-\frac{1}{(\text{BPH})_t} \frac{d(\text{BPH})}{dt} \right]. \quad (\text{XX})$$

Thus for ROOH formed by reaction (XVIII)

$$(\text{ROOH})_t^{\text{XVIII}} = \frac{k_{\text{RH}}(\text{RH})}{k_{\text{BPH}}} n \frac{(\text{BPH})_0}{(\text{BPH})_t}. \quad (\text{XXI})$$

When $k_{\text{BPH}} (\text{BPH}) \leq k_{\text{RH}} (\text{RH})$ exponential increases in $(\text{ROOH})_t$ and in R_i occur and lead to the observed strong convexity of curves B and C in Figure 2.

At this point we are in a position to initiate stirred flow reactor experiments on PETH and n-hexadecane systems containing BPH. The validity of eq. (XVII) for a general description of the BPH inhibited systems can be readily tested since the volume of reacted material generated from a single experiment may be sufficient to determine the hydroperoxide concentrations and allow the isolation by preparative liquid chromatography of the various intermediate products. In addition, it will be possible to carry out experiments with admixture of BPH and its intermediate products and thus determine with considerable precision the values of the ratios of rate constants such as $k_{\text{QM}}/k_{\text{BPH}}$.

MAXIMUM INHIBITION PERIODS - Independent of mechanism, the results reported in Tables I and II have considerable technological significance. Values of $t_{inh}/(BPH)_0$, i.e., $1/(R_i/n)$, calculated from the results of the present study with pure PETH are likely to represent the maximum inhibition periods per molar unit of BPH that can be realized in the service use of PETH at a given temperature. Since the maximum concentrations of BPH utilized in the fully formulated lubricants are in the range of 10^{-2} M one would calculate that if PETH containing 10^{-2} M BPH were exposed to an oxidation environment at 220°C rapid autoxidation would occur within one hour or less.⁴ The present calculation does not take into account the effects of partial pressure of oxygen which would increase the time period of protection. However, such effects are likely to be counterbalanced by the effects due to impurities present in technical grade PETH. From the results in Table II we see that the values of $t_{inh}/(BPH)_0$ are a factor of 6 smaller with technical grade PETH than with the purified material. Percolation over alumina of the technical grade material results in a material with inhibition times 4 times lower than the pure material.

⁴ Calculation of t_{inh} for BPH by methods presented in section IV of the present report is also possible. We are currently modifying the equations utilized in this work to reflect the complex stoichiometry of reactions of Q,I and P leading to formation of ROOH.

TABLE II
 AUTOXIDATION OF PETH INHIBITED BY
 BPH - EFFECT OF PETH PURIFICATION
 (Inhibition Period Experiments at 180°C)

PETH	$10^4 \cdot (BPH)_0$ (M)	$10^{-3} t_{inh}$ (s)	$10^{-6} t_{inh}/(BPH)_0$ ($M^{-1} s$)
Technical Grade	3.50	ca. 1.0	ca. 2.9
Percolated - Alumina ^a	3.60	ca. 1.8	ca. 5.0
Highly Purified ^a	3.45	6.28	18

^a For purification procedures see ref. (1).

EXPERIMENTAL

MATERIALS - Pentaerythrityl tetraheptanoate, PETH, was purified by methods previously described to yield a PDP material.⁽¹⁾

4,4'-methylenebis(2,6-di-tert-butylphenol), BPH, obtained from Aldrich Chemical Company was recrystallized twice from ethanol: mp 155°C. The sample of 2,6,3',5'-tetra-tert-butyl-4-hydroxyphenyl-4-methylene-2,5-cyclohexadiene-1-one, the quinone methide, QM, was prepared by the method of Copperger.⁽⁵⁾

BATCH REACTOR - The batch reactor design and procedure were previously described.⁽¹⁾ Samples of the reacting mixture withdrawn at various time intervals were quenched to room temperature and analyzed for hydroperoxide by titration⁽¹⁾ and for BPH and QM by HPLC.

HPLC ANALYSIS - A Waters' HPLC system was used for analysis. The system consists of two Model 6000 solvent delivery pumps, a model U6K Septumless injector, a model 660 gradient programmer and a model 440 dual micro UV-VIS detector. A model FS-970 LC Spectrofluorometer from Schoeffel was connected downstream of the UV detector for fluorescence measurements.

HPLC analysis was accomplished by reverse-phase separation on a μ -Bondapak C₁₈ column obtained from Waters. The column was operated at room

temperature, and a 10 minute linear gradient of the mobile phase from 60/40 $\text{CH}_3\text{CN}/\text{H}_2\text{O}$ to 100% CH_3CN was used for all the analyses reported here. The chromatographic peaks corresponding to bisphenol and quinone methide were identified by: a) retention time, b) co-injection of the standard and the mixture, and c) the ratios of their UV-Vis absorption response (peak areas) at 280 nm and 405 nm. The fluorescence response of BPH provides yet another means of identification and peak purity check.

Quantification was achieved using peak heights or peak areas compared with standard calibration mixtures. A Hewlett Packard Model 3380A integrator was used for all the peak area integrations.

REFERENCES

1. E. J. Hamilton, Jr., S. Korcek, L. R. Mahoney, and M. Zinbo, "Kinetics and Mechanism of the Autoxidation of Pentaerythrityl Tetraheptanoate at 180 and 220°C," Int. J. Chem. Kinet., in press; Attachment I.
2. L. R. Mahoney, Angew. Chem., Int. Ed. Engl., 8, 547 (1969). The simplest case refers to constant rate of initiation and a constant value of n.
3. a) L. R. Mahoney, S. Korcek, S. Hoffman and P. Willermet, Ind. and Eng. Chem. Prod. Res. and Dev., 17, 250 (1978).
b) R. K. Jensen, unpublished results.
4. S. A. Weiner and L. R. Mahoney, J. Am. Chem. Soc., 91, 5029 (1972).
5. G. M. Coppinger, J. Am. Chem. Soc., 79, 501 (1957).

IV EFFECTS OF STRUCTURE ON THE THERMOXIDATIVE STABILITY OF SYNTHETIC ESTER LUBRICANTS: THEORY AND PREDICTIVE METHOD DEVELOPMENT

(L. R. Mahoney, S. Korcek, and J. Norbeck)

The establishment of structure - reactivity relationships is of considerable scientific and technological importance. In the following sections we develop both the theoretical basis and the method for the prediction of the effects of structure changes on the thermoxidative stability of synthetic ester lubricants.

BACKGROUND. Chao and coworkers⁽¹⁾ have recently reported the results of a systematic study of the effects of structural changes in the alkanoyloxy group on the physical and chemical properties of synthetic polyol ester lubricants. The relative thermoxidative stabilities of the materials were determined by measurements of the lengths of inhibition periods in the presence of the same amount of an amine antioxidant, N-phenyl- α -naphthylamine (PAN). Although the inhibition periods in homologous series of esters were found to decrease monotonically with increasing number of reactive hydrogens in the alkanoyloxy group the effects were not additive. In Figure 1 are shown the results of their measurements for the pentanoate, n-C₅, through octanoate, n-C₈, tetraesters of pentaerythritol versus a reactivity parameter, I/N₃ (RH), based on the gram atoms of reactive hydrogens available for intermolecular abstraction reaction per liter of the substrate.

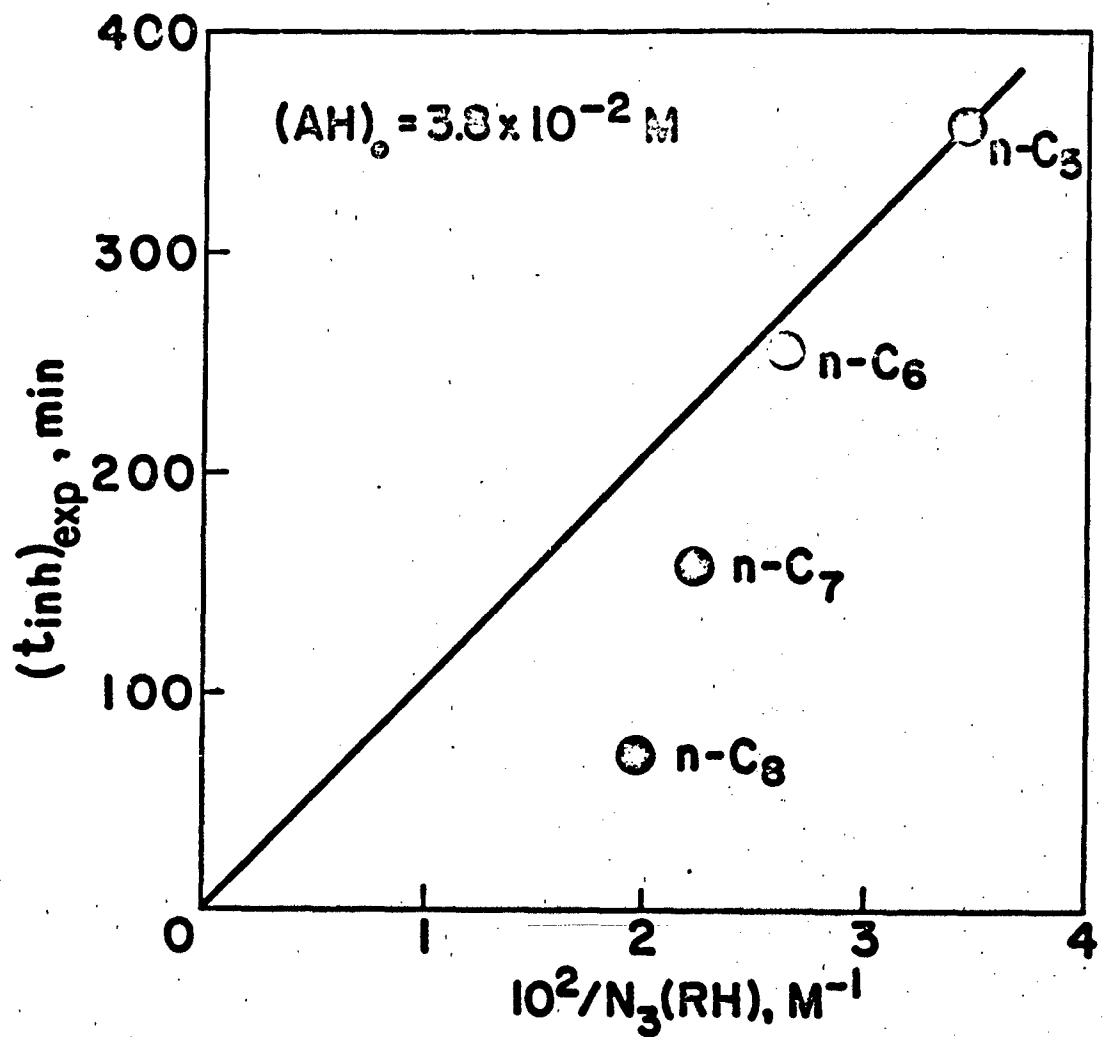


Figure 1 A plot of inhibition periods from the PAN inhibited autoxidation of straight-chain pentaerythrityl alkanoates at 232°C (1) vs. a reactivity parameter, $1/N_3(\text{RH})$.

Such non-additive effects on the stability of these lubricants must be at least in part due to the increasing importance of α, γ and α, δ intramolecular hydrogen abstraction reactions as the number of $-\text{CH}_2-$ units in the alkanoyloxy group increases.^(2, 3) The occurrence of intramolecular reactions leads to increased rates of formation of hydroperoxide products. This, then, results in an enhancement of autocatalytic character of oxidation process and thus in a decrease of thermoxidative stability of higher members of a homologous series.

Based upon these considerations we now develop a kinetic-mathematic model relating the length of experimental inhibition period, t_{inh} , with these structural effects and compare the predicted values of t_{inh} derived from the model with the results of Chao et al.⁽¹⁾

DERIVATION OF KINETIC EQUATIONS. The autoxidation of PETH at 180 to 220°C is described by the reaction scheme (1) - (7) shown in Figure 2. Upon the addition of an efficient¹ antioxidant, AH, reaction (6) is replaced by

¹ By efficient we mean that reaction (3) is not reversible under the conditions of the inhibition period measurement. By this definition hindered phenols and N-phenyl- α -naphthylamine, PAN, are efficient while 4,4'-dioctyldiphenyl amine, cf. section III of this report, is not efficient.

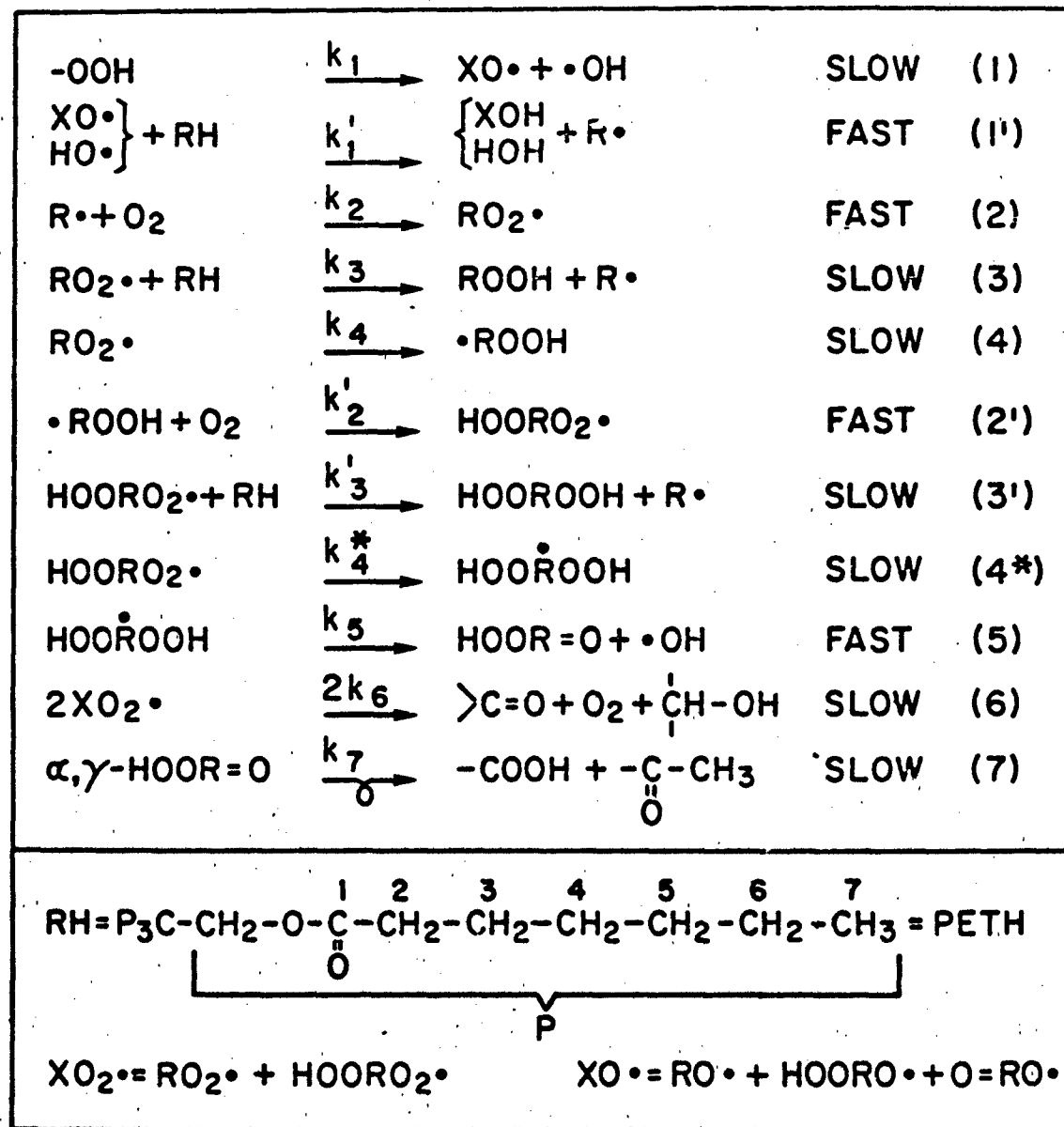
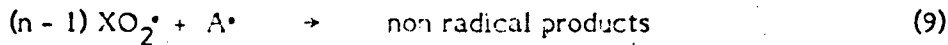
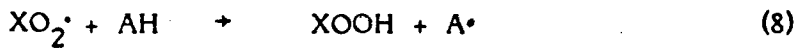


Figure 2 Reaction scheme for the autoxidation of PETH.



where n is equal to the number of peroxy radicals consumed by reaction with a molecule of AH. Under these conditions

$$(XO_2^\cdot) = \frac{1}{k_g(AH)} \frac{-d(AH)}{dt} \quad (I)$$

and

$$2 k_1 (-OOH) = \frac{-n d(AH)}{dt} \quad (II)$$

At elevated temperature, α , γ -hydroperoxyketone products rapidly decompose via reaction (7); $t_{1/2}^{(7)}$ is equal to 108 s at 180°C and 2.5 s at 232°C compared to $t_{1/2}^{(1)}$ equal to 4330 s at 180°C and 87 s at 232°C .⁽³⁾ Based upon the assumption that α , γ -hydroperoxyketone species do not significantly contribute to the total hydroperoxide concentration, the rates of formation of total hydroperoxide groups are then given by,

$$\frac{d(-OOH)_t}{dt} = \left[1+A+B \frac{k_3}{H} N_3(RH) + (1+A) k_g(AH) \right] \frac{1}{k_g(AH)} \frac{-d(AH)}{dt} - \frac{n}{2} \frac{-d(AH)}{dt} \quad (III)$$

where A and B represent composite rate constants for intra and intermolecular abstraction reactions, see Appendix 1. When intramolecular reactions do not occur $A = B = 0$. Noting that the time derivative may be eliminated from equation (III),

$$d(-OOH)_t = G'(a_i, b_i, k_g/(k_3/H), N_j, (RH), n, (AH)) d(AH) \quad (IV)$$

The values of a_i , b_i , and N_j are constants calculated from the structure of the reacting molecule and kinetic data (cf. Appendix I). The values of $k_g/(k_3/H)$ and n are now adjustable parameters but they may also be obtained from experimental data if available.²

Upon integration

$$\begin{aligned} (-OOH)_t &= \int_{(AH)_0}^{(AH)_t} G'(a_i, b_i, k_g/(k_3/H), N_j, (RH), n, (AH)) d(AH) \\ &= G(a_i, b_i, k_g/(k_3/H), N_j, (RH), n, (AH)_t, (AH)_0) \end{aligned} \quad (V)$$

Combining (II) and (V)

$$-\frac{n}{2k_1} \frac{d(AH)}{dt} = G(a_i, b_i, k_g/(k_3/H), N_j, (RH), n, (AH)_t, (AH)_0) \quad (VI)$$

² The absolute values of k_g are normally much less sensitive to the structure of the reacting peroxy radical than are the values of k_3/H .⁽⁴⁾

Rearranging and integration results in

$$-\frac{2k_1}{n} (t_2 - t_1) = \int_{(AH)_{t_1}}^{(AH)_{t_2}} \bar{G}(a_i, b_i, k_8/(k_3/H), N_j, (RH), n, (AH)_t, (AH)_o) d(AH)$$

(VII)

The inhibition period for a system equals $\frac{-n}{2k_1}$ times the value of the integral as $(AH)_{t_1} \rightarrow (AH)_o$ and $(AH)_{t_2} \rightarrow 0$. Unfortunately, the integral is undefined at $(AH)_{t_1} = (AH)_o$ and the integral slowly diverges as $(AH)_{t_1} \rightarrow (AH)_o$. However, the ratio of integrals for a system I where $A = 0, B = 0$ and a system II where $A \neq 0, B \neq 0$ can be calculated using numerical procedures described in Appendix 2. Thus the ratio of the inhibition periods of systems I and II can be obtained from the equation,

$$\frac{n^I k_1^I}{n^II k_1^II} \frac{t_{inh}^I}{t_{inh}^{II}} = \frac{\int_0^{(AH)_t + (AH)_o} \bar{G}^I(k_8/(k_3/H), N_j, (RH), n, (AH)_t, (AH)_o) d(AH)}{\int_0^{(AH)_t + (AH)_o} \bar{G}^{II}(a_i, b_i, k_8/(k_3/H), N_j, (RH), n, (AH)_t, (AH)_o) d(AH)}$$

(VIII)

Equation (VIII) is utilized for the calculation of the ratios of t_{inh}^I/t_{inh}^{II} for a variety of polyol ester systems. The ratios are then compared with literature values. System I is a C_5 or lower member of a series since intramolecular abstractions in such structures are not possible.

$n\text{-C}_5\text{---n-C}_8$ ESTERS OF PENTAERYTHRITOL. In Figure 3 are plots of the inhibition periods at 232°C for the $n\text{-C}_5\text{---n-C}_8$ tetraesters of pentaerythritol reported by Chao et al.⁽¹⁾ versus corresponding values calculated from eq. (VIII) as a function of the value of $k_8/(k_3/\text{H})$ with n equal to 2.0 and t_{inh}^1 equal to 358 min. A value of $k_8/(k_3/\text{H})$ equal to 2.5×10^4 results in a poor correlation. The correlation improves as the value is decreased until there appears to be little effect as the value is decreased from 2.5×10^3 to 1×10^2 . A value in the range of 3×10^3 would in fact be predicted for $k_8/(k_3/\text{H})$ from the limited kinetic data on N-phenyl- α -naphthylamine. Brownlie and Ingold⁽⁵⁾ reported a value of k_8 equal to $7 \times 10^4 \text{ M}^{-1}\text{s}$ for n equal 2.0 in styrene at 65°C . We estimate from the temperature dependence of the autoxidation of pure PETH that k_3/H will equal $23 \text{ M}^{-1}\text{s}$ at 232°C .⁽³⁾

The largest differences between experimental and calculated values of t_{inh} occur for the $n\text{-C}_8$ ester. It is likely that due to steric effects there will in fact be a slight increase in the value of k_3/H as one increases the length of the ester chain. Utilizing a value of $k_8/(k_3/\text{H})$ equal to 1.6×10^3 for $n\text{-C}_8$ ester and 2.5×10^3 for $n\text{-C}_5$ results in a precise agreement of calculated and experimental values.

FUTURE WORK. Based upon the results obtained for the $n\text{-C}_5$ through $n\text{-C}_8$ esters we believe that eq. (VIII) will be useful for the prediction of the effects of structural changes on the thermoxidative stability of many ester systems.

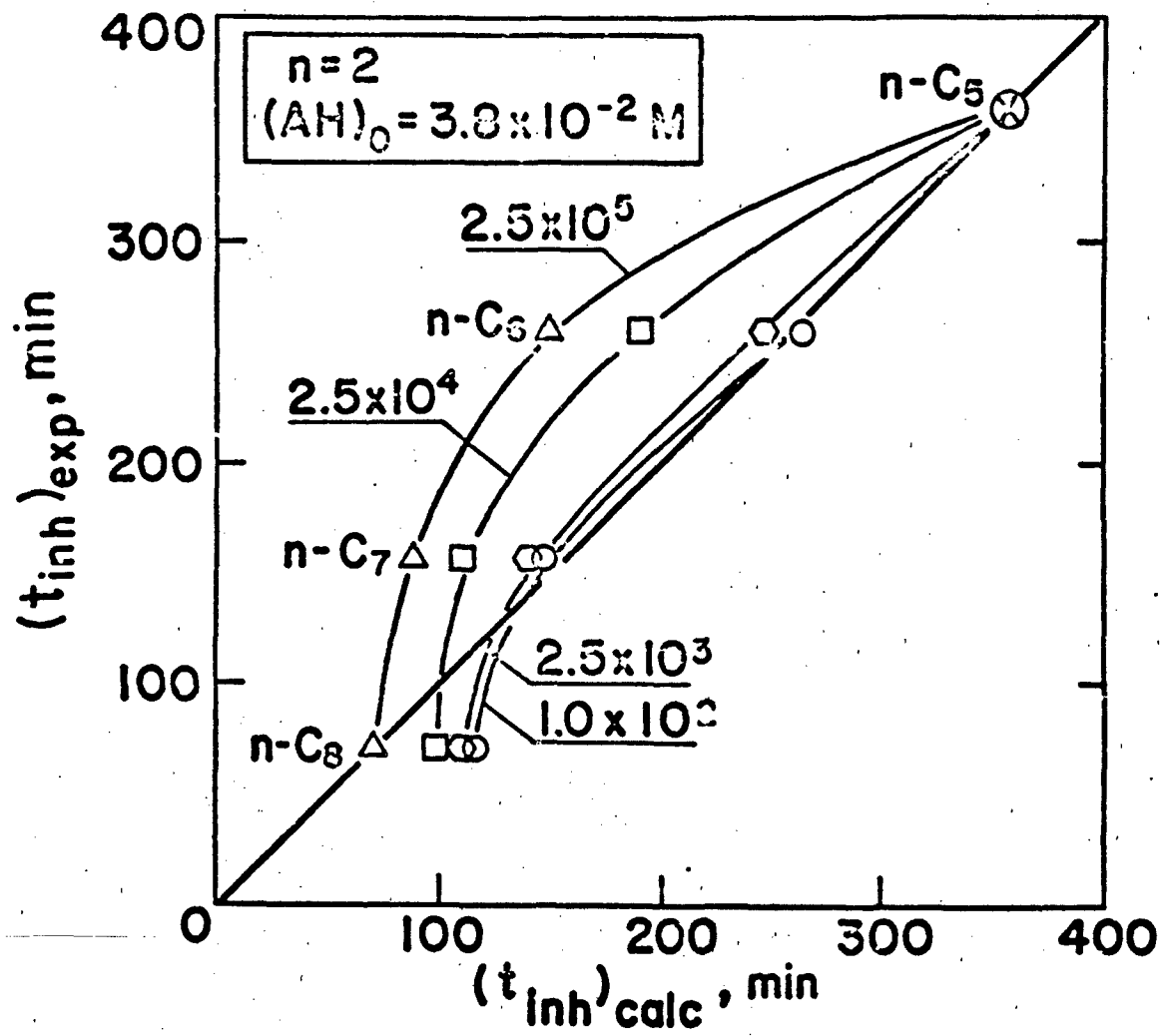
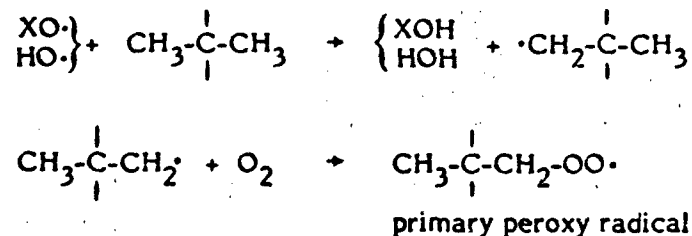
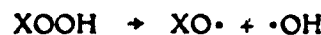


Figure 3 Plots of experimental inhibition periods from the PAN inhibited autoxidation of straight-chain pentaerythrityl alkanoates at 232°C (1) vs. corresponding values calculated from eq. (VIII) as a function of $k_8/(k_3/H)$.

For example, by a suitable choices of the values of $k_8/(k_3/H)$, it is possible to generate agreement between experimental and calculated values of t_{inh} . In Figure 4 is the result of such an exercise for some gem-dimethyl substituted pentaerythrityl alkanoates.

In these gem-dimethyl systems the values of k_3/H include significant contribution of primary peroxy radicals produced from reactions of initiation derived radicals, i.e.,



For systems other than the 3,3-dimethyl-C₃ ester these radical species can undergo intramolecular reactions,



The occurrence of these reactions would lead to increased values of k_3/H and thus the lower values of $k_8/(k_3/H)$ necessary to obtain the fit shown in Figure 4.

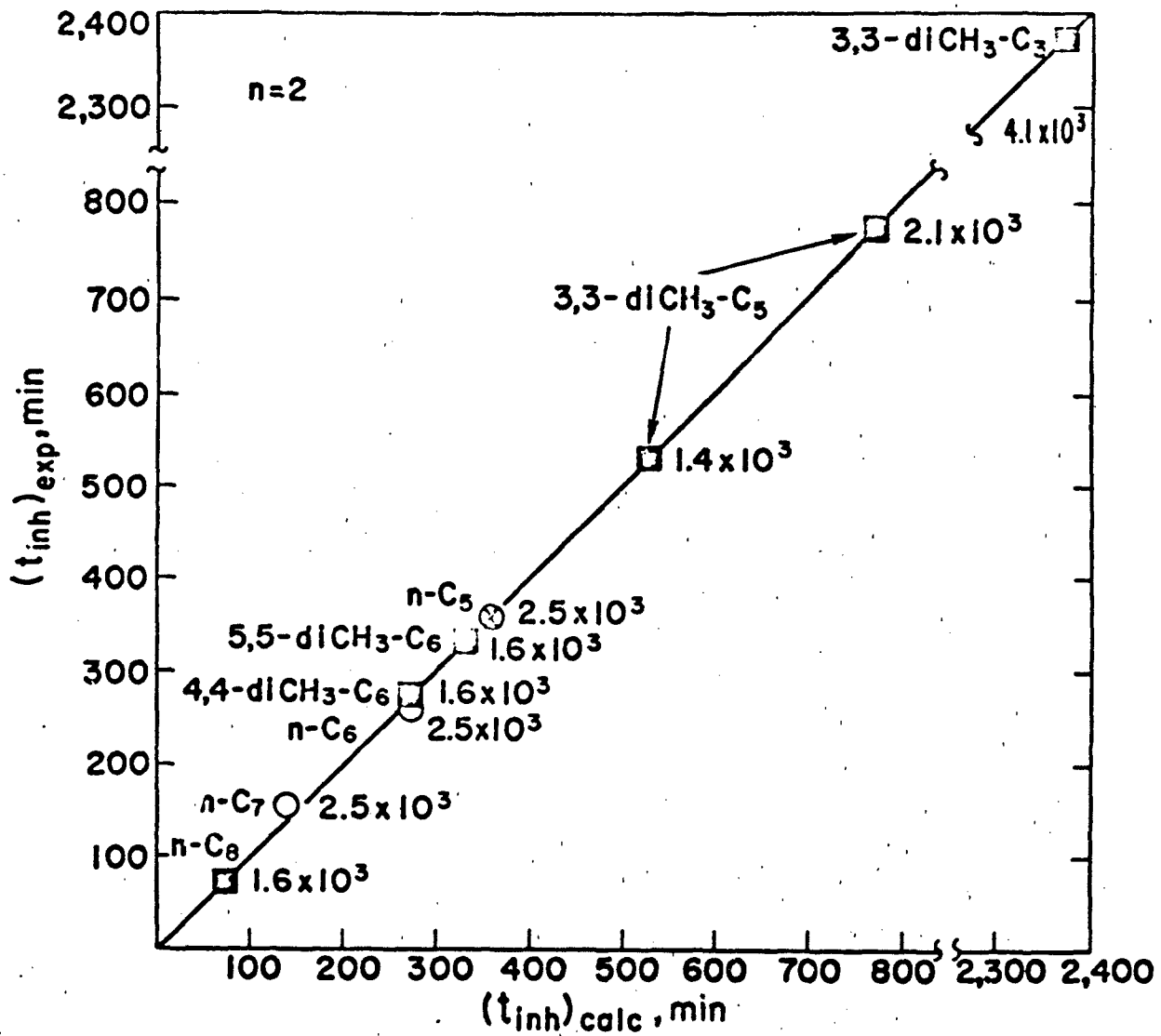


Figure 4 A plot of experimental inhibition periods from the PAN inhibited autoxidation of straight-chain and gem-dimethyl substituted pentaerythryl alkanoates at 232°C (1) vs. corresponding values calculated from eq. (VIII) using values of $k_3/(k_3/H)$ designated in the figure.

In the case of 3,3-dimethyl-C₃ ester the only reactive hydrogen is on a tertiary carbon. Due to the extreme steric effects involved in its abstraction the value of k_3/H may be lower than that observed for a secondary C-H abstraction and lead to the higher value of $k_8/(k_3/H)$ shown in Figure 4.

REFERENCES

1. (a) T. S. Chao, M. Kjonaas, and J. DeJovine, Preprints, Div. Petrol. Chem., ACS, 24, No. 3, 836 (1979); (b) T. S. Chao, M. Kjonaas, and W. D. Hoffman, U. S. Patent 3,441,600, 1969 and U. S. Patent 3,523,084, 1970; in "Synthetic Lubricants", M. W. Ranney, Ed.; Noyes Data Corporation, Park Ridge, N. J., 1972, p. 7.
2. R. K. Jensen, S. Korcek, L. R. Mahoney, and M. Zimbo, J. Am. Chem. Soc., 101, in press.
3. E. J. Hamilton, Jr., S. Korcek, L. R. Mahoney, and M. Zimbo, "Kinetics and Mechanism of the Autoxidation of Pentaerythrityl tetraheptanoate at 180 to 220°C," Int. J. Chem. Kinet., in press; Attachment I.
4. L. R. Mahoney and M. A. DaRooge, J. Am. Chem. Soc., 92, 4063 (1970).
5. I. T. Brownlie and K. U. Ingold, Can. J. Chem., 45, 2419 (1967).

APPENDIX I

DERIVATION OF KINETIC EXPRESSIONS

The composite rate constants A and B in eq. (III) were derived from kinetic analyses of the reaction scheme (cf. Figure 2) in which reaction (6) was replaced by reactions (8) and (9):^{1, 2}

$$A = \frac{\frac{a_G}{1 + b_G + c(AH)} + \frac{a_D}{1 + b_D + c(AH)}}{1 + \frac{a_G}{1 + b_G + c(AH)} + \frac{a_D}{1 + b_D + c(AH)}} \quad (AI)$$

$$B = \frac{\frac{a_D b_D}{1 + b_D + c(AH)}}{1 + \frac{a_G}{1 + b_G + c(AH)} + \frac{a_D}{1 + b_D + c(AH)}} \quad (AI)$$

¹ This reaction scheme does not include a reaction sequence analogous to that of reactions (4), (2'), and (3') but starting with HOOR_2^{\bullet} which leads to formation of trihydroperoxide and dihydroperoxy ketone products. In the cases where these reactions could occur, i.e., in esters containing C_7 and C_8 alkanoyloxy groups, this simplification was found to introduce an error of less than 1 percent.

² Expression AI was derived assuming that all metastable $\alpha, \gamma\text{-HOOR} = O$ species produced during induction period decompose immediately and do not contribute to $(-\text{OOH})$.

In expressions (AI) and (AII), a_G , a_D , b_G , and b_D represent ratios of rate constants for intra- and intermolecular abstraction reactions, k_4-a , γ/k_3 (RH), k_4- , γ/k_3 (RH), k_{4-a}^* , γ/k_3 (RH), and $k_{4-a,\delta}^*/k_3$ (RH), respectively, and c the ratio k_8/k_3 (RH). In these ratios, all rate constants may be expressed by the products of corresponding rate constants on per hydrogen atom basis and of average number of available hydrogen atoms for corresponding abstraction reaction, N_i . Thus

$$a_i = \frac{k_{4-i}}{k_3(\text{RH})} = \frac{k_{4-i}/\text{H-atom}}{k_3/\text{H-atom}} \quad \frac{N_{4i}}{N_3(\text{RH})} = a_i/\text{H} \quad \frac{N_{4i}}{N_3(\text{RH})} \quad (\text{AIII})$$

$$b_i = (b_i/\text{H}) \quad \frac{N_{4i}^*}{N_3(\text{RH})} \quad (\text{AIV})$$

and

$$c = \frac{k_8}{k_3/\text{H-atom}} \quad \frac{1}{N_3(\text{RH})} \quad (\text{AV})$$

where i represents G or D.

The values of a_i and b_i may be calculated from eq. (AIII) and (AIV) assuming that the ratios of rate constants expressed on per hydrogen atom basis, a_i/H and b_i/H , for similar ester systems are the same. The values of a_i and b_i listed in Table A1-1 were obtained using the values of ratios a_G/H , a_D/H , b_G/H , and b_D/H equal to 26.3, 26.3, 1035, and 329, respectively. These values were derived from the study of PETH autoxidation at 180°C assuming that the ratios do not change with temperature significantly. The average numbers of hydrogen atoms for abstraction reactions (N_i in Table A1-1) were estimated from the structure of ester systems and availability of hydrogens assuming that the concentrations of abstracting isomeric peroxy radicals of given type are equal.

TABLE A1 - 1

**AVERAGE NUMBER OF AVAILABLE HYDROGEN ATOMS AND
COMPOSITE RATE CONSTANTS FOR TETRAESTERS OF PENTAERYTHRITOL**

Alkanoyloxy Substituent	(RH) ₂₃₂ (M)	N _j				$\frac{a_i}{a_G}$	$\frac{b_i}{b_G}$	a	b	α	β	γ	δ
		N ₃	N _{4G}	N _{4D}	N _{4*} ^a								
n - C ₅	1.80	16	0	0	0	0	0	0	0	1	2	0	0
n - C ₆	1.58	24	1.33	0	1	0	0.92	0	27.3	0	29.2	30.2	0.92
n - C ₇	1.40	32	2	1.	1.	1	1.18	0.59	23.1	7.3	224	34.2	1.77
n - C ₈	1.27	40	2.4	1.6	1	1	1.24	0.83	20.4	6.5	18	31.0	2.07
3,3-diCH ₃ -C ₅	1.40	8	0	0	0	0	0	0	0	1	2	0	0
5,5-diCH ₃ -C ₆	1.27	16	0	0	0	0	0	0	0	1	2	0	0
4,4-diCH ₃ -C ₆	1.27	16	2	0	1	0	2.59	0	50.9	0	54.5	55.5	2.59
3,3-diCH ₃ -C ₃	1.80	4 ^a	0	0	0	0	0	0	0	1	2	0	0

^a Tertiary hydrogens

Substituting a_i , b_i , and c into eq. (III) gives G-function in eq. (IV)

$$G(a_i, b_i, k_3/(k_3/H), N_j, (RH), n, (AH)) = \frac{n}{2} - 1 - \frac{1}{c(AH)} - \frac{\alpha + \beta c(AH) + \gamma/c(AH)}{a + bc(AH) + c^2(AH)^2} \quad (AVI)$$

$$\text{where } \alpha = a_G + a_D$$

$$\beta = (1 + b_D)(\alpha + b_G a_D)$$

$$\gamma = \alpha(2 + b_D) + b_G a_D$$

$$a = b - 1 + b_G a_D + b_D (a_G + b_G)$$

$$b = \alpha + b_G + b_D + 2$$

and c is defined by eq. (AV).

Upon integration of eq. (IV) we obtain G-function in eq. (V).

$$G(a_i, b_i, k_3/(k_3/H), N_j, (RH), n, (AH)_t, (AH)_o) =$$

$$\begin{aligned} & \left[\frac{n}{2} - 1 \right] \left[(AH)_t - (AH)_o \right] - \frac{1}{c} \ln \frac{(AH)_t}{(AH)_o} - \\ & \frac{1}{2c} \left[\alpha \ln \frac{a + bc(AH)_t + c^2(AH)_t^2}{a + bc(AH)_o + c^2(AH)_o^2} + \frac{\beta}{a} \ln \frac{(AH)_t^2 (a + bc(AH)_o + c^2(AH)_o^2)}{(AH)_o^2 (a + bc(AH)_t + c^2(AH)_t^2)} + \right. \\ & \left. \delta \ln \frac{(2c(AH)_t + b - q) (2c(AH)_o + b + q)}{(2c(AH)_t + b + q) (2c(AH)_o + b - q)} \right] \quad (AVII) \end{aligned}$$

where $q = \sqrt{b^2 - 4a}$

$$\delta = \frac{2\gamma - b \left(\alpha + \frac{\beta}{a} \right)}{q}$$

The values of all composite constants used in eq. (AVII) for all ester systems discussed in this study are in Table A1-1.

In the absence of intramolecular abstraction reactions the composite rate constants α , β , and δ are all equal to zero. For such systems (systems I in this work) eq. (A VII) becomes

$$G^1 \left(k_g / (k_3 / H), N_j, (RH), n, (AH)_t, (AH)_o \right) = \\ \left[\frac{n}{2} - 1 \right] \left[(AH)_t - (AH)_o \right] - \frac{1}{c} \ln \frac{(AH)_t}{(AH)_o} \quad (AVIII)$$

APPENDIX 2

NUMERICAL EVALUATION OF THE RATIO OF INTEGRALS IN EQ. VIII

The values for the ratio of integrals in eq. VIII were obtained numerically using the CADRE numerical quadrature algorithm in the IMSL library⁽¹⁾. The calculations were done in single precision using a DEC-10 computer system.

As mentioned above, each integral equation used to obtain an individual inhibition period (eq. VII) slowly diverges as $(AH)_t$ approaches $(AH)_0$, where at $(AH)_t = (AH)_0$ the integral is not defined. To avoid this singularity each integration was done from a value $(AH)_t = \epsilon (AH)_0$ for a value ϵ near but not equal to 1. To show how sensitive the integrals and their ratio are to values of ϵ the results of a typical calculation for two systems, I and II, are given in Table A2-1. Notice that the values of individual integrals increase as ϵ approaches 1. However the ratio of integrals, I/I^{II} , converges to a constant value (column 4, Table 2A-1).

The results in Table 2A-1 demonstrate an interesting dichotomy. The values obtained for the individual integrals depend on what value is chosen for ϵ . If one defines a critical concentration $(AH)_c = (AH)_0 - \epsilon (AH)_0$, it is seen from Table A2-1 that as $(AH)_c$ changes from 1×10^{-3} to 1×10^{-6} the integrals for both system increase by a factor of 3 or more. The limits of integration as given by eq. VII, correspond to a system having an infinite inhibition time. One must

TABLE A2-1

CALCULATED VALUES OF INDIVIDUAL INTEGRALS IN EQ. VII
 FOR SYSTEMS I AND II^a AND OF RATIO OF THESE INTEGRALS
 IN EQ. VIII FOR VARIOUS VALUES OF ϵ

ϵ	I ^I	I ^{II}	I ^I /I ^{II}
.50	12.4	4.13	3.00
.80	37.2	11.9	3.12
.90	58.2	18.4	3.16
.99	132.	41.1	3.21
.9999	283.	87.3	3.24
.99999	358.	110.	3.25
.999999	434.	134.	3.25

^a System I was n-C₅ and system II n-C₇ ester; n=2, $(AH)_0 = 3.2 \times 10^{-2}$ M,
 $k_8/(k_3/H) = 2.5 \times 10^4$

introduce some value of ϵ other than 1 or change the form of the kinetics to obtain a finite value for the inhibition period. Thus, one can speculate what, if any, physical significance can be placed on ϵ and is it the same for all systems, as was assumed here. This should be contrasted to the fact that the ratio of integrals converges to a constant value as ϵ approaches 1. This implies that eq. VIII is simply a function of I^I and I^{II} which is determined primarily by the value at $(AH)_0$. Thus the ratio should be able to be obtained without doing the integration.

For this paper we have chosen to obtain the ratio numerically, using $\epsilon = .9999$. However the possibility of obtaining the same result from I^I and I^{II} directly is being explored.

REFERENCES

1. DCADRE Routine, IMSL Library - July, 1977, International Mathematical and Statistical Libraries, 7500 Bellaire Blvd., Houston, Texas.
2. de Boor, C., "CADRE: An Algorithm for Numerical Quadrature", Mathematical Software, New York, Academic Press, 1971, Chapter 7.

ACKNOWLEDGMENTS

The authors wish to acknowledge Dr. F. S. Lee for HPLC antioxidant analyses described in Section III and Ms. S. Tsang for assistance rendered during the final preparation of this report.

ATTACHMENT I

KINETICS AND MECHANISM OF THE AUTOXIDATION OF PENTAERYTHRITYL
TETRAHEPTANOATE AT 180 TO 220°C¹

Edwin J. Hamilton, Jr., Stefan Korcek, Lee R. Mahoney,
and Mikio Zinbo

Engineering & Research Staff
Research
Ford Motor Company
Dearborn, Michigan 48121

ABSTRACT

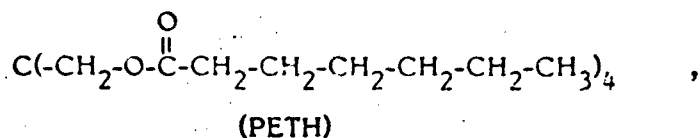
A kinetic and mechanistic study of the autoxidation of liquid pentaerythrityl tetraheptanoate, PETH, at 180 to 220°C has been carried out utilizing a stirred flow reactor. The results are consistent with the occurrence of a chain reaction scheme similar to that proposed for n-hexadecane autoxidation, namely the formation of monohydroperoxides by the intermolecular abstraction reaction (3), formation of α, γ - and α, δ -dihydroperoxides and α, γ - and α, δ -hydroperoxyketones by intramolecular peroxy radical abstraction reactions (4) and (4*), bimolecular termination of peroxy radicals, reaction (6), and rapid conversion of α, γ -hydroperoxyketones to the corresponding cleavage acids and methyl ketones, reaction (7). Comparisons of various rate parameters for the n-hexadecane and PETH systems reveal that the values of k_7 and $(k_3/H\text{-atom})/(2 k_6)^{1/2}$ are within experimental uncertainties identical for the two systems at 180°C.

¹ Presented in part at the 17th National Meeting of the Am. Chem. Soc., Phys 10,
Chicago, Ill., August, 1977.

The proposed reaction scheme includes the concurrent formation of hydroxy radicals and hydroperoxyketone species. The results of kinetic analysis and the experimentally observed isomer distributions of primary and secondary mono-hydroperoxide products at high and low oxygen pressures suggest that ca. 60 percent of the hydrogen abstractions from PETH at high oxygen pressures occur by hydroxy radicals.

INTRODUCTION

The present work, which describes the results of a kinetic and mechanistic study of the autoxidation of pentaerythrityl tetraheptanoate,



at elevated temperatures, is an extention of our stirred flow reactor study of n-hexadecane (1) to other thermally stable organic liquid systems. PETH is representative of a class of neopentyl type ester materials used in high temperature applications. Due to the absence of hydrogens on the central carbon which is in a position β to heptanoyloxy groups, PETH is not susceptible to the usual cyclic elimination processes which yield olefin and acid products (2). Thus, in the absence of oxygen, PETH possesses thermal stability comparable to that of hydrocarbons.

A review of the limited literature in the area suggests that the kinetics and mechanism of reactions in the autoxidation of esters are likely to be as complex as those shown by hydrocarbons at elevated temperatures. In his careful investigations VanSickle (3) studied the initiated oxidations of isobutyl acetate and of cyclohexylenedimethylene diacetate at temperatures up to 120°C and reported that his results were not amenable to kinetic analyses since the systems were strongly autocatalytic and the products were complex mixtures derived from secondary reactions of primary products. In a model study for pentaerythrityl systems,

Sniegoski (4) determined the isomer distribution of monohydroperoxide species from the air autoxidation of neopentyl hexanoate at 150 to 200°C. The results of recent studies in which only the hydroperoxide by titration and/or the rates of oxygen absorption for pentaerythrityl ester systems were determined have been reported by Agliullina et al. (5,6) and Kovtun et al. (7). The former studied the initiated oxidation of pentaerythrityl tetrapentanoate at temperatures up to 150°C and the autoxidation of the same material at temperature up to 220°C while the latter group studied the initiated oxidation of a mixture of pentaerythrityl C₅-C₉ tetraalkanoates at 95 to 140°C.

The stirred flow reactor technique has proven advantageous for kinetic investigation of complex chemical systems such as autoxidation of hydrocarbons at increased temperatures (8). As shown by Denbigh (9), in a stirred flow reactor the instantaneous rate of reaction of a species X is given by the equation

$$\frac{d(X)}{dt} = \frac{(X)_{\tau} - (X)_0}{\tau} \quad (1)$$

where $(X)_{\tau}$ is the concentration of X in the fluid both in the reactor and exiting the reactor, $(X)_0$ is the concentration in the entering fluid, and τ is the residence time of the fluid in the reactor. Thus, measurement of the concentration of a product in the exiting fluid allows a direct determination of its rate of formation in the reactor. The empirical rate law is then determined by finding a relation that describes this rate of formation as a function of the concentrations of species in the stirred flow reactor.

EXPERIMENTAL

Materials. Pentaerythrityl tetraheptanoate, PETH, was obtained from Stauffer Chemical Company as technical grade material. Oxygen was Matheson UHP (min. purity 99.99%), argon was Matheson Grade (min. purity 99.9995%). 4,4'-methylenebis(2,6-di-*tert*-butylphenol), BPH, was obtained from Aldrich Chemical Company and recrystallized twice from ethanol: mp 155°C. Alumina was ALCOA Type F-20 (80-200 mesh) obtained from Matheson, Coleman and Bell and activated at 400° for 16 hours. Lithium aluminum hydride was obtained from J. T. Baker Chemical Company.

Samples of acids and alcohols utilized as standards for analysis were obtained from commercial sources. Samples of 1,4- and 1,6-heptanediols were prepared by LiAlH_4 reductions of γ -heptanoic lactone (K and K Lab.) and of 6-oxoheptanoic acid (Sapon Labs.), respectively. The sample of 1,7-heptanediol was obtained from Aldrich Chemical Company.

p-Bromophenacyl ester derivatization kits and the reagents for preparing pertrimethylsilyl derivatives were obtained from Applied Science Laboratories, Inc. Isopropyl alcohol was distilled from NaBH_4 or CaH_2 prior to use. Diethyl ether was distilled from LiAlH_4 prior to use. Other solvents and reagents utilized were ACS reagent grade materials.

Purification of PETH. The purification of technical grade PETH for use as standard material for this investigation was accomplished utilizing combinations of

vacuum distillation, designated as D, and percolation through alumina, designated as P.

The deep-yellow technical grade PETH material was percolated through a 60 cm x 4 cm glass column dry packed with 550 grams of activated alumina. The first two liters of the pale yellow eluent were collected. The eluent was then distilled at reduced pressure under argon utilizing a 30 cm Vigreux column and an argon bubbler in the pot to minimize bumping. Following a small yellow lower boiling fraction, a pale yellow main fraction corresponding to ca. 75 percent of the original eluent was collected at a head temperature of ca. 230°C and a gauge pressure of less than 0.005 torr. This distilled material was then percolated through a 100 cm x 3 cm glass column dry packed with 550 grams of activated alumina. The first 600 ml of eluent was collected and designated PDP-1. The next 200 ml of eluent was collected and designated PDP-2. A portion of PDP-1 was redistilled and the middle fraction collected as described above. This redistilled material was then percolated through a 50 cm x 3 cm glass column dry packed with 275 grams of activated alumina. The first 400 ml of eluent from this percolation was collected and designated PDPDP.

The purity of various PETH materials prepared as described above was assessed from their relative oxidation kinetics. The results of this evaluation are presented in Figure 1. The figure shows plots of the instantaneous rate of formation of total hydroperoxides expressed by titer vs. the square root of hydroperoxide titer obtained in stirred flow reactor oxidation experiments at 180°C for PETH materials of different purities. Examination of these plots reveals that the purified PETH

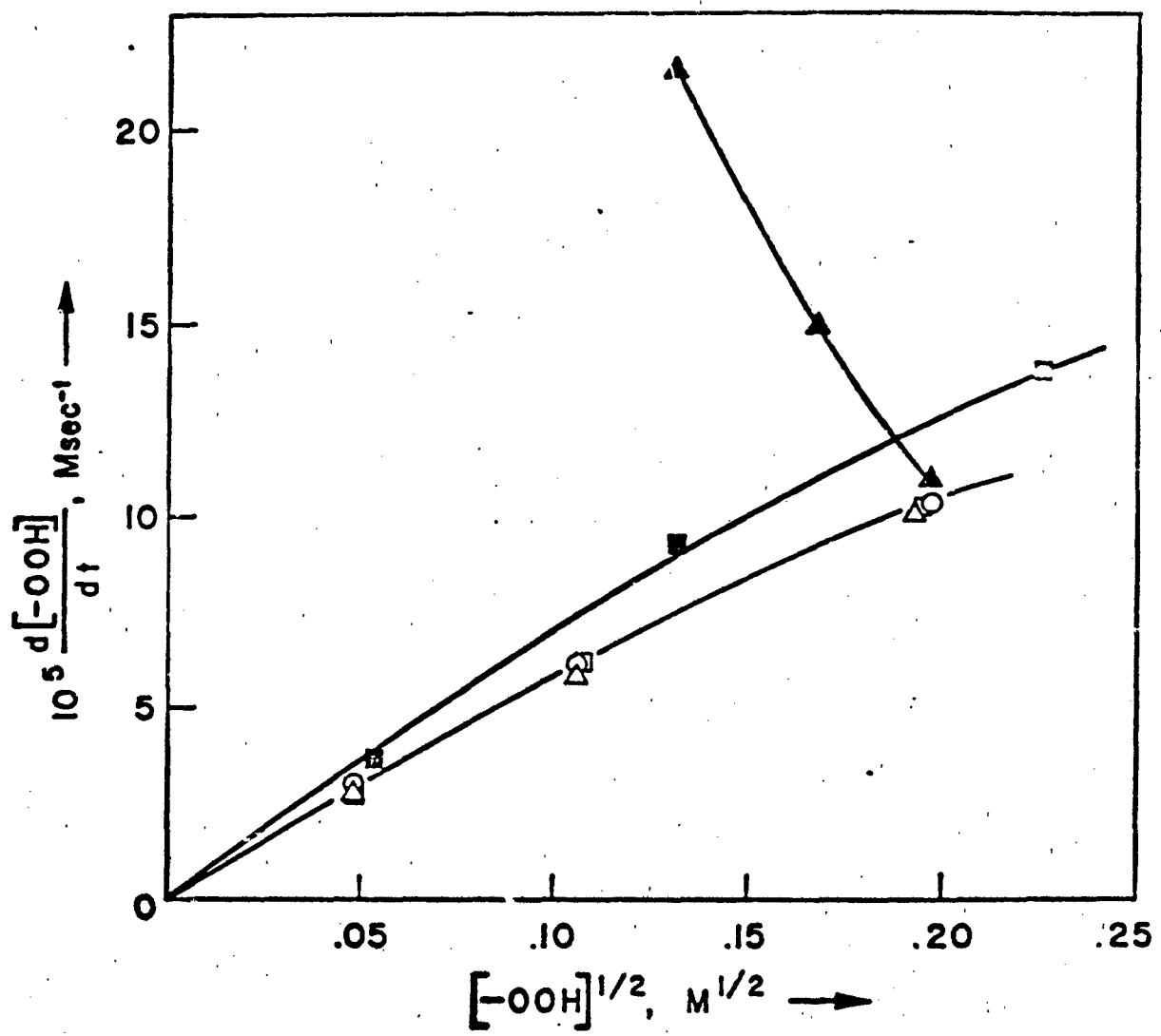


Figure 1. Rate of formation of hydroperoxide for PETH samples of different purities. ▲ - technical grade; ■ - distilled; □ - PDP-1; △ - PDP-2; ○ - PDPDP.

materials PDP-1, PDP-2, and PDPDP exhibited, in the range of hydroperoxide concentrations studied, essentially equal rates of hydroperoxide formation at a given hydroperoxide titer. Since further purification did not change the measured oxidative reactivity, the PETH material purified by the PDP procedure was judged to be of sufficient purity for this study and was, therefore, prepared in large quantity by collecting and combining eluents equivalent to PDP-1 and PDP-2. The PDP PETH material was used throughout this work unless otherwise noted.

Optical absorption spectra of the PETH materials evaluated by a kinetic oxidation method revealed that absorption at the wavelengths between 255 and 500 nm, in the range where saturated alkyl esters do not absorb, decreased with increasing degree of purification. Thus, absorption in the above spectral range was used for monitoring the purity during the preparation of PDP material.

The NMR and IR spectra and C and H analyses of the PDP and PDPDP PETH materials did not reveal any presence of impurities. The LiAlH_4 reductions of these materials (cf. Table I) indicated that PDP and PDPDP PETH contained pentaerythrityl heptanoate-hexanoate impurities (ca. 1.6% of total number of side chains were hexanoyloxy) and trace amounts of acyl chain substituted impurities (< 0.2% in PDP and < 0.1% in PDPDP) which upon oxidation and subsequent LiAlH_4 reduction presumably yield 1,x-heptanediols.

Determination of PETH Density. The density of PETH (g/ml) determined by pycnometry is 0.9746 at 25.9°C , 0.8732 at 160°C , 0.8577 at 180°C , 0.8425 at 200°C ,

and 0.8269 at 220°C. The pycnometer volume at 160°C was determined using n-hexadecane ($\rho_{160} = 0.6745$ g/ml (10)); the volume at 180, 200 and 220°C was calculated from the volume at 160°C using the coefficient of thermal volumetric expansion for glass ($\beta = 2.5 \times 10^{-5} \text{ K}^{-1}$ (11)).

Stirred Flow Microreactor Experiments. The apparatus and procedures are described elsewhere (8).

Batch Reactor - Design and Procedure. The batch reactor, whose design resembled that of the stirred flow reactor (8), was constructed from a 100 ml round bottom flask (55 mm i.d.) with a lengthened neck (25 mm i.d. x 130 mm). A glass tube through the neck led down to an eccentrically located inner sphere (20 mm o.d.) which was perforated in its lower spherical segment (7 holes, 0.5 mm diameter). This inner sphere was used to continuously introduce oxygen or inert gas into the reactor and insure efficient mixing of the reaction mixture in the flask. The batch reactor was used with the same gas supply system and constant temperature bath as those used for the stirred flow reactor. Increased heat transfer with the constant temperature bath was accomplished using a vigorous flow of the thermostating fluid around the outside reactor wall. The temperature in the reactor was measured continuously using a glass shielded Chromel-Alumel thermocouple.

The purified PETH (35 or 40 ml) was introduced under a flow of argon into the flask and mixed using the argon flow during the heating period followed by oxygen during the oxidation period. Oxygen was introduced into the reactor at a flow rate

of $24.5 \text{ ml. sec}^{-1}$ at 180° , argon at $21.6 \text{ ml. sec}^{-1}$ at 180° . Solid samples of the antioxidant, 4,4'-methylenebis(2,6-di-tert-butylphenol), were introduced into the reactor at varying degrees of oxidation by means of a small glass ladle. The antioxidant added into the reactor was completely dissolved within a few seconds. Aliquots of the reaction mixture were withdrawn from the reactor at various time intervals, quenched to room temperature, and analyzed for hydroperoxide, (-OOH), by titration.

Gas Chromatography. GLC analyses were performed with an F & M Model 310 or a Hewlett-Packard Model 5730A Gas Chromatographs operating in the flame ionization mode using an all glass column system and equipped with an Autolab System IV Computing Integrator.

Reaction products obtained from the reduction procedures described below were analyzed by GLC on a 6 ft x 4 mm glass column using 3% Silar-10C, 3% OV-1 or 3% OV-17 on 100-120 mesh Gas-Chrom Q, obtained from Applied Science Laboratories, Inc. The details of GLC analyses were described previously (12).

Gas Chromatography-Mass Spectrometry. Electron impact and chemical ionization mass spectra were obtained on a VG Micromass MM 16 with an Incos Data System (Data General Computer) following gas chromatographic separations of reaction products obtained from the reduction and derivatization procedures with a 3% Silar-10C or a 3% OV-101 column (glass tubing; 10 ft x 4 mm).

Lithium Aluminum Hydride Reduction - Method I. LiAlH_4 (1.2 g) was slowly added to the solution of the PETH sample (2 g) in distilled diethyl ether (50 ml)

stirred in a glass-stoppered 200 ml round bottom flask. After stirring for at least 5 hours at room temperature, $\text{Na}_2\text{SO}_4 \cdot 10\text{H}_2\text{O}$ (8.2 g) was slowly added to this mixture which contained dark grey solids. The color of the solids gradually lightened. After 16 hours all solids were entirely white and crystalline. Ether was then added to fill the flask and stirring continued for at least 15 min. The solids were allowed to settle and ca. 85 percent of the supernatant liquid was transferred to another round bottom flask. The solution was then evaporated from an ice bath using a rotary evaporator and water aspirator (final pressure equal to 15 to 20 torr). This same cycle of filling with ether, stirring, supernatant transfer, and evaporation was repeated twice more. The total residue was typically two colorless liquid phases (presumably mainly 1-heptanol and water) and a slight amount of solid carried over during supernatant transfer. This liquid residue was quantitatively dissolved in acetone to give a 10 ml sample for the subsequent GLC analysis.

Figure 2a presents a typical gas chromatogram obtained from the separation of the products of the method I LiAlH_4 reduction of an oxidized sample of PETH. The peaks designated A through G have been identified by comparison of their chromatographic retention times with those of standard samples and by their $M+1$ ions in combined gas chromatography-chemical ionization mass spectrometry.

Figure 2a shows that the method I procedure allows determination of 1-heptanol, 1-hexanol and 1,3- through 1,7-heptanediols. Heptanetriols, which are sparingly soluble in ether, were not detected by this method.

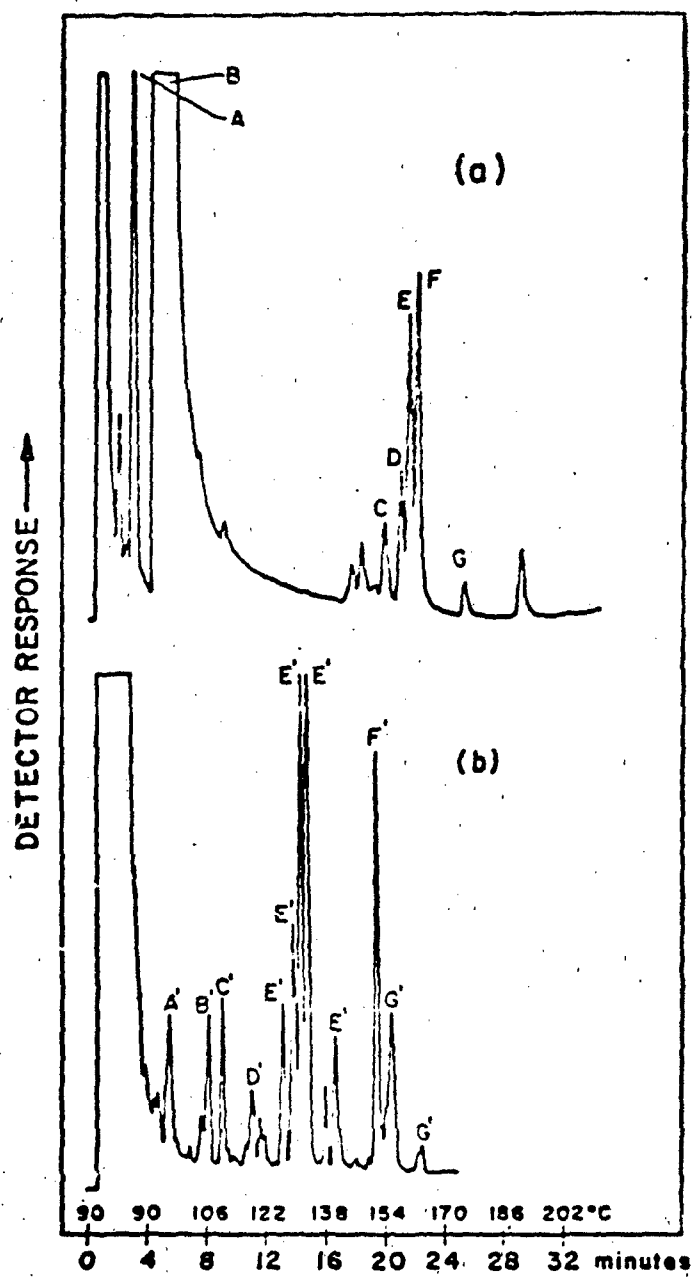


Figure 2. GLC of products from the LiAlH_4 reductions of an oxidized PETH sample.

a) Method I reduction. The compounds giving the lettered peaks are: A — 1-hexanol; B — 1-heptanol; C — 1,3-heptanediol; D — 1,4-heptanediol; E — 1,5-heptanediol; F — 1,6-heptanediol; G — 1,7-heptanediol.

b) Method II reduction. The lettered peaks correspond to the pertrimethylsilylated derivatives of the following compounds: A' — 1,3-butanediol; B' — 1,4-butanediol; C' — 1,4-pentanediol; D' — 1,5-pentanediol; E' — heptanediols; F' — pentaerythritol; G' — heptanetriols.

The quantitative recovery of products from this LiAlH_4 reduction was assessed by control experiments with pure and oxidized PETH and with standard solution of heptanediols in PETH (Table I). Recovery of 1-heptanol plus 1-hexanol was essentially quantitative (better than 97%) after three supernatant liquid transfers. Recoveries of 1,4-, 1,5- and 1,7-heptanediols which were initially added in PETH were also essentially quantitative (better than 95% after only two supernatant liquid transfers). For each of these five compounds analyzed and for the sum of the 1,4-, 1,5-, and 1,6-heptanediols the amount found in the supernatant liquid portions obtained after the first and second transfers agreed with the amounts expected from the weighings of those portions. This demonstrates that these compounds, at the concentrations used, were not strongly adsorbed by the solids during the supernatant liquid transfer.

Lithium Aluminum Hydride Reduction - Method II. The method II procedure was adopted from the work of Adams and Govindachari (13). LiAlH_4 (0.86 g) was slowly added to the solution of the PETH sample (2 g) in distilled diethyl ether (60 ml) stirred in a glass stoppered 200 ml round bottom flask. After stirring for at least two more hours, the flask was cooled in an ice-water bath and 3.25 ml of distilled water was slowly added. All solids became white within ca. 2 hours. Subsequently, 65 ml of 10% (v/v) aqueous H_2SO_4 was added to the ice-water cooled flask, whereupon the solids rapidly dissolved. The aqueous layer was separated and the ether layer was washed with three 5.4 ml portions of distilled water. The combined aqueous solution was cooled and neutralized with 50% aqueous NaOH to pH ca. 7. The resulting precipitate was filtered and repeatedly washed with distilled

TABLE I.
 LiAlH_4 Reduction of PETH - Method I. Control Experiments

Reduced PETH Sample	Supernatant		Recovery, wt. %			
	Liquid Transfer	Supernatant Liquid	1-Heptanol ^a	1-Heptanol ^{a,b}	1-Hexanol ^a	1-Hexanol ^{a,b}
PDP	1	76.8	76.6	-	76.6	
	1 + 2	96.6	95.9	-	95.9	
PDP	1	81.7	78.5	-	78.5	
	1 + 2	97.0	92.8	-	92.8	
PDP	1 + 2 + 3	99.7	95.8	1.4	97.2	
Heptane nediols ^d	1	86.2	84.2	1.4	85.6	83.8
	1 + 2	98.9	96.6	1.6	98.2	95.0
PDPDP	1 + 2 + 3	99.7	98.1	1.7	99.8	
PDPDP, Oxidized ^e	1	86.4	85.8	1.5	87.3	
	1 + 2	98.7	97.5	1.6	99.1	

^a Calculated assuming the samples were pure PETH.

^b Corrected for the difference in molecular weights of 1-hexanol and 1-heptanol.

^c Corrected for the heptanediol yields from the PETH sample alone.

^d Initial concentrations of 1,4-, 1,6-, and 1,7-heptanediols were 177, 140 and $62.6 \times 10^{-4} \text{M}$, respectively.

^e PDPDP oxidized in SFR at 180°C , residence time 368 sec.

water. The combined filtrate was then concentrated to ca. 80-100 ml of solution remained. This solution then was continuously extracted with ether for at least 48 hours using a simple extraction column (14). The supernatant ether extract was quantitatively removed from some undissolved solid, presumably pentaerythritol, and rotary evaporated to leave a residue which was dissolved in acetone to give a 5 ml sample for subsequent analysis by GLC, either directly or after trimethylsilylation (8, 12).

In Figure 2b is presented a gas chromatogram of trimethylsilylated products. The indicated peaks (A'-G') were identified by comparison of their chromatographic retention times with those of standard samples and/or by their M+1 ions in combined gas chromatography-chemical ionization mass spectrometry. Figure 2b shows that the method II procedure in addition to the products quantitatively determined by the method I allows determination of 1,3- and 1,4-butanediols, 1,4- and 1,5-pentanediols, and heptanetriols.

Product recoveries in the method II reduction procedure were assessed from the results of two sequential reductions. An oxidized PETH sample (PDDP, 180°C, residence time 368 sec) was first reduced and the products were analysed as described above. Products from this first reduction were then combined with unoxidized PETH to give a sample which contained known concentrations of reduced oxidation products. This sample was then subjected to a second method II reduction followed again by analysis. From these analyses it was found that the recoveries of diols were generally 60-70 percent and the recovery of heptanetriols was ca. 80

percent. Thus, the method II reduction procedure did not give quantitative product recoveries.

Determination of Hydroperoxide and Acid Products. The total yields of hydroperoxide groups, (-OOH), were determined by the iodometric titration of Mair and Graupner (Method I) (15).

The total yields of organic acids, (-COOH), were determined by potentiometric acid-base titration. An appropriate volume of oxidized PETH was dissolved in 15 ml toluene and the solution mixed with 23 ml of 2.7 M KCl under argon. Two milliliters of 0.01 N $\text{Ba}(\text{OH})_2$ was then added and the two phases vigorously mixed under argon for ca. 10 min. Following phase separation, the resulting basic aqueous phase was titrated with a 0.01 N HCl solution using a Metrohm E535/6 Recording Titrator apparatus. The total acid concentration was calculated from the difference in the volumes of HCl titrant utilized for the PETH sample and for a blank without the PETH sample. Purified PETH samples yielded end points identical to those of the blank sample.

Determination of Individual Alcanoic Acid Products. The concentration of C_2 through C_6 alcanoic acids were determined by the following method. The PETH sample (1 to 10 ml) was diluted 5 to 20 fold with toluene and extracted in a 50 ml separatory funnel first with 10 ml of aqueous KOH at $\text{pH} \approx 10$ and then three times with 10 ml of distilled water. The aqueous KOH was prepared directly in the funnel by adding 10 ml of distilled water and 2-3 drops of 20% (w/v) of methanolic KOH.

The combined extracts were evaporated to dryness. Potassium carboxylates obtained by this procedure were derivatized using 0.20 mmole of α,β -dibromoacetophenone and 0.02 mmole of dicyclohexyl-18-crown-6 ether both in one ml of acetonitrile (Applied Science Laboratories) (16). The resulting p-bromophenacyl esters were dissolved in 5 ml chloroform and analyzed by GLC on an OV-225 column.

The concentration of heptanoic acid was determined by direct injection of the PETH sample onto an AT-1000 (Altech Associates) packed GLC column since the above extraction method gave additional heptanoic acid formed from PETH.

Each of these two methods of acid determination gave an accurate analysis for standard PET_n solutions of the alkanoic acids for which it was employed.

Acid Exchange Experiment. A sample of PETH containing 45×10^{-4} M each of C₅ and C₆ acids was heated under argon in a batch reactor at 180°C. Samples were taken as a function of time and analyzed for C₅, C₆, and C₇ acids. In a 400 second time period less than 1×10^{-4} M of C₇ acid was detected. The C₅ and C₆ acid concentrations decreased to 30 and 36×10^{-4} M, presumably due to evaporation.

RESULTS AND DISCUSSION

Reaction Scheme. A reaction scheme which accounts for the results obtained in the present study of the autoxidation of PETH at 180 to 220°C is presented in Figure 3. In the scheme, RH represents PETH; ROOH represents 3- through 7- mono-hydroperoxy derivatives of PETH; HOOROOH and HOOR=O represent α, γ - and α, δ -dihydroperoxy and hydroperoxyoxo derivatives of PETH², and R \cdot , RO \cdot , RO₂ \cdot , HOOR \cdot , HOOROOH, HOORO \cdot , O=RO \cdot , and HOORO₂ \cdot represent carbon, alkoxy and peroxy radicals corresponding to the above listed PETH derivatives.

This reaction scheme is somewhat simpler but kinetically equivalent to that proposed earlier for the autoxidation of n-hexadecane at 120-180°C (8, 18). In addition to established initiation,³ propagation,⁴ and termination reactions the scheme includes intramolecular α, γ and α, δ hydrogen abstraction reactions (4) and (4*) leading to the formation of a variety of disubstituted autoxidation products and

- 2 α, γ designates 3,5-, 4,6-, and 5,7-substituted products and α, δ designates 3,6- and 4,7-substituted products.
- 3 It is likely that the various hydroperoxide products decompose at different rates. Thus, k_1 represents a complex composite first order rate constant for radical formation.
- 4 Intermolecular hydrogen abstraction reaction (3) includes abstractions from other heptanoyloxy groups of the same molecule.

-OOH	$\xrightarrow{k_1}$	$\text{XO} \cdot + \text{OH}$	SLOW	(1)
$\text{XO} \cdot \} + \text{RH}$	$\xrightarrow{k'_1}$	$\{\text{HOH} + \text{R} \cdot$	FAST	(1')
$\text{R} \cdot + \text{O}_2$	$\xrightarrow{k_2}$	$\text{RO}_2 \cdot$	FAST	(2)
$\text{RO}_2 \cdot + \text{RH}$	$\xrightarrow{k_3}$	$\text{ROOH} + \text{R} \cdot$	SLOW	(3)
$\text{RO}_2 \cdot$	$\xrightarrow{k_4}$	$\cdot\text{ROOH}$	SLOW	(4)
$\cdot\text{ROOH} + \text{O}_2$	$\xrightarrow{k'_2}$	$\text{HOORO}_2 \cdot$	FAST	(2')
$\text{HOORO}_2 \cdot + \text{RH}$	$\xrightarrow{k'_3}$	$\text{HOOROOH} + \text{R} \cdot$	SLOW	(3')
$\text{HOORO}_2 \cdot$	$\xrightarrow{k'_4}$	HOOROOH	SLOW	(4*)
HOOROOH	$\xrightarrow{k_5}$	$\text{HOOR=O} + \text{OH} \cdot$	FAST	(5)
$2\text{XO}_2 \cdot$	$\xrightarrow{2k_6}$	$\text{>C=O} + \text{O}_2 + \text{CH}-\text{OH}$	SLOW	(6)
$\alpha, \gamma\text{-HOOR=O}$	$\xrightarrow[O]{k_7}$	$-\text{COOH} + -\text{C}-\text{CH}_3$	SLOW	(7)

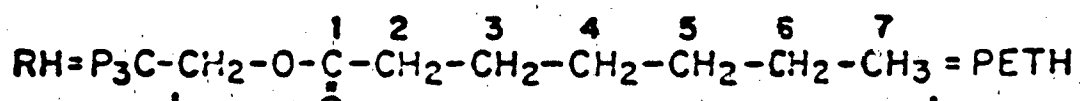
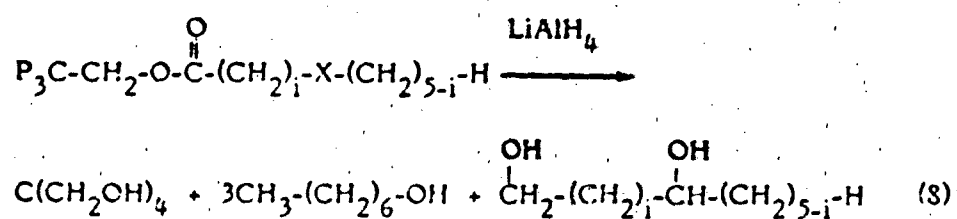


Figure 3. Reaction scheme.

hydroxy radicals via reactions (2'), (3'), and (5). The most important of the disubstituted products are α, γ -hydroperoxyketone species. These species are precursors of acid and methyl ketone products formed via cleavage reaction (7).

Product Analysis. Table II summarizes the results from the analyses of total hydroperoxide and acid products in autoxidized PETH samples obtained from the stirred flow reactor experiments at 180, 200, and 220°C. The results show that the yields of hydroperoxide and acid products are independent of oxygen pressure at residence times up to 365 seconds at 180°C and up to 70 seconds at 200°C if the partial pressure of oxygen is greater than 90 kPa. In the 200°C experiments at longer residence times and in all 220°C experiments the yields of hydroperoxide and acid products increase with increasing oxygen pressure.

The results from analyses of LiAlH_4 reduced samples of autoxidized PETH are summarized in Table III. Upon LiAlH_4 reduction the monosubstituted products of the PETH autoxidation, ROOH , ROH , and R=O , are converted to pentaerythritol, 1-heptanol, and 1, ω -heptanediols, i.e.,



where i is 1, 2, 3, 4 or 5 and X represents $\text{CH}-\text{OOH}$, $\text{CH}-\text{OH}$, or $\text{C}=\text{O}$. The absence of 1,2-heptanediol in the reduced samples suggests very low reactivity of hydrogens in

TABLE II.
Hydroperoxide and Acid Products from the Autoxidation
of PETH

Temperature (°C)	Residence Time (sec)	Oxygen Pressure (kPa)	(-OOH) ^a (M/10 ⁴)	(-COOH) ^a (M/10 ⁴)	PETH ^b
180	77	119	23.1	3.6	PDPDP
	77	121	24.0	-	
	79	118	23.2	3.6	PDP-2
	81	119	23.6	3.5	PDP-1
	182	113	113	30	PDPDP
	185	114	115	29	PDP-1
	187	113	112	30	PDP-2
	188	116	125	-	
	363	110	385	-	DP
	364	111	364	134	
	365	112	378 ^c	143	PDP-1
	367	110	374	136	PDP-2
	368	109	384	146	PDPDP
	366	82	403	-	DP
200	20	143	23.8	3.4	
	36	128	71	15	
	53	123	128	31	
	69	121	208 ^c	63	
	69	90	206	57	
	70	24	97	14	
	101	119	415	148	
	103	89	382	118	
	220	191	208	60	
	17	146	178	50	

^aAt the temperature of the autoxidation

^bPDP purity material used except as otherwise noted.

^cTitration of water extract of 365 (69.1) sec sample gave (H₂O₂) equal less than 0.045 (-OOH) (0.03 (-OOH)).

TABLE III.
Heptanediols and Heptanetriols from LiAlH_4 Reduction^a
of PETH Samples

Residence Time (sec)	(-OOH)	(1, x-heptanediol)					[HD]	[HT] ^{b,c}
		1,3-	1,4-	1,5- (N/10 ⁴)	1,6-	1,7-		
180°C								
77	23	-	1.2	2.4	4.1	(0)	7.7	
77	24	1.1	0.6	2.9	3.5	(0)	8.1	
182	113	5.2	5.3	14.7	21.1	1.8	48	
188	125	5.2	6.4	17.0	21.7	2.4	53	
368	384	19.9	27.6	62	77	9.4	196	
368	384	(11) ^b	(21) ^b	(57) ^b	(72) ^b	(9.4) ^b	(170) ^b	(31) ^b
200°C								
20	24	(3) ^d	(2) ^d	(3) ^d	(2) ^d	(1) ^d	(11) ^d	
36	71	5	4	11	19	(1)	40	
53	128	2	6	17	25	3	53	
69	208	6	11	31	38	5	91	
101	415	30	36	80	93	13	252 (220) ^e	
70 ^f	97	11	8	17	15	1	52	

^a Method I, except as footnoted.

^b Method II LiAlH_4 reduction; due to nonquantitative character of this method values are only approximate.

^c Analyzed as per-trimethylsilylated derivatives.

^d Due to substantial blank sample corrections values are only approximate.

^e Value in brackets was obtained by the cutting and weighing of appropriate CLC peaks.

^f PETH sample from the reduced oxygen pressure experiment (24 kPa).

position 2 of heptanoyloxy group. This finding is consistent with the results reported by Sniegoski (4) from the autoxidation of neopentyl hexanoate and by Anbar et al. (17) from their studies of reactivities of various carbon-hydrogen bonds in abstraction reactions by hydroxy radicals.

At sufficiently long kinetic chain length the yields of 1, x-heptanediols from LiAlH_4 reductions of ROH and R=O arising from initiation and termination reactions are low and the sum of the yields of 1, x-heptanediols, HD, may be approximately equated with the yields of monohydroperoxide products formed in reaction (3), i.e.,

$$(HD) \approx (ROOH) \quad (II)$$

The data of Table III show that HD accounts for only 30 to 50 percent of the total hydroperoxide titers at 180°C and for 40 to 60 percent at 200°C and that the contribution of hydrogen peroxide to the titer amounts to less than 5 percent of the total. Based upon the results of our studies of n-hexadecane autoxidation (8), the residual hydroperoxide titer is expected to come in large part from polysubstituted PETH derivatives arising from the intramolecular hydrogen abstraction reactions.

In analogy with the LiAlH_4 reduction of monosubstituted products (cf. eq 8), the disubstituted products HOOROOH and HOOR=O yield upon LiAlH_4 reduction

pentaerythritol, 1-heptanol, and various isomeric 1,x,y-heptanetriols. The application of the method II LiAlH_4 reduction, although not quantitative⁵, led to identification of heptanetriols, HT, in a reduced sample obtained at the residence time 368 seconds and 180°C . Although the yield, $31 \times 10^{-4}\text{M}$, represents only about 20 percent of the residual titer⁶, the result does support the notion that large amounts of primary disubstituted products are formed in the autoxidation of PETH.

Table IV summarizes the results obtained from the analyses of the individual n-alkanoic cleavage acids in the autoxidized PETH and from the analyses of some low molecular weight diols in trimethylsilylated samples obtained from the non-quantitative method II LiAlH_4 reduction of selected oxidized PETH samples. The isomeric composition and the concentrations of the low molecular weight diols relative to the concentrations of n-alkanoic acids in the PETH autoxidation are explained by the novel sequence of reactions (4*), (5), and (7). This sequence is also consistent with the results obtained in the study of the autoxidation of n-hexadecane in our laboratory (8, 18). In that system it was observed that the rapid first order decay of α, γ -hydroperoxyketone species or their equivalent⁷ resulted in the simultaneous formation of ca. equal amounts of cleavage methyl ketones and n-alkanoic acids. The results from the kinetic analysis of total hydroperoxide plus acid

5. cf. Experimental Section for recoveries.

6. Based on the distribution of disubstituted oxidation products calculated using the values of rate parameters from Table VI.

7. The half life of α, γ -hydroperoxyketone species or their equivalent was found to be equal to 95 seconds at 180°C .

TABLE IV.

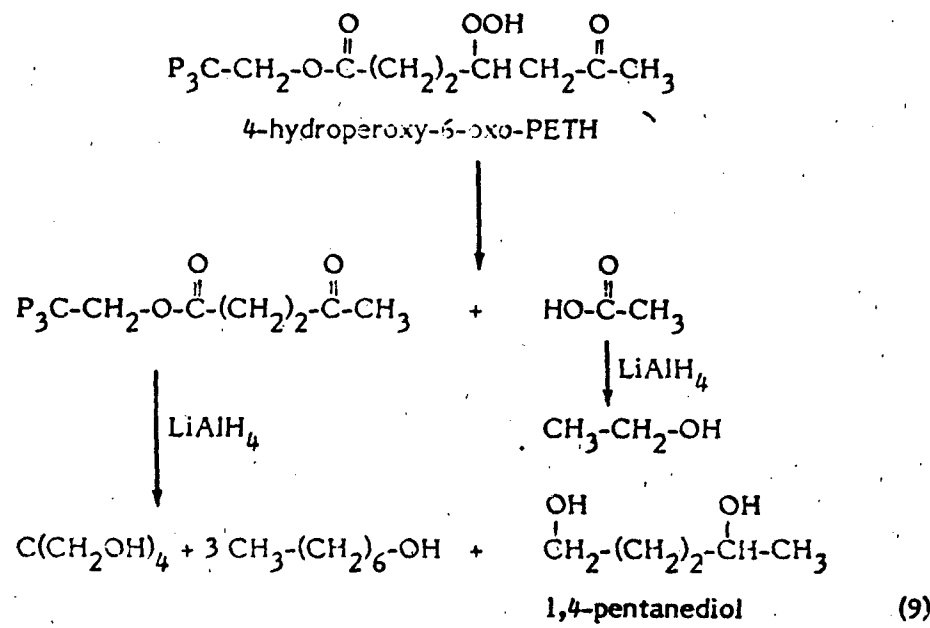
Scission Products from the Autoroxidation of PETH at 180°C

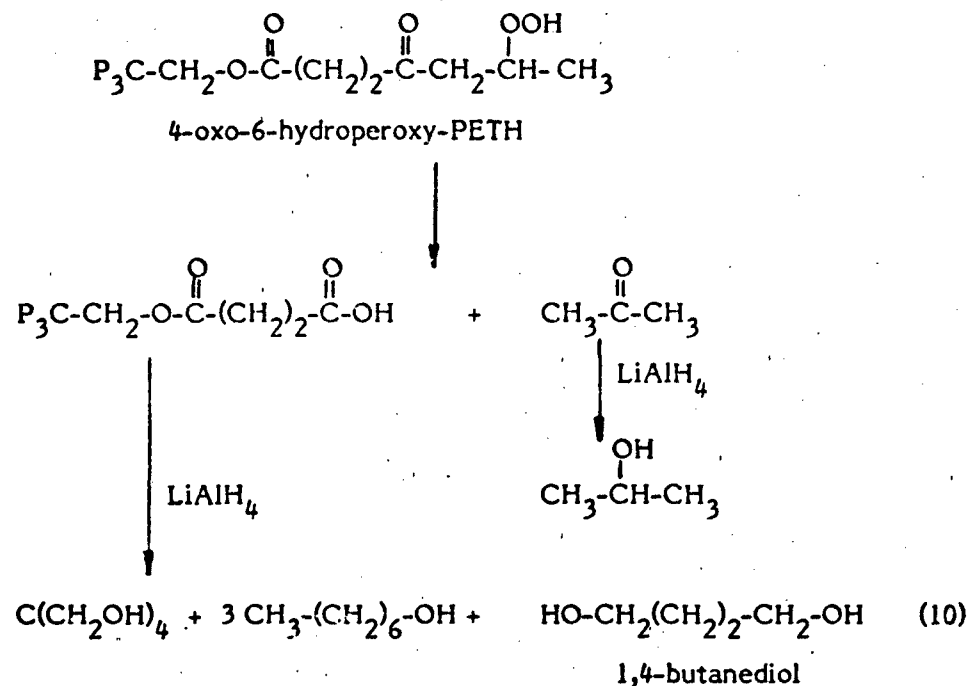
Residence Time (sec)	(-COOH) (M/10 ⁴)	(Alkanoic Acids) (M/10 ⁴)						(Diols) ^a (M/10 ⁴)		
		C ₂	C ₃	C ₄	C ₅	C ₆	C ₇	$\Sigma(C_2-C_7)$	1,3-butane	1,4-butane
182	30	6.3	3.2	0.6	0.25	0.20	12.5	23	-	-
368	146	21.5	12.5	2.5	1.3	1.0	42	81	-	-
365	143	-	-	-	-	-	-	-	18	21
									23	9

^aObtained from the Method II LiAlH₄ reduction.

formation (cf. Figure 5) strongly suggest the concurrent formation of one molecule of acid and consumption of one hydroperoxy group. Based upon this observation, the unstable intermediates in the PETH system are likely to be α, γ -hydroperoxyketone species, α, γ -HOOR=O.

To illustrate this transformation in the PETH system, consider the decomposition of two isomeric α , γ -hydroperoxyketone species, 4-hydroperoxy-6-oxo-PETH and 4-oxo-6-hydroperoxy-PETH, followed by the LiAlH_4 reduction of resulting cleavage product:





Thus, acid and methylketone products formed in decomposition reactions of α , γ -hydroperoxyketone species will consist of low molecular weight n-alkanoic acids and methyl ketones and high molecular weight carboxy and acetyl substituted tetraesters. In Table V are summarized the cleavage products expected to be formed from all possible α , γ -substituted hydroperoxyketone derivatives of PETH and the products from their LiAlH_4 reductions. The products are listed in order of expected decreasing yields and with a designation in brackets of those products analyzed in this work. The occurrence of the proposed mechanism requires the yield of 1,4-butanediol to be equal to that of C_2 acid and the yield of 1,3-butanediol to that of C_3 acid. The results in Table IV are in good agreement with that requirement in the first case but in the second case the yield of 1,3-butanediol is somewhat larger than that of C_3 acid. Nevertheless, the substantially higher yields

TABLE V.

Scission Products Expected from the Decomposition of α,γ -Hydroperoxyketone
PETH Oxidation Products

α,γ -Hydroperoxyketone PETH Derivative $\xrightarrow{x, Y-100R=0}$	Original $\underline{x-RO_2}$ \underline{x}	Type/Number of H Available for Intramolecular Abstraction	Scission Products			Products from LiAlH_4 Reduction Of		
			Acids	Methyl Ketones	Acids	Methyl Ketone		
6-oxo-4-hydroperoxy-	6-	4-/2			$\text{CH}_3\text{CO}-$ tetraester			$1,4\text{-pentanediol}$
5-oxo-3-hydroperoxy-	5-	3-/2			$\text{CH}_3\text{CO}-$ tetraester			$1,3\text{-butanediol}$
4-oxo-6-hydroperoxy-	4-	6-/2			-COOH tetraester			
3-oxo-5-hydroperoxy-	3-	5-/2			CH_3COCH_3			
5-oxo-7-hydroperoxy-	5-	7-/3 (primary)			$\text{CH}_3\text{COC}_2\text{H}_5$			
7-oxo-5-hydroperoxy-	7- (primary)	5-/2			CH_3CHO			$1,5\text{-pentanediol ethanol}$
			C_1		$\text{CH}_3\text{CO}-$ tetraester			$1,5\text{-hexanediol}$

of C_2 and C_3 acids than those of C_4 – C_6 acids, occurrence of high yields of non-terminal diols, 1,3-butanediol and 1,4-pentanediol, and finally substantially lower yield of 1,5-pentanediol than that of 1,4-butanediol virtually demand that cleavage principally occurs via reactions of α , γ -substituted difunctional oxidation products. If cleavage processes were occurring via conventional β -scission of alkoxy radicals one would expect 1) a high yield of 1,5-pentanediol, 2) monotonically decreasing yields of lower terminal diol homologues, and 3) monotonically decreasing yields of acids with increasing carbon number.

A summation of the yields of C_2 – C_7 acids and the yields of carboxy substituted tetraesters, estimated from the yields of terminal diols assuming that the yield of 1,3-propanediol is equal to that of 1,4-butanediol, gives a value equal to 90 percent of the titrated acids in the 365–8 sec samples.

Reaction pathways which might account for the large amounts of C_7 acid are intra- and intermolecular exchange reactions of cleavage acids with PETH molecules. From the results of the exchange experiment described in the experimental section, the occurrence of facile intermolecular exchange reactions with the low molecular weight cleavage acids does not appear likely. It is then plausible that the carboxy groups attached to the PETH moiety are undergoing various intra-and intermolecular reactions to produce the C_7 acid. The elucidation of the mechanism of such reactions is a complex task, beyond the scope of the present work. Subsequent kinetic analyses are then based on the assumption that all acid products originate from a cleavage process involving decomposition of α , γ -substituted hydroperoxyketone oxidation products.

Rate of Initiation. For the purpose of subsequent kinetic analyses of the autoxidation of PETH it is desirable to estimate the rates of radical formation, R_i , as a function of hydroperoxide concentration³ and to compare the values of R_i obtained for PETH and n-hexadecane systems under the same reaction conditions.

The present method of determination of R_i is based on the measurement of the length of inhibition period, t_{inh} , caused by the addition of varying amounts of 4,4'-methylenebis (2,6-di-*tert*-butylphenol), BPH, to the autoxidizing substrate. Upon the introduction of BPH the steady state concentration of peroxy radicals in the system is decreased by many orders of magnitude and the formation of hydroperoxide products is strongly inhibited until the initial antioxidant and its antioxidant reactive products are all consumed. At that point the autoxidation of substrate resumes. At a constant rate of radical formation the value of $(BPH)_0/t_{inh}$ is equal to R_i/n where $(BPH)_0$ is initial concentration of BPH and n , the stoichiometric factor (19), is equal to the total number of peroxy radicals consumed by reactions with a molecule of BPH and with molecules of the antioxidant reactive products resulting from BPH-peroxy radical interactions. At 60°C n for BPH is equal to 4.0 (20).

Figure 4 shows the results from a series of batch reactor experiments in which values of t_{inh} were determined as functions of $(BPH)_0$ and of the average concentration of hydroperoxides⁸ during the period of strong inhibition, $(-OOH)$, for

8 The decrease from the initial hydroperoxide concentration during the inhibition period was less than 10 percent.

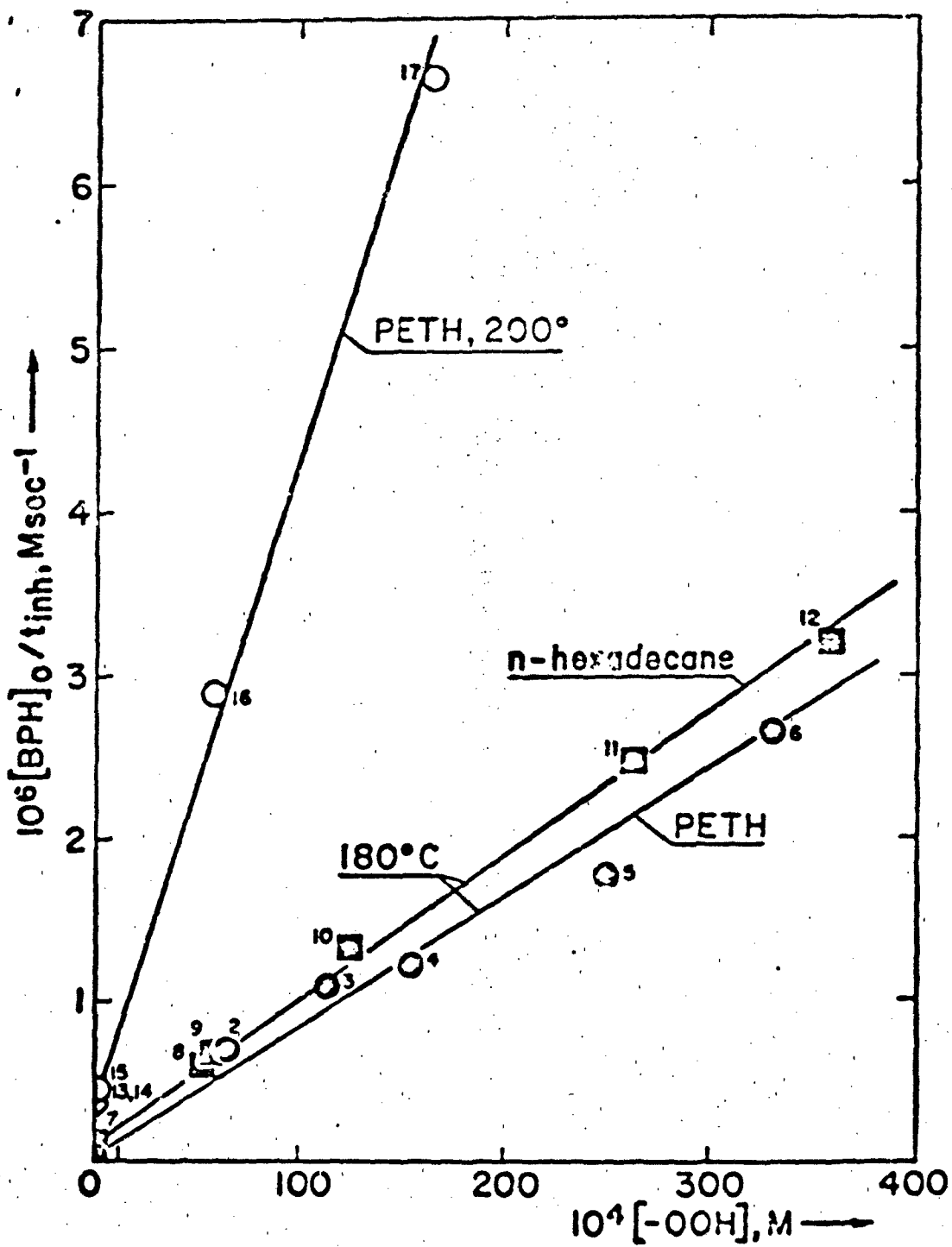


Figure 6. Plot of $(BPH)_0/t_{inh}$ versus $(-\text{OOH})$. The numbered points correspond to the following $(BPH)_0$ ($\text{M}/10^4$): 1-1.9, 2-7.5, 3-17.3, 4-62, 5-64, 6-31, 7-2.1, 8-19.5, 9-13.0, 10-22, 11-38, 12-76, 13-5.3, 14-10.6, 15-13.7, 16-12.8, 17-40.

PETH system at 180 and 200°C and for n-hexadecane at 180°C. For both systems

$$\frac{(BPH)_0}{t_{inh}} = \frac{R_1}{n} = \underline{a} + \underline{b} (-OOH) \quad (III)$$

where \underline{a} ($M \text{ sec}^{-1}$) and \underline{b} (sec^{-1}) are at 180°C equal to 5×10^{-8} and 8×10^{-5} for PETH and 1×10^{-7} and 9×10^{-5} for n-hexadecane. The results from a limited number of experiments with PETH at 200°C suggests the same relationship with values of \underline{a} equal to ca. $4 \times 10^{-7} M \text{ sec}^{-1}$ and \underline{b} ca. $4 \times 10^{-4} \text{ sec}^{-1}$.

The values $n \underline{a}$ and $n \underline{b}$ may be interpreted as equal to the rate of formation of free radicals from the direct reactions of substrate with oxygen and to the composite first order rate constant for the homolysis of hydroperoxide products, $2k_1$, respectively. If the value of n is equal to 4.0 in both PETH and n-hexadecane at 180 and 200°C, then $(BPH)_0/t_{inh}$ is equal to $R_1/4$ and the values of k_1 are found to be equal to $1.6 \times 10^{-4} \text{ sec}^{-1}$ for PETH and to $1.8 \times 10^{-4} \text{ sec}^{-1}$ for n-hexadecane at 180°C and to $8 \times 10^{-4} \text{ sec}^{-1}$ for PETH at 200°C.

Kinetic-Analysis. A kinetic analysis for the sequence of reactions (1) -- (7) presented in Figure 3 leads to the following rate expressions for formation of hydroperoxide, $-OOH$, acid, $-COOH$, and monohydroperoxy, $ROOH$, and α, γ -hydroperoxyoxo, α, γ -HOOR=O, substituted PETH autoxidation products:⁹

9 Eqs. (IV), (VI), and (VII) were derived using the steady state approximation for each peroxy radical at sufficiently long kinetic chain length and assuming k_3 to be equal to k_3' and k_7 to be much greater than k_1 . Kinetic chain lengths in the range of conversions studied were equal to or larger than 11 (8) at 180 (200)°C.

$$\frac{d(-\text{OOH})}{dt} + \frac{d(-\text{COOH})}{dt} = \left(\frac{k_1}{k_6}\right)^{\frac{1}{2}} k_3(\text{RH}) \frac{\frac{k_{4-\alpha, \gamma}}{k_3(\text{RH})} \left(2 + \frac{k_{4-\alpha, \gamma}}{k_3(\text{RH})}\right) + \frac{k_{4-\alpha, \delta}}{k_3(\text{RH})} \left(2 + \frac{k_{4-\alpha, \delta}}{k_3(\text{RH})}\right)}{1 + \frac{k_{4-\alpha, \gamma}}{k_3(\text{RH})} + \frac{k_{4-\alpha, \delta}}{k_3(\text{RH})}} (-\text{OOH})^{\frac{1}{2}}$$

$$= \eta(-\text{OOH})^{\frac{1}{2}} \quad (\text{IV})$$

$$\frac{d(-\text{COOH})}{dt} = k_7(\alpha, \gamma - \text{HOOR} = \text{O}) \quad (\text{V})$$

$$\frac{d(\text{ROOH})}{dt} = \left(\frac{k_1}{k_6}\right)^{\frac{1}{2}} k_3(\text{RH}) \frac{\frac{1}{k_{4-\alpha, \gamma}} + \frac{k_{4-\alpha, \delta}}{k_3(\text{RH})}}{1 + \frac{k_{4-\alpha, \gamma}}{k_3(\text{RH})} + \frac{k_{4-\alpha, \delta}}{k_3(\text{RH})}} (\text{OOH})^{\frac{1}{2}}$$

$$= v(-\text{OOH})^{\frac{1}{2}} \approx \frac{d(\text{HD})}{dt} \quad (\text{VI})$$

$$\begin{aligned}
 \frac{d(\alpha, \gamma\text{-HOOR=O})}{dt} &= \left(\frac{k_1}{k_6}\right)^{\frac{1}{2}} k_3(\text{RH}) \frac{\left(\frac{k_{4-\alpha, \gamma}}{k_3(\text{RH})}\right) \left(\frac{k_{4-\alpha, \gamma}^*}{k_3(\text{RH})}\right)}{1 + \frac{k_{4-\alpha, \gamma}}{k_3(\text{RH})}} (-\text{OOH})^{\frac{1}{2}} \\
 &\quad - \frac{\frac{k_{4-\alpha, \delta}}{k_3(\text{RH})}}{1 + \frac{k_{4-\alpha, \gamma}}{k_3(\text{RH})}} + \frac{\frac{k_{4-\alpha, \delta}^*}{k_3(\text{RH})}}{1 + \frac{k_{4-\alpha, \delta}}{k_3(\text{RH})}} \\
 &= -k_7(\alpha, \gamma\text{-HOOR=O}) \\
 &= \omega (-\text{OOH})^{\frac{1}{2}} - k_7(\alpha, \gamma\text{-HOOR=O}) \tag{VII}
 \end{aligned}$$

where

$$(-\text{OOH}) = (\text{ROOH}) + 2(\text{HOOROOH}) + (\text{HOOR=O}) \tag{VIII}$$

The values η and ν are obtained from plots of experimental data in Figure 5.¹⁰ In the absence of experimental data on yields of $\alpha, \gamma\text{-HOOR=O}$, the values of ω and k_7 are obtained from experimental data plotted in Figure 6 in accordance with eq. (IX).

10 It should be noted that the 200°C/101 sec data at highest oxygen pressure also fit eq. (IV) and (VI). The 200°C data, apparently oxygen dependent, will be separately discussed below.

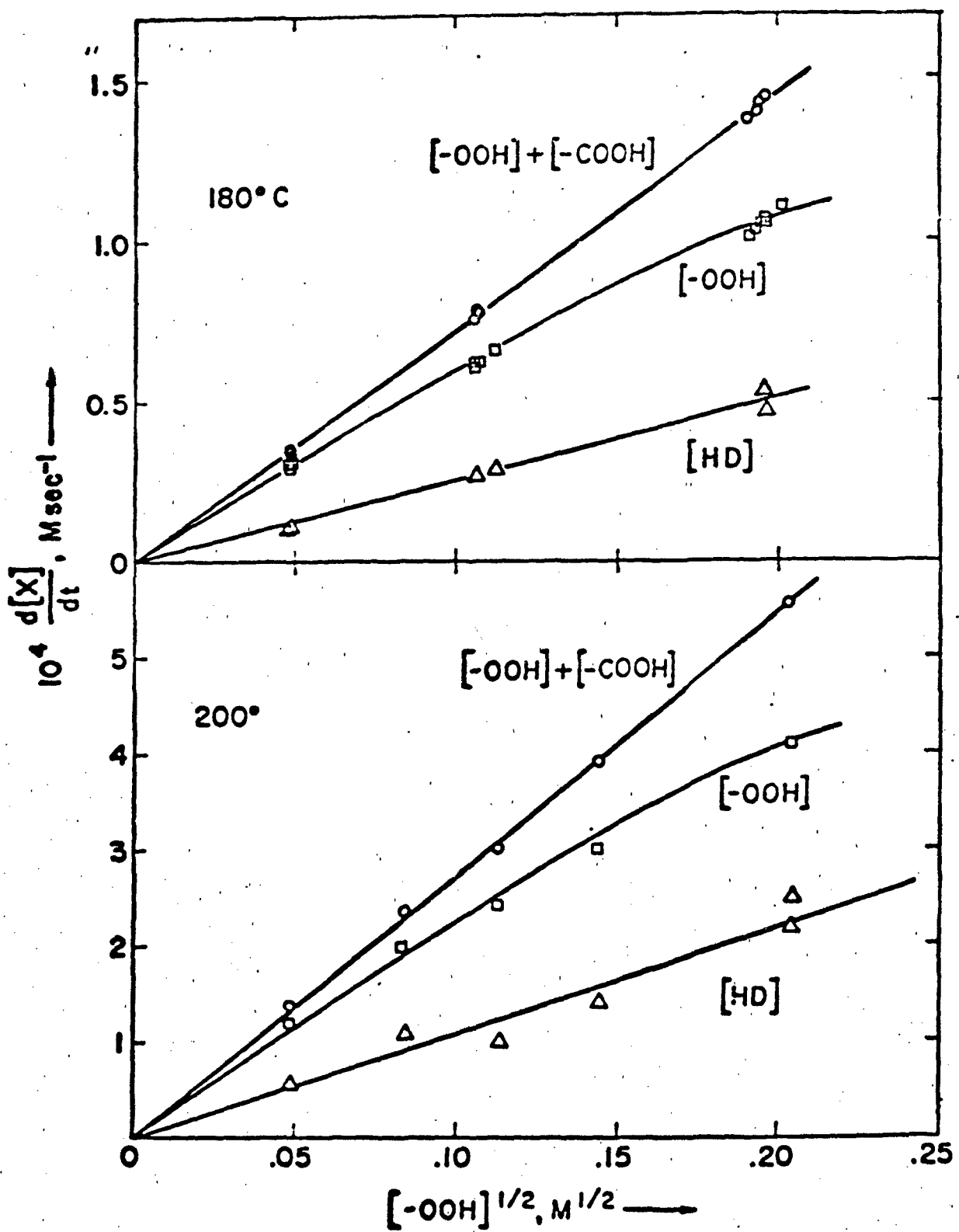


Figure 5. Plots of $\{d(-\text{OOH})/dt + d(-\text{COOH})/dt\}$ and $d(\text{HD})/dt$ versus $(-\text{OOH})^{1/2}$ at 180 and 200°C.

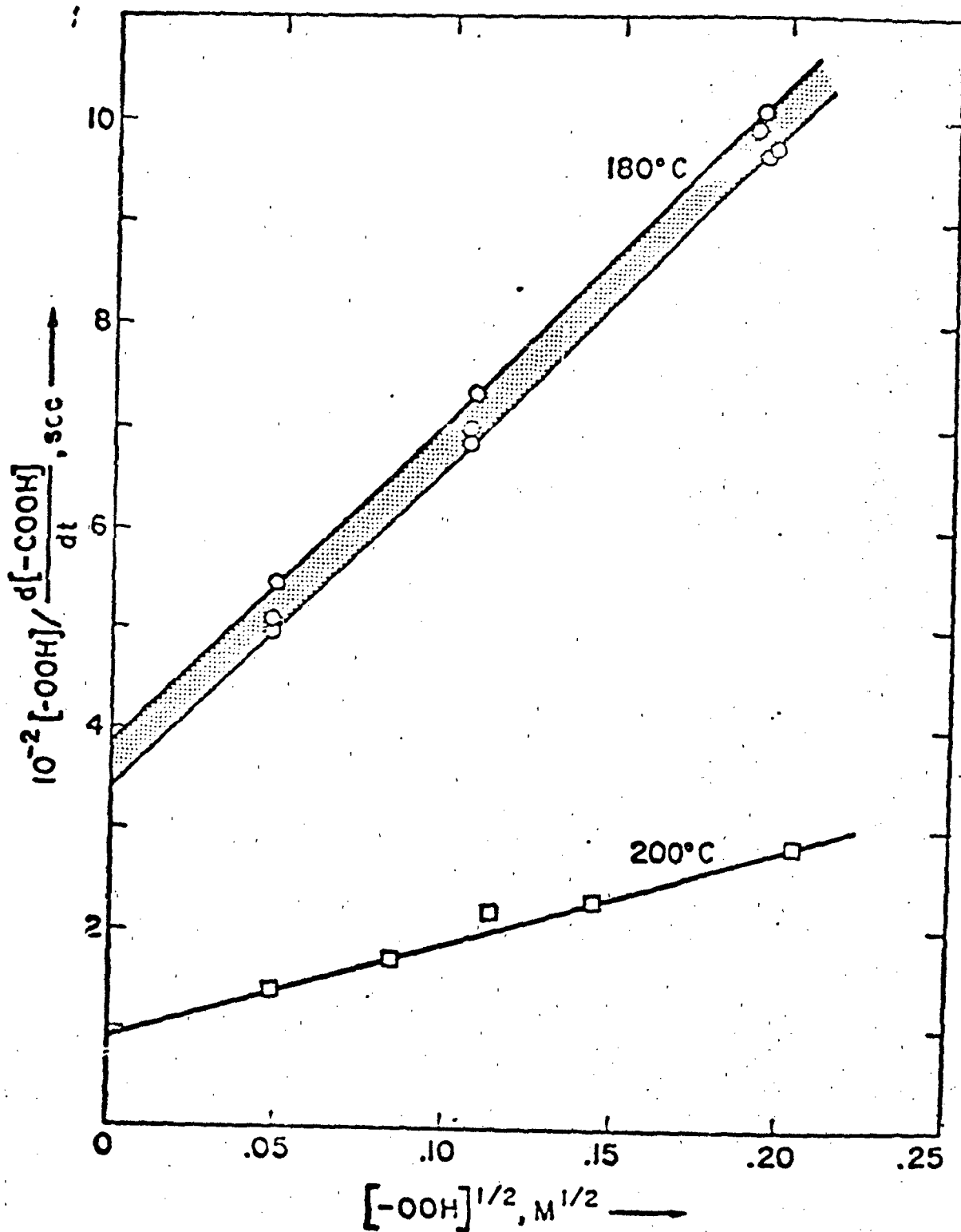


Figure 6. Plots of $\{[-\text{OOH}] / (d[-\text{COOH}] / dt)\}$ versus $(-\text{OOH})^{1/2}$ at 180 and 200°C.

$$\frac{(-\text{OOH})}{d(-\text{COOH})/dt} = \frac{\eta}{c k_7 \omega} + \frac{1}{c \omega} (-\text{OOH})^{\frac{1}{2}} \quad (\text{IX})$$

The derivation of eq. (IX) and detailed procedure for calculation of ω and k_7 are described in the Appendix. The values of η , ν , ω , and k_7 obtained at 180 and 200°C are summarized in Table VI.

Comparison of PETH and n-hexadecane rate parameters. Value of the rate constant for cleavage of α, γ -hydroperoxyoxo-PETH, k_7 , are strikingly similar to those obtained in n-hexadecane autoxidation. Direct measurements of the rates of decomposition of α, γ -hydroperoxyketone species or their equivalent and of formation of C_{14} methylketone product in n-hexadecane (18) yielded first order rate constants which in temperature range of 120 to 180°C were found to obey the Arrhenius equation

$$\log k_7 = 12.4 - \frac{30,200}{4.6T} \quad (\text{X})$$

This equation gives values of $k_7^{180^\circ}$ equal to $7.1 \times 10^{-3} \text{ sec}^{-1}$ and $k_7^{200^\circ}$ equal to $33 \times 10^{-3} \text{ sec}^{-1}$ for the n-hexadecane system. These findings strongly support the notion that cleavage product formation occurs in the PETH and n-hexadecane via the same mechanism, i.e., via decomposition of α, γ -hydroperoxyketone species.

Values of the ratios of rate constants for intramolecular and intermolecular hydrogen abstraction reactions, $k_4/k_3(\text{RH})$ and $k_4^*/k_3(\text{RH})$ and values of

TABLE VI.

PETH Autoxidation - Summary of Rate Constants^a

Rate Constant	Temperature, °C	
	180 ^c	200 ^c
$k_1, \text{ sec}^{-1}$ ^b	1.6×10^{-4}	8.0×10^{-4}
$n, \text{ M}^{\frac{1}{2}} \text{sec}^{-1}$ (eq. X)	7.3×10^{-4}	28×10^{-4}
$v, \text{ M}^{\frac{1}{2}} \text{sec}^{-1}$ (eq. XI)	2.6×10^{-4}	$10.7 (12) \times 10^{-4}$
$w, \text{ M}^{\frac{1}{2}} \text{sec}^{-1}$ (eq. XII)	2.8×10^{-4}	9.4×10^{-4}
$k_7, \text{ sec}^{-1}$ (eq. XII)	$6.4 (3) \times 10^{-3}$ ^b	30×10^{-3}
w/v	1.08; 1.1 ^c	0.88 (11) ^b ; 1.0 ^c
$k_{4-\alpha, \gamma}/k_3$ (RH)	1.14	0.97 (14) ^b ; 1.11 ^c
$k_{4-\alpha, \delta}/k_3$ (RH)	0.50	0.43 (6) ^b ; 0.49 ^c
$k_{4-\alpha, \gamma}^*/k_3$ (RH)	18	14 (5) ^b ; 19 ^c
$k_{4-\alpha, \delta}^*/k_3$ (RH)	4.9	3.6 (15) ^b ; 5.1 ^b
$(2k_1/2k_6)^{\frac{1}{2}} k_3$ (RH), $\text{M}^{\frac{1}{2}} \text{sec}^{-1}$	3.0×10^{-4}	$12.7(5) \times 10^{-4}$
$(k_{4-\alpha, \gamma}/H)/(k_3/H), \text{ M}$	26	22(4) ^b
$(k_{4-\alpha, \delta}/H)/(k_3/H), \text{ M}$	22	18(3) ^b
$(k_{4-\alpha, \gamma}^*/H)/(k_3/H), \text{ M}$	840	620(250) ^b
$(k_{4-\alpha, \delta}^*/H)/(k_3/H), \text{ M}$	230	170(70) ^b
$(k_3/H)/(2k_6)^{\frac{1}{2}}, \text{ M}^{-\frac{1}{2}} \text{sec}^{-\frac{1}{2}}$ ^b	3.6×10^{-4}	$6.9(3) \times 10^{-4}$ ^b

^a Concentrations of PETH, [RH], at 180 and 200° were 1.47 and 1.44 M, respectively.

^b The uncertainties of the values obtained are indicated in parenthesis. For example, $10.7(12) \times 10^{-4}$ denotes that values obtained lay in the range $(10.7 \pm 1.2) \times 10^{-4}$. The values of k_1 and $(k_3/H)/(2k_6)^{\frac{1}{2}}$ are based upon the assumption that $n = 4$ for the bisphenol antioxidant used (cf. Rate of Initiation Section).

^c Obtained combining eqs (VI) and (VII) and using k_7 derived from eq (IX).

$(2k_1/2k_6)^{1/2}k_3(RH)$ (cf. Table VI) may be then derived from values of η , v , and w assuming that the ratios of rate constants for intramolecular α , γ and α , δ abstractions are on a per hydrogen basis the same as those in n-hexadecane autoxidation, i.e., $(k_{4-\alpha,\gamma}/H)/(k_{4-\alpha,\delta}/H)$ is equal to 1.2 and $(k_{4-\alpha,\gamma}^*/H)/(k_{4-\alpha,\delta}^*/H)$ to 3.7 (18).¹¹ The ratio $(k_3/H)/(2k_6)^{1/2}$ can then be obtained from $(2k_1/2k_6)^{1/2}k_3(RH)$ using values of k_1 measured in this work. At 180°C $(k_3/H)/(2k_6)^{1/2}$ for PETH is equal to $3.6 \times 10^{-4} \text{ M}^{-1/2} \text{ sec}^{-1/2}$ which is ca. 20 percent lower than the corresponding value obtained for n-hexadecane ($4.6 \times 10^{-4} \text{ M}^{-1/2} \text{ sec}^{-1/2}$) (18) and by a factor of 2.5 lower than the value $9.2 \times 10^{-4} \text{ M}^{-1/2} \text{ sec}^{-1/2}$ reported by Agliullina et al. (5) for autoxidation of pentaerythrityl tetrapentanoate, a system in which the availability of hydrogens limits the extent of intramolecular abstractions.

Due to the steric hindrance of PETH peroxy radicals it is anticipated that the values of $2k_6$ are smaller for the PETH than for the n-hexadecane system. This would lead to lower values of k_3/H in PETH and would in turn account for the higher values of the ratios of intramolecular to intermolecular abstraction rate constants in PETH than in n-hexadecane (18). The values of $(k_4/H)/(k_3/H)$ derived for PETH are greater than those derived for n-hexadecane by factor of 3.7 and values of $(k_4^*/H)/(k_3/H)$ by factor of 2.6. As observed in n-hexadecane, these ratios in PETH show little temperature dependence since the values at 200°C are, within experimental error, the same as those at 180°C.

11 The ratios of rate constants for n-hexadecane were calculated using methyl ketone product formation as a measure of $\alpha,\gamma\text{-HOO}\text{R}=\text{O}$ decomposed.

The value of the composite rate constant η at 200°C determined from the single experiment at the highest partial pressure of oxygen used in this study (191 kPa) and the value of η at 220°C obtained by extrapolation of an Arrhenius plot of the data at 180 and 200°C are found to be the same, i.e., $110 \times 10^{-4} \text{ M}^{-\frac{1}{2}} \text{ sec}^{-1}$. This finding suggests that the minimum oxygen pressure at which the yields of hydroperoxide and acid products are independent of oxygen pressure was exceeded in that experiment. Thus, a valid value of $(k_3/\text{H})/(2k_6)^{\frac{1}{2}}$ at 220°C may be extracted from η using an extrapolated value for k_1 at 220°C ($31 \times 10^{-4} \text{ sec}^{-1}$) and assuming that the ratios of $k_4/k_3(\text{RH})$ and $k_4^*/k_3(\text{RH})$ remain at 220°C the same as those at 180 and 200°C . The ratio $(k_3/\text{H})/(2k_6)^{\frac{1}{2}}$ at 220°C is then calculated to be equal to $12 \times 10^{-4} \text{ M}^{-\frac{1}{2}} \text{ sec}^{-\frac{1}{2}}$. This value together with those at the lower temperatures yields for $(k_3/\text{H})/(2k_6)^{\frac{1}{2}}$ an activation energy approximately equal to 13 kcal/mole, a value consistent with that observed in the autoxidation of n-butane at 100 and 125°C (21).

Evidence for ·OH Abstractions. From the values of $k_4/k_3(\text{RH})$ and $k_4^*/k_3(\text{RH})$ we conclude that ca. 60 percent of all hydrogen abstractions from PETH occur by ·OH radicals generated via reaction (5). The remaining abstraction reactions occur by chain carrying peroxy radicals and radical species derived from initiation reactions.¹² The relative reactivities of secondary to primary hydrogen atoms at the above distribution of free radicals species may be calculated from the expression

12 Since the kinetic chain lengths are equal to or larger than 8, an upper limit of 12 percent may be assigned to abstraction by species from initiation.

$$\frac{k_{sec}/H}{k_{prim}/H} = x \left(\frac{k_{sec}/H}{k_{prim}/H} \right) \cdot OH + (1-x) \left(\frac{k_{sec}/H}{k_{prim}/H} \right) RO_2^{\cdot} \quad (XI)$$

where x is a fraction of abstracting radicals corresponding to $\cdot OH$ and $\left(\frac{k_{sec}/H}{k_{prim}/H} \right) \cdot OH$ and $\left(\frac{k_{sec}/H}{k_{prim}/H} \right) RO_2^{\cdot}$ are relative reactivities of secondary to primary hydrogens for abstractions by hydroxy and peroxy radicals which may be obtained from the literature. Using values of $\left(\frac{k_{sec}/H}{k_{prim}/H} \right) \cdot OH$ equal to 5.4(5.2) (22) and of $\left(\frac{k_{sec}/H}{k_{prim}/H} \right) RO_2^{\cdot}$ equal to 30(28)¹³ the calculated values of $\left(\frac{k_{sec}/H}{k_{prim}/H} \right)$ are found to be equal to 16(15) at 180°C (200°C). From the experimental values of yields of 1,6- and 1,7-heptanediois (cf. Table III) apparent values¹⁴ of $\left(\frac{k_{sec}/H}{k_{prim}/H} \right)$ are found to be in the range of 11 to 18. The reasonable agreement of the calculated and the experimental values of $\left(\frac{k_{sec}/H}{k_{prim}/H} \right)$ strongly supports the notion that in PETH a high percentage of hydrogen atom abstractions occur via $\cdot OH$ radicals.

13 In a study of n-butane oxidation, Mill et al. (21) have determined that the ratio $\left(\frac{k_{sec}/H}{k_{prim}/H} \right)$ for abstraction by sec-butyperoxy radicals is 45 at 100°C. Based on difference in activation energy for the two abstractions of 1.65 kcal/mole (23), equal to 0.55 times the difference in strengths of the two C-H bonds, this ratio is calculated to be 30 at 180°C and 28 at 200°C.

14 These values are apparent since the relative yields of these products also reflect the relative values of $k_3(RH)/(k_3(RH) + k_4)$ for the corresponding primary and secondary peroxy radicals. In the case of internal secondary peroxy radicals these values may vary significantly.

We note that at a low oxygen pressure of 24 kPa at 200°C the apparent value of $(k_{sec}/H)/(k_{prim}/H)$ obtained from the yields of 1,6- and 1,7-heptanediols increases to ca. 23. This suggests that a lower percentage of hydroxy radicals participate in abstraction reactions at lower oxygen pressures. Since $\cdot\text{OH}$ are generated concurrently with hydroperoxyketone formation, reaction (5), the result further implies that yields of hydroperoxyketone species decreases with decreasing oxygen pressure. Indeed, the yield of α, γ -hydroperoxyketone species, as measured by the rate of acid formation, decreases compared to the 121 kPa experiment by a factor of five while the yield of total hydroperoxide and monohydroperoxide products decrease by a factor of only two. Strongly decreasing relative yields of α, γ -disubstituted products with decreasing oxygen pressure below ca. 60 kPa have also been observed in the n-hexadecane autoxidation at 180°C (18).¹⁵ This phenomenon of decreased rate of formation of α, γ -disubstituted products at lower oxygen pressures is now being further investigated in the n-hexadecane system.

15 The source of this sensitivity to oxygen pressure may be the reversibility of intramolecular α, γ abstraction reaction (4) at decreased oxygen pressures. The reverse reaction may under these conditions become competitive with oxygen addition since peroxy radical abstraction from $-\text{CH}_2-$ is endothermic by ca. 6 kcal/mole and intramolecular reactions have high preexponential factors (18).

ACKNOWLEDGMENT

The authors wish to acknowledge R. K. Jensen for many helpful discussions and for his assistance in the measurement of rates of initiations and Dr. T. M. Harvey, R. Marano, and T. J. Prater for mass spectrometric analyses. This work was supported by the Air Force Office of Scientific Research under contract F44620-76-C-0097.

REFERENCES

1. L. R. Mahoney, S. Korcek, R. K. Jensen, and M. Zinbo, Preprints, Div. Petrol. Chem., ACS, 21, No. 4, 852 (1976).
2. C. H. DePuy and R. W. King, Chem. Rev., 60, 431 (1960).
3. D. E. VanSickle, J. Org. Chem., 37, 1392, 1398 (1972).
4. P. J. Sniegoski, ASLE Trans., 20, 282 (1977).
5. G. G. Agliullina, V. S. Martemianov, E. T. Denisov, O. A. Kulagina, and M. M. Kukovitskii, Neftekhimiya, 16, 262 (1976).
6. G. G. Agliullina, V. S. Martemianov, E. T. Denisov, and T. I. Eliseeva, Izv. Akad. Nauk SSSR, Ser. Khim., 50 (1977).
7. G. A. Kovtun, G. L. Lukyanova, A. S. Berenblyum, and I. I. Moiseev, Izv. Akad. Nauk SSSR, Ser. Khim., 2179 (1976).
8. R. K. Jensen, S. Korcek, L. R. Mahoney, and M. Zinbo, "Liquid Phase Autoxidation of Organic Compounds at Elevated Temperatures," Part I, J. Am. Chem. Soc., 101, 7574 (1979).
9. (a) K. G. Denbigh, Trans. Faraday Soc., 40, 352 (1944); (b) B. Stead, F. M. Page, and K. G. Denbigh, Faraday Soc. Disc. 2, 263 (1947); (c) K. G. Denbigh, M. Hicks, and F. M. Page, Trans. Faraday Soc., 44, 479 (1948).
10. F. D. Rossini et al., "Selected Values of Physical and Thermodynamic Properties of Hydrocarbons and Related Compounds", American Petroleum Institute Research Project 44, Carnegie Press, Pittsburgh, Pa., 1953.

11. "Handbook of Chemistry and Physics", 52nd ed.; R. C. Weast, Ed.; The Chemical Rubber Co., Cleveland, Ohio, 1971, D-100.
12. M. Zinbo, R. K. Jensen, and S. Korcek, Anal. Lett., 10, 119 (1977).
13. R. Adams and T. R. Govindachari, J. Amer. Chem. Soc., 72, 158 (1950).
14. M. J. Rosen and H. A. Goldsmith, "Systematic Analysis of Surface-Active Agents," Wiley - Interscience, New York, N. Y., 1972, p. 43.
15. R. D. Mair and A. J. Graupner, Anal. Chem., 36, 194 (1964).
16. "Fatty Acid Analysis", GAS-CHROM Newsletter, Applied Science Laboratories, Inc., Jan./Feb., 1976.
17. M. Anbar, D. Meyerstein, and P. Neta, J. Chem. Soc., B. Phys. Org. 1966, 742.
18. R. K. Jensen, S. Korcek, L. R. Mahoney, and M. Zinbo, "Liquid Phase Autoxidation of Organic Compounds at Elevated Temperatures," Part II, III, and IV, manuscripts in preparation.
19. L. R. Mahoney, Angew. Chem., Int. Ed. Engl., 8, 547 (1969).
20. L. R. Mahoney, S. Korcek, S. Hoffman, and P. A. Willermet, Ind. Eng. Chem. Prod. Res. Dev., 17, 250 (1978).
21. T. Mill, F. Mayo, H. Richardson, K. Irwin, and D. L. Allara, J. Amer. Chem. Soc., 94, 6802 (1972).
22. N. R. Greiner, J. Chem. Phys., 53, 1070 (1970).
23. S. Korcek, J. H. B. Chenier, J. A. Howard, and K. U. Ingold, Can. J. Chem., 50, 2285 (1972).

APPENDIX

DERIVATION OF EQ. IX AND CALCULATION OF ω AND k_7

In the stirred flow reactor experiments the ratio of rates of formation of any two products is equal to the ratio of their concentrations in the reactor. Thus,

$$\frac{d(\alpha, \gamma\text{-HOOR}=O)}{dt} = \frac{d(-\text{OOH})}{dt} \frac{(\alpha, \gamma\text{-HOOR}=O)}{(-\text{OOH})} \quad (\text{XII})$$

Combining eqs. (IV), (V), (VII), and (XII) yields an equation quadratic in $(\alpha, \gamma\text{-HOOR}=O)$, i.e.,

$$\frac{k_7}{(-\text{OOH})} (\alpha, \gamma\text{-HOOR}=O)^2 - \left(k_7 + \frac{\eta}{(-\text{OOH})} \right) (\alpha, \gamma\text{-HOOR}=O) + \omega (-\text{OOH})^{\frac{1}{2}} = 0 \quad (\text{XIII})$$

The solution of eq. (XIII) for $(\alpha, \gamma\text{-HOOR}=O)$ and expansion of the square root term in combination with eq. (V) yields for the rate of formation of acid products

$$\frac{d(-\text{COOH})}{dt} = \frac{\frac{k_7 \omega}{\eta} (-\text{OOH})}{1 + \frac{k_7}{\eta} (-\text{OOH})^{\frac{1}{2}}} \left\{ 1 + \frac{k_7 \omega (-\text{OOH})^{\frac{1}{2}}}{[k_7 (-\text{OOH})^{\frac{1}{2}} + \eta]^2} \right. \\ \left. + 2 \left[\frac{k_7 \omega (-\text{OOH})^{\frac{1}{2}}}{[k_7 (-\text{OOH})^{\frac{1}{2}} + \eta]^2} \right]^2 + 5 \left[\frac{k_7 \omega (-\text{OOH})^{\frac{1}{2}}}{[k_7 (-\text{OOH})^{\frac{1}{2}} + \eta]^2} \right]^3 + \dots \right\} \quad (\text{XIV})$$

If the expression in braces in eq (XIV) is approximately constant, equal to c, then the rate of formation of acid products should obey the equation

$$\frac{(-\text{OOH})}{d[-\text{COOH}]} = \frac{\eta}{c k_7 \omega} + \frac{1}{c \omega} (-\text{OOH})^{\frac{1}{2}} \quad (\text{IX})$$

Figure 6 shows that eq (IX) does indeed describe well the observed instantaneous rates of formation of total acid products at 180 and 200°C. From these plots, the values of $\frac{\eta}{c k_7 \omega}$ and $\frac{1}{c \omega}$ are equal to 360(20) sec and $3200 \text{ M}^{-\frac{1}{2}}$ sec at 180°C and to 90 sec and $970 \text{ M}^{-\frac{1}{2}}$ sec at 200°C. The ratio of these values in combination with previously determined values of η yields the values of k_7 which are listed in Table VI. These values of k_7 are used for the calculations of ω and c from eq (XIV) and (IX) by a method of successive approximations (for final values of ω see Table (XVI)). The values of c derived by this procedure are found to be independent of $(-\text{OOH})$ and temperature and are equal to 1.10(1). This finding validates the assumption used in the derivation of eq (IX).

ATTACHMENT II

LUBRICANT DEGRADATION AND WEAR IV. THE
EFFECT OF OXIDATION ON THE WEAR BEHAVIOR OF
PENTAERYTHRITYL TETRAHEPTANOATE

P. A. Willermet, L. R. Mahoney
and S. K. Kandah

Engineering and Research Staff
Research
Ford Motor Company
Dearborn, Michigan 48121

ABSTRACT

Wear studies carried out in conjunction with a study of the kinetics and mechanism of the autoxidation of pentaerythrityl tetraheptanoate (PETH) showed that small degrees of oxidation produced large increases in wear rate. The results indicate that monoesters of dicarboxylic acids in conjunction with hydroperoxides are the oxidation products which result in the increased wear.

INTRODUCTION

The reactions of molecular oxygen with lubricants produce polar oxidation products. At low conversions these processes may not result in any measurable change in lubrication-related physical properties. It is, however, well known that low concentrations of surface active molecules can have large influences on the wear of materials under boundary lubrication conditions⁽¹⁾.

In order to determine which specific chemical species are responsible for any wear effects found upon oxidation of a lubricant, it is necessary to have quantitative information on the nature of the oxidation products. Our laboratory has recently carried out a kinetic study of the oxidation of pentaerythrityl tetraheptanoate, PETH, at elevated temperatures⁽²⁾. In the course of that study large quantities of oxidized PETH were generated and the oxidation products were quantitatively defined. This paper reports the results of a laboratory wear study utilizing these materials.

EXPERIMENTAL

Preparation and Composition of Pure Oxidized PETH

Detailed descriptions of the purification and oxidation of PETH and the analysis of the oxidation products have been presented earlier⁽²⁾. Purification of technical grade PETH was accomplished by percolation through alumina followed by vacuum distillation and a final percolation.

The purified PETH was oxidized in a stirred flow reactor. This technique provides large quantities of material oxidized under precisely controlled conditions⁽²⁾. The reaction conditions and the major products of the oxidations are summarized in Table 1.

Model Compounds

Succinic acid mononeopentyl ester was synthesized by refluxing equimolar concentrations of succinic anhydride and neopentyl alcohol in xylene. The resulting product was purified by vacuum distillation and assayed at 95% purity by titration

with KOH. Tertiary butyl hydroperoxide was a redistilled commercial material which was assayed at 97% purity by iodometric titration⁽²⁾. All other model compounds were commercial materials of 99+% purity.

Wear Measurements

Wear measurements were conducted using a Brown/GE modified 4-Ball apparatus operated at 600 RPM. Except where indicated, 40Kg load was employed. The wear specimens were AISI 52100 steel balls, grade 25. Before each test, the balls, top ball chuck, and sample container were thoroughly washed with Stoddard solvent, followed by reagent grade toluene, acetone and pentane. The sample container and top ball chuck were assembled, dried at 100°C, then cooled to room temperature in a dessicator. The spindle and drawbar were washed with pentane to remove any contaminants from the previous run. Syringes used for adding or withdrawing samples were cleaned and dried in the same way.

Solutions were purged with dry air after being made up, then stored in a desiccator. At the beginning of each run, 8 ml of the test solution was added to the sample container and the apparatus assembled. The liquid seal employed to maintain a controlled atmosphere was filled with base oil. 40 kg pressure was applied and purging with dry air started. The sample temperature was then brought to 100°C (except where indicated) and the test begun. After termination of the experiment, a sample of used fluid was withdrawn and the wear scar diameters measured in the usual manner.

For purposes of data analysis, the measured average wear scar diameters were converted to calculated wear volumes using Feng's equation⁽³⁾.

$$V = 4.65 \times 10^{-2} d^4 - 3.21 \times 10^{-5} Wd$$

Where V equal wear volume in mm³ for 3 balls, d is equal to wear scar diameter in mm and W equals load in kg.

Wear of the rotating ball was measured with a stylus profilometer.

Experimental Results for Pure and Oxidized PETH

A series of wear runs of 5 minutes duration was made with highly purified PETH and ESFR-62 in which the load was increased in 10 kg increments to 90 kg. Plots of wear scar diameter versus load indicated that the initial seizure load was above 50 kg. A 40 kg. load was chosen for the remainder of the wear experiments in order to produce readily measured wear while operating in the mild wear regime.

Data for wear volume versus time for ESFR-62, fresh PETH and admixtures are presented in Fig. 1. The data represent steady state wear rates for the fluids which were found to be linearly dependent on the volume fraction of oxidized PETH (Fig 1, insert). This is equivalent to a linear dependence on the concentration of oxidation products, or for these experiments:

$$\frac{dV}{dt} = A + B \sum_1^n [P]_n$$

where dV/dt denote the volumetric wear rate,

$[P]_n$ denotes the concentration of an oxidation product, and

A and B are experimental constants.

The distribution of oxidation products depends in part on the oxygen partial pressure ⁽²⁾ (Table 1). The effect of product distribution on wear was examined by comparing the results obtained with ESFR-36 with data for admixtures composed of 25 volume percent ESFR-62 or ESFR-65 and 75 volume percent pure PETH (Fig. 2). These fluids had equivalent concentrations of total hydroperoxides. The steady state wear rates were found to be proportional to the total acid concentration in the solution (Fig. 3). The initial wear for the ESFR-65 admixture and for ESFR-36 was, however, significantly greater. For these experiments in which the total initial hydroperoxide were equal to about $100 \times 10^{-4} M$,

$$\frac{dV}{dt} = C + D \sum_1^n [RCOH]_n$$

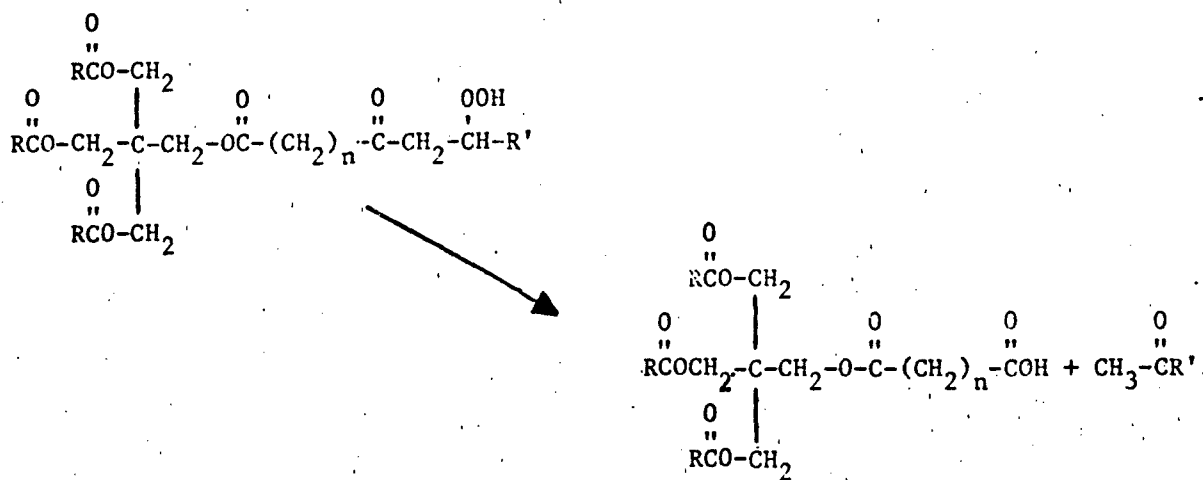
where $[RCOH]$ denotes the concentration of a product acid and C and D are experimental

constants.

It should be noted that the wear rate results for oxidized PETH and mixtures of pure and oxidized PETH, (Figure 1 and 3), which contain higher concentration of hydroperoxide species also obey equation (2). This result suggests that at these high hydroperoxide concentrations the wear rates may be independent of hydroperoxide concentration. Results from model system experiments, vide infra, lead to the same conclusions.

Experimental Results for Model Systems

Acids and hydroperoxide added to pure PETH. The acids formed upon oxidation of PETH and other ester lubricants are about equally divided into monobasic short chain acids and diacid monoesters in which the ester substituent is the PETH moiety, via the reaction:



Monobasic acids were added in amounts comparable to their concentrations in oxidized PETH to assess their effect on wear. The influence of the diacid monoesters was assessed by adding the monomethyl esters and succinic acid mono-neopentyl ester as model compounds. These acids were added to both pure PETH and pure PETH containing added tertiary butyl hydroperoxide.

Table II presents results which show the effect of the addition of the various acids to pure PETH on the amount of wear generated in 30 minutes.

test time. The lower molecular weight monobasic acids formed during PETH oxidation produced only a small increase in wear. The diacid monomethyl esters produced substantial increases in wear. The influence of the mononeopentyl ester was intermediate.

Table III shows the effect of adding the various acids to pure PETH containing 420×10^{-4} tertiary butyl hydroperoxide. The presence of the hydroperoxide brought about further large increases in wear. As in the system without hydroperoxide, the effects of the monobasic acids were minimal or, in the case of heptanoic acid, wear was decreased. The model dibasic acid monoesters increased the amount of wear. In the presence of hydroperoxide, succinic acid mononeopentyl ester was as effective in increasing wear as were the other monoesters. Results obtained employing succinic acid and adipic acid in place of the monoesters are presented in Tables II and III for comparison.

Experiments in which the initial concentration of hydroperoxide was varied (Fig. 4) suggest that the wear rates become independent of hydroperoxide concentration above about 100×10^{-4} M for the model systems. It should be noted that this result is in general agreement with the behavior observed for oxidized PETH and its admixtures with pure PETH.

The concentration of hydroperoxide was monitored by iodometric titration for several wear experiments and in a blank experiment in which the balls were not in contact. Due to the volatility of tertiary butyl hydroperoxide, the concentration of hydroperoxide decreased significantly during the wear experiments on the model systems; about 85% of the initial hydroperoxide being lost in 30 minutes running time.

Acids Added to Oxidized PETH

To further test the hypothesis that diacid monoesters play a crucial rôle in determining the wear behavior of oxidized PETH, model compounds and monobasic acids were added to 25 volume percent ESFR-65 in fresh PETH (Table IV). The results are in general agreement with those seen for the model systems described

previously. Little effect was observed upon the addition of propionic acid, wear was decreased upon the addition of dodecanoic acid, and the wear increased upon the addition of dibasic acid monoesters.

Wear of the Rotating Ball

The results of wear measurements on the rotating ball for selected specimens are presented in Table V. The data are consistent with the 3 ball wear results. Greater wear is noted for oxidized PETH than for fresh PETH. The addition of hydroperoxide and monoesters of dibasic acids to fresh PETH results in wear increases. Although insufficient data has been accumulated at this time to allow unambiguous interpretation, it may be noted that the relative wear on the rotating ball decreased when the concentration of the diacid monoesters became sufficiently high, suggesting a change in the wear mechanism.

Conclusions

Although it is premature to propose a detailed mechanochemical mechanism for the increased wear observed with autoxidized PETH, the experimental results are consistent with the following description of the wear kinetics:

- The wear rates are proportional to the concentration of acid products.
- The wear rates are independent of the concentration of hydroperoxides above ca 100×10^{-4} M.

Further, specific structural effects must play a rôle. Monoacid products have little effect while low concentrations of dibasic acids or dibasic acid monoesters of comparable molecular weights greatly accelerated the wear process. The results suggest that similar studies on simpler systems for which specific oxidation products can be readily synthesized may lead to a better understanding of the mechanochemical processes which produce these large effects.

Acknowledgement

This work was supported by the Air Force Office of Scientific Research
under contract F44620-76-C0097.

REFERENCES

1. Be...r, A., "Boundary Lubrication", Scientific and Technical Applications Forecast, AD 747336, June 1972.
2. Hamilton, E. J. Jr., Korcek, S., Mahoney, L. R., and Zinbo, M., "Kinetics and Mechanism of the Autoxidation of Pentaerythritol Tetraheptanoate at 180 to 220°C." International Journal of Chemical Kinetics; in press.
3. Feng, I-Ming, "A New Approach in Interpreting the Four-Ball Wear Results", Wear, 5, pp. 275-288 (1962).

TABLE I

A. Principal Products and Oxidation Conditions for Autoxidized PETH

Sample	Temp., °C	Residence Time Sec.	O ₂ Pressure kPa	Total Hydroperoxides ^{a/} Mx10 ⁴	Total Acids, Mx10 ⁴
ESFR-62	180	368	109	436	165
ESFR-65	180	364	111	413	152
ESFR-36	200	70	24	110	16

B. Distribution of Acids for ESFR-62^{b/}

Monoacids, Mx10 ⁴ ^{c/}						Principal Diacid Half Esters, Mx10 ⁴ ^{d/}			
C ₂	C ₃	C ₄	C ₅	C ₆	C ₇	$\Sigma (C_2 - C_7)$	C ₃	C ₄	C ₅
24.4	14.2	2.8	1.5	1.1	47.7	91.7	11-23	24	10

^{a/} All product concentrations are at 26°C^{b/} Subscript to C denotes the number of carbon atoms^{c/} Based on direct analysis for monoacids (2).^{d/} Based on analysis of terminal diols from LiAlH₄ reductions of the oxidized sample (2).

TABLE II
Effect of Monoacids, Diacids and Diacid Monoesters
on the 4-Ball Wear Behavior of Pure PETH

Additive	Concentration, Mx10 ⁴	Wear Scar Diameter, mm		Wear Volume for 3 Balls, mm ³ x10 ³
		Wear Scar Diameter, mm	Wear Volume for 3 Balls, mm ³ x10 ³	
None	--	0.535		3.1
<u>Monobasic Acids</u>				
Decanoic acid	2	0.541		3.3
	20	0.511		2.5
Heptanoic acid	3	0.503		2.5
Propionic acid	65	0.567		3.9
Acetic acid	9.5	0.550		3.6
	87	0.588		4.7
<u>Dibasic Acids</u>				
Succinic acid	5	0.549		3.5
	10	0.618		6.0
	20	0.670		8.5
	100	0.738		12.8
Adipic acid	10	0.653		7.6
	100	0.851		23.3
<u>Dibasic Acid Monoesters</u>				
Succinic acid monomethyl ester	50	0.649		7.4
	100	0.670		8.5
Adipic acid monomethyl ester	27	0.654		7.7
	50	0.663		8.1
Succinic acid mononeopentyl ester	50	0.607		5.1

TABLE III

Effect of Monoacids, Diacids and Diacid Monoesters
on the 4-Ball Wear Behavior of an Admixture of Pure
PEIH and Tertiary Butyl Hydroperoxide. Initial
Hydroperoxide Concentration: 420×10^{-4} M

Additive	Concentration, $M \times 10^4$	Wear Scar Diameter, mm	Wear Volume for 3 Balls, $mm^3 \times 10^3$
None	--	0.656	7.8
<u>Monobasic Acids</u>			
Heptanoic acid	50	0.563	4.0
Propionic acid	50	0.651	7.5
<u>Dibasic Acids</u>			
Succinic acid	27	0.849	23.1
	50	0.903	29.8
Adipic acid	27	0.735	12.6
<u>Dibasic Acid Monoesters</u>			
Succinic acid monomethyl ester	50	0.786	16.7
Adipic acid monomethyl ester	10	0.714	11.2
	27	0.723	11.8
	50	0.764	14.9
Succinic acid mononeopentyl ester	28.5	0.737	12.8
	39	0.725	11.9
	50	0.873	27.0

TABLE IV

Effect of Monoacids and Diacid Monoesters on
 the 4-Ball Wear Behavior of an Admixture of 25
 Volume Percent ESFR-65 in Pure PETH.

Test Time: 30 min.

Additive	Concentration, Mx10 ⁴	Wear Scar Diameter, mm	Wear Volume for 3 Balls, mm ³ x10 ³
None	--	0.692	9.8
<u>Monobasic Acids</u>			
Dodecanoic acid	8	0.604	5.4
Propionic acid	10	0.642	7.1
	50	0.716	11.3
<u>Dibasic Acid Monoesters</u>			
Succinic acid mononeopentyl ester	10	0.691	9.7
	50	0.719	11.5

Test Time: 60 min.

Additive	Concentration, Mx10 ⁴	Wear Scar Diameter, mm	Wear Volume for 3 Balls, mm ³ x10 ³
None	--	0.754	14.3
<u>Monobasic Acids</u>			
Dodecanoic acid	8	0.689	9.6
Propionic acid	10	0.779	16.1
	50	0.791	17.2
<u>Dibasic Acid Monoesters</u>			
Succinic acid monomethyl ester	10	0.833	21.3
	40	0.872	25.8
Succinic acid mononeopentyl ester	10	0.847	23.9
	50	0.830	21.1

TABLE V
Results of Wear Measurements on the Rotating Ball

<u>Base Fluid</u>	<u>Additives</u>	<u>Run Time</u> <u>min.</u>	<u>Total Wear</u> <u>mm³ x 10³</u>	<u>Wear*</u> <u>Ratio</u>
Pure PETM	---	15	6.8	2.3
		60	15.5	1.9
	Adipic acid monomethyl ester, 2.7×10^{-4} M	30	15.6	1.9
	Adipic acid monomethyl ester, 10×10^{-4} M	30	14.6	0.9
	Adipic acid monomethyl ester, 250×10^{-4} M	30	18.9	0.7
	Succinic acid monomethyl ester, 100×10^{-4} M	30	25.1	0.7
	Tertiary butyl hydroperoxide, 420×10^{-4} M	30	28	2.6
	Tertiary butyl hydroperoxide, 420×10^{-4} M	60	32	3.2
	Tertiary butyl hydroperoxide, 420×10^{-4} M	30	31.2	1.1
	Adipic acid monomethyl ester, 50×10^{-4} M			
	Tertiary butyl hydroperoxide, 420×10^{-4} M	30	42.6	1.6
	Succinic acid monomethyl ester, 50×10^{-4} M			
	Tertiary butyl hydroperoxide, 420×10^{-4} M	30	38.3	0.4
	Succinic acid mononeopentyl ester 50×10^{-4} M			
ESFR-36	---	20	13.1	1.1
	---	60	24.4	1.2
25 volume percent	---	30	18.6	2.5
ESFR-62	---	60	27.7	1.8
25 volume percent	---	20	14.3	0.9
ESFR-65	---	60	36.8	1.8
	Succinic acid monomethyl ester, 40×10^{-4} M	60	46.0	0.9
	Succinic acid monomethyl ester, 10×10^{-4} M	60	68.1	2.2
	Succinic acid mononeopentyl ester, 50×10^{-4} M	30	29.3	1.6
		60	45.2	1.1

*The wear volume for the rotating ball divided by the wear volume for the 3 stationary balls.

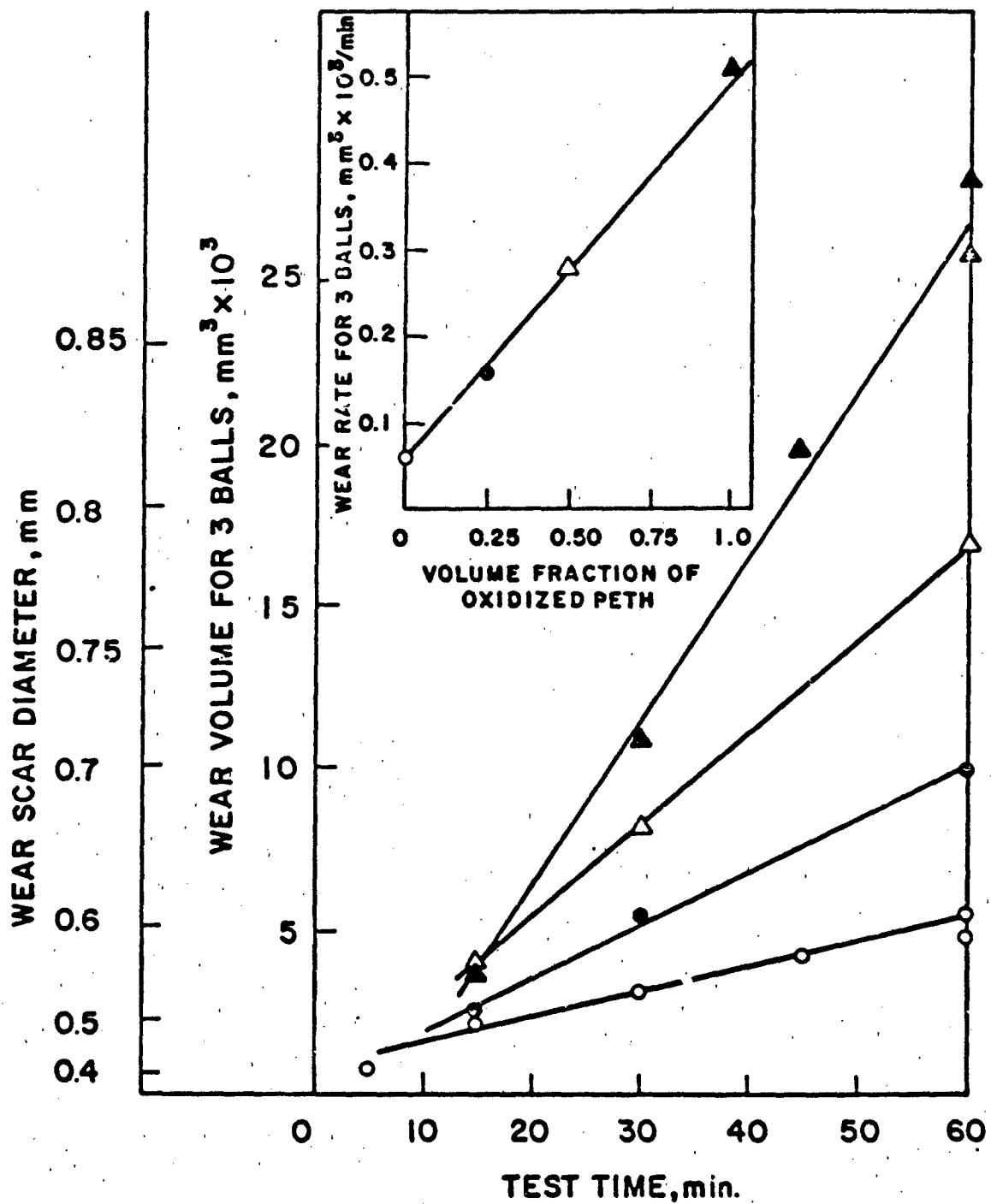


Fig. 1 - Wear volume and wear scar diameter for 3 stationary balls versus time for pure PETH, oxidized PETH and admixtures.

- Pure PETH
- ▲ Oxidized PETH, ESFR-62
- △ 0.50 volume fraction of ESFR-62 in pure PETH
- 0.25 volume fraction of ESFR-62 in pure PETH

Inset - Wear rate calculated for 3 balls versus volume fraction of oxidized PETH, ESFR-62, for admixtures of oxidized and pure

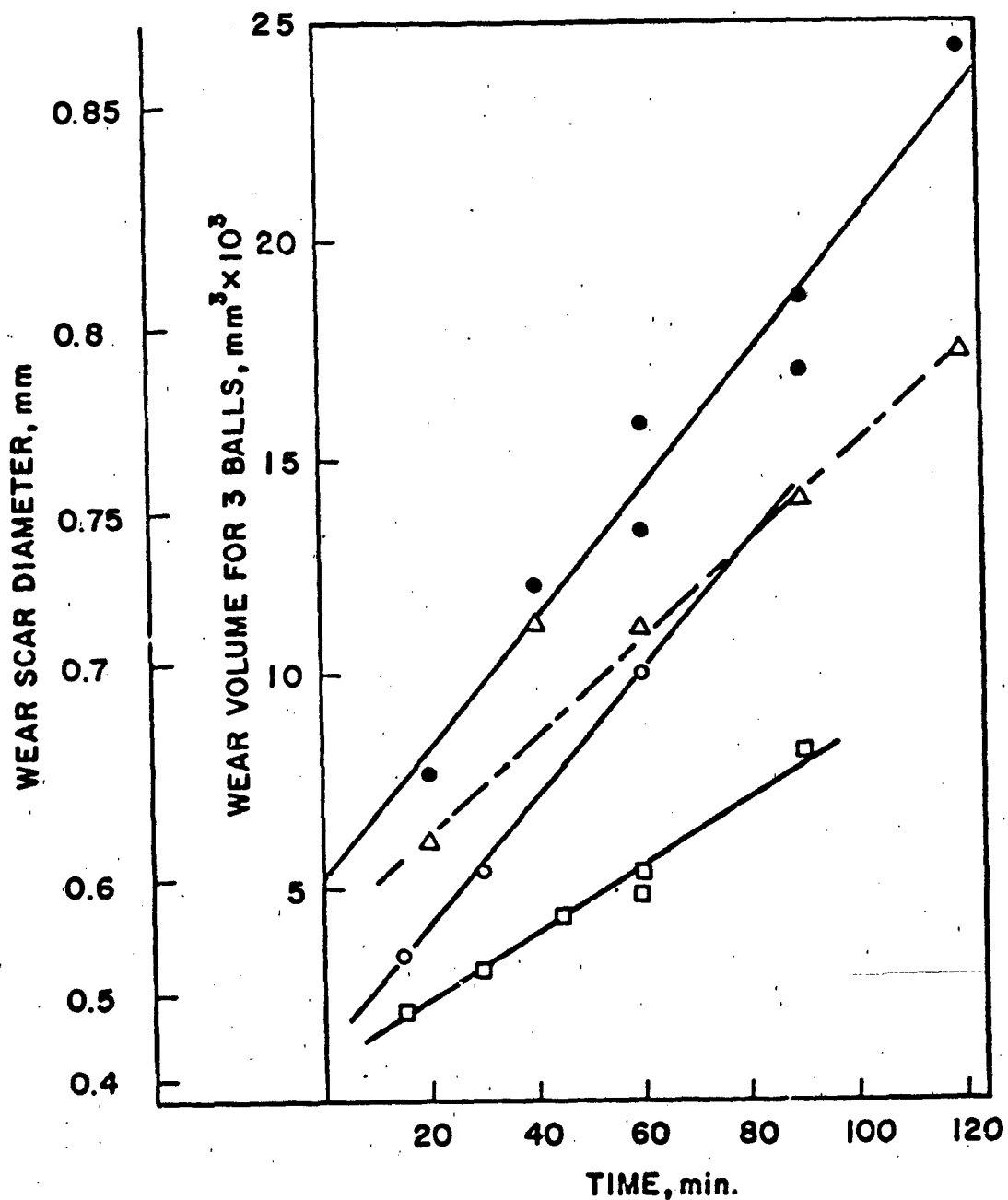


Fig. 2 - Wear volume and wear scar diameter for 3 stationary balls versus time for ESFR-36 (oxidized under reduced oxygen pressure) and for admixtures of ESFR-62 and ESFR-65 with pure PETH, having equivalent total hydroperoxide concentrations.

- 0.25 volume fraction ESFR-62 in pure PETH, total hydroperoxide concentration = $100 \times 10^{-4} M$, total acid concentration = $41 \times 10^{-4} M$
- 0.25 volume fraction ESFR-65 in pure PETH, total hydroperoxide concentration = $103 \times 10^{-4} M$, total acid concentration = $38 \times 10^{-4} M$
- △ ESFR-36, total hydroperoxide concentration = $110 \times 10^{-4} M$, total acid concentration = $16 \times 10^{-4} M$
- Pure PETH

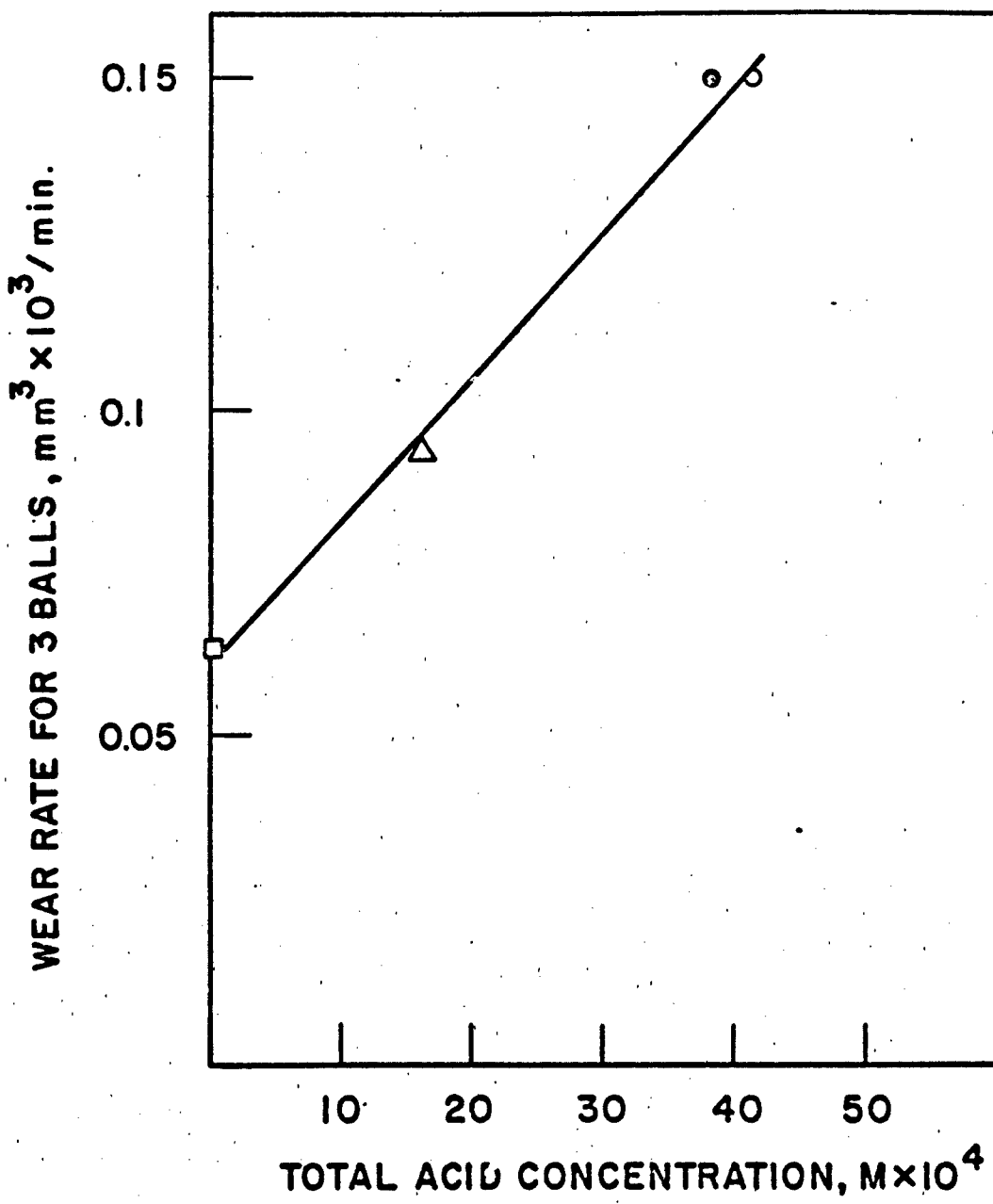


Fig. 3 - Wear rate for 3 balls versus total acid concentration for ESFR-36, 0.25 volume fraction ESFR-65 and 62 and fresh PETH

- Fresh PETH
- 0.25 volume fraction ESFR-65 in pure PETH
- 0.25 volume fraction ESFR-62 in pure PETH
- △ ESFR-36

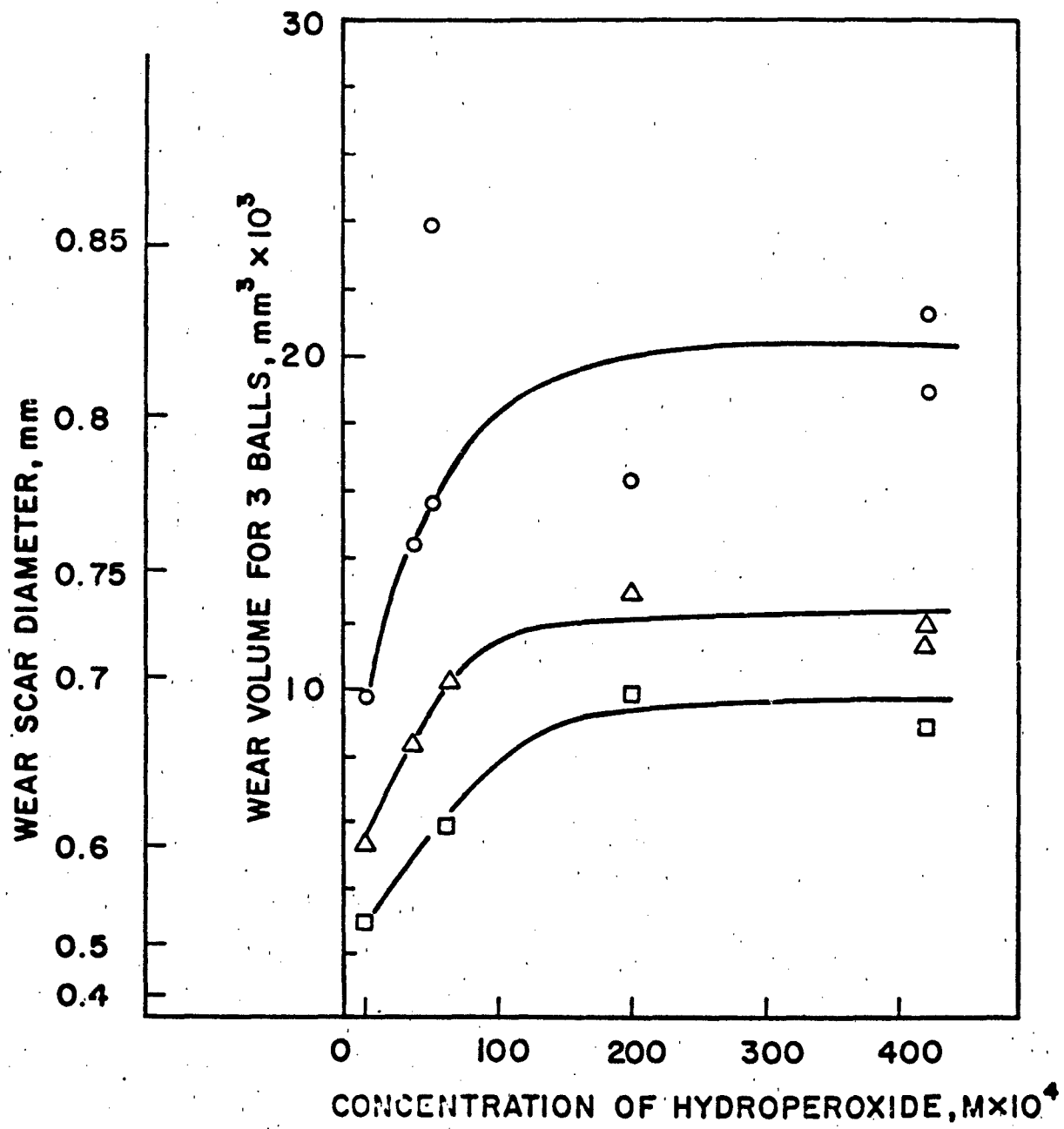


Fig. 4 - Wear volume and wear scar diameter for 3 stationary balls for admixtures of 2.7×10^{-4} M adipic acid monomethyl ester and tertiary butyl hydroperoxide in pure PETH versus the initial concentration of added tertiary butyl hydroperoxide.

- 60 minutes run time
- △ 30 minutes run time
- 20 minutes run time